arXiv:1101.5420v1 [hep-ph] 28 Jan 2011

# CP violation and FCNC in a warped $A_4$ flavor model

**Avihay Kadosh**[a] **and Elisabetta Pallante**[a]

[a] *Centre for Theoretical Physics, University of Groningen, 9747 AG, Netherlands*
`a.kadosh@rug.nl, e.pallante@rug.nl`

## Abstract

We recently proposed a spontaneous $A_4$ flavor symmetry breaking scheme implemented in a warped extra dimensional setup to explain the observed pattern of quark and lepton masses and mixings. The quark mixing is induced by bulk $A_4$ flavons mediating "cross-brane" interactions and a "cross-talk" between the quark and neutrino sectors. In this work we explore the phenomenology of RS-$A_4$ and systematically obtain bounds on the Kaluza-Klein mass scale implied by flavor changing neutral current (FCNC) processes. In particular, we study the constraints arising from $Re(\epsilon'/\epsilon_K)$, $b \to s\gamma$, the neutron EDM and Higgs mediated FCNCs, while the tree level contribution to $\epsilon_K$ through a KK gluon exchange vanishes. We find an overall lower bound on the Kaluza-Klein mass scale $M_{KK} \gtrsim 1.3$ TeV from FCNCs, induced by $b \to s\gamma$ differently from flavor anarchic models. This bound is still weaker than the bound $M_{KK} \gtrsim 4.6$ TeV induced by $Zb_L\bar{b}_L$ in RS-$A_4$. The little CP problem, related to the largely enhanced new physics contributions to the neutron EDM in flavor anarchic models, is absent. The subtleties of having the Higgs and flavons in the bulk are taken into account and final predictions are derived in the complete three-generation case.

# 1 Introduction

In a recent paper [1] we have proposed a model based on a bulk $\mathrm{A}_4$ flavor symmetry [2] in warped geometry [3], in an attempt to describe masses and mixing patterns of Standard Model (SM) quarks and leptons. As in previous models based on $\mathrm{A}_4$ [4], the three generations of left-handed quarks transform as triplets of $\mathrm{A}_4$; this assignment forbids tree level gauge mediated FCNCs and allows to obtain realistic masses and almost realistic mixing angles in the quark sector. The scalar sector of the RS-$\mathrm{A}_4$ model contains two bulk flavon fields, in addition to a bulk Higgs field. The bulk flavons transform as triplets of $\mathrm{A}_4$, and allow for a complete "cross-talk" [5] between the $\mathrm{A}_4 \to Z_2$ spontaneous symmetry breaking (SSB) pattern associated with the heavy neutrino sector – with scalar mediator peaked towards the UV brane – and the $\mathrm{A}_4 \to Z_3$ SSB pattern associated with the quark and charged lepton sectors – with scalar mediator peaked towards the IR brane. A bulk custodial symmetry, broken differently at the two branes [6], guarantees the suppression of large contributions to electroweak precision observables [7], such as the Peskin-Takeuchi $S, T$ parameters. However, the mixing between zero modes of the 5D theory and their Kaluza-Klein (KK) excitations – after 4D reduction – may still cause significant new physics (NP) contributions to SM suppressed flavor changing neutral current (FCNC) processes.

In the most general case, without imposing any additional flavor symmetry and assuming anarchical 5D Yukawa couplings, new physics contributions can already be generated at tree level through a KK gauge boson exchange. Even if a RS-GIM suppression mechanism [8, 9] is at work, stringent constraints on the KK scale come from the $K^0 - \overline{K^0}$ oscillation parameter $\epsilon_K$ and the radiative decays $b \to s(d)\gamma$ [10, 15], the direct CP violation parameter $\epsilon'/\epsilon_K$ [16], and especially the neutron electric dipole moment [10], where a KK mass of $\mathcal{O}(3$ TeV) gives rise to a NP contribution which is roughly forty times larger than the current experimental bound – a CP problem in itself, referred to as little CP problem. The bounds become increasingly stringent by IR localizing the Higgs field.

Conclusions may differ if a flavor pattern of the Yukawa couplings is assumed to hold in the 5D theory due to bulk flavor symmetries. They typically imply an increased alignment between the 4D fermion mass matrix and the Yukawa and gauge couplings, thus suppressing the amount of flavor violation induced by the interactions with KK states. One example that removes or suppresses all tree level contributions is the generalization to 5D of minimal flavor violation in the quark sector [11] and in the lepton sector [12, 13]. In these settings, the bulk mass matrices are aligned with the 5D Yukawa matrices as a result of a bulk $[U(3)]^6$ flavor symmetry that is broken in a controlled manner. In [14] a shining mechanism is proposed, where the suppression of flavor violation in the effective 4D theory on the IR brane is obtained by confining the sources of flavor violation to the UV brane, and communicating its effects through gauge bosons of the gauged bulk flavor symmetry.

In our case, the most relevant consequence of imposing an $\mathrm{A}_4$ flavor symmetry is the degeneracy of the left-handed fermion bulk profiles $f_Q$, i.e. $diag(f_{Q_1,Q_2,Q_3}) = f_Q \times \mathbb{1}$. In addition, the distribution of phases, CKM and Majorana-like, in the mixing matrices might induce zeros in the imaginary components of the Wilson coefficients contributing to CP violating quantities. In [1] we already observed a few consequences of the $\mathrm{A}_4$ flavor symmetry. First, the new physics contribution to $\epsilon_K$ coming from a KK gluon exchange at tree level vanishes [1], thus relaxing the most stringent bound on the KK scale induced by $\epsilon_K$ in flavor anarchic models [16]. This leaves $b \to s(d)\gamma$, $\epsilon'/\epsilon_K$, the neutron EDM and Higgs mediated FCNCs as possible candidates to produce the most stringent lower bounds on the KK scale. In addition, a milder lower bound from the EDM and $\epsilon'/\epsilon_K$ should be expected in our model due to the vanishing of down-type dipole contributions in the naive spurion analysis and mass insertion approximation. It should also be interesting to compare this pattern to the case of larger realizations of the flavor symmetry, like $T'$ [17], usually associated with a rather richer flavon sector.

In this paper we analyze the above processes, $b \to s(d)\gamma$, $\epsilon'/\epsilon_K$, the neutron EDM and Higgs mediated FCNC (HMFCNC) processes [18, 19], in the context of RS-$\mathrm{A}_4$. Differently from flavor anarchy, it is particularly relevant in this case to properly describe the flavor pattern of Yukawa interactions and the mixing among generations. For this reason, we predict all quantities at various levels of approximation, starting with the generalization of the spurion analysis in the mass insertion approximation to include bulk effects parameterized by overlap factors. The latter quantities measure the deviation from the case of a IR localized Higgs. We then proceed beyond the mass insertion approximation, for each generation separately: this means that KK mass eigenstates for each separate generation are obtained by disregarding generational mixing, while the latter is approximately described by the flavor structure of the spurion analysis. Finally, we compare with the *exact* three-generation case, where all contributions are obtained in terms of the KK mass eigenstates, after the complete mass matrix for the zero modes and KK modes is diagonalized numerically, or by means of an approximate analytical procedure.

The paper is organized as follows. In Sec. 2 we recall the important components of the RS-$\mathrm{A}_4$ model proposed in [1], focusing on the Yukawa sector of the theory. In Sec. 3 we derive new physics contributions to the Wilson coefficients of magnetic and chromo-magnetic dipole operators, relevant for the estimate of the neutron EDM, $b \to s\gamma$ and $Re(\epsilon'/\epsilon_K)$. In particular, we describe the various degrees of approximation, in which the KK mixing within each generation and the mixing among generations can be incorporated. The analysis is then performed separately for each observable in Sec. 5 and predictions are studied by varying the model input parameters. Sec. 6 describes Higgs mediated FCNC processes. We conclude in Sec. 7. A few appendices are included. The overlap factors are defined and computed in Appendix A. Appendix B contains details of the diagonalization of the KK mass matrices in the one-generation approximation and for three-generations.

## 2 Quark sector of the $\mathrm{A}_4$ warped model

We start by reviewing some useful results and definitions for the quark sector in RS-$\mathrm{A}_4$. In this model [1] we adopt a custodial RS setup without an additional $P_{LR}$ symmetry [21]. We then assign the three generations of left-handed fermion weak doublets to triplets of the discrete non-abelian flavor symmetry, $\mathrm{A}_4$. The right-handed charged fermions are assigned to the 3 distinct one-dimensional representations of $A_4$. The SSB pattern $A_4 \to$ *nothing* is driven by the VEVs of two flavons $\Phi$ and $\chi$, which are assigned to be triplets of $A_4$ peaked towards the IR and UV branes, respectively, and it is responsible for the generation of fermion masses and mixings in good agreement with the experimental results [20].

## 2.1 The 4D Yukawa Lagrangian

Since the Higgs field and the $A_4$ flavons $\Phi$ and $\chi$ live in the bulk, it will be instructive to generalize [16] and write the 4D Yukawa lagrangian in terms of overlap correction factors $r$'s, which quantify the deviation from the IR localized case. All overlap factors, defined as the ratio between the bulk wave function overlaps and the approximate coupling on the IR brane, are derived in Appendix A.

The leading order (LO) 4D Yukawa lagrangian, generated by the LO 5D and $A_4$-invariant Yukawa lagrangian in [1], and including all the effective interactions in the KK tower, carries similar structure in the up- and down-quark sector. In particular, the leading order interactions with the neutral Higgs can be written as follows

$$\begin{aligned}\mathcal{L}^{4D} \supset\ & \hat{Y}^{u,d}_{ij} h^{(*)}_{0(4D)} \Big[ \psi^{0\dagger}_{Q_i} f^{-1}_{Q_i} \psi^{0}_{u_j,d_j} f^{-1}_{u_j,d_j} r^{H\Phi}_{00}(c_{Q_i}, c_{u_j,d_j}, \beta) + \textstyle\sum_n \psi^{0\dagger}_{Q_i} f^{-1}_{Q_i} \psi^{n}_{u_j,d_j} r^{H\Phi}_{0n}(c_{Q_i}, c_{u_j,d_j}, \beta) \\ & + \textstyle\sum_n \psi^{0\dagger}_{Q_i} f^{-1}_{Q_i} \psi^{n^{-+}}_{u_j,d_j} r^{H\Phi}_{0n^{-+}}(c_{Q_i}, c_{d_j,u_j}, \beta) + \textstyle\sum_n \psi^{n\dagger}_{Q_i} \psi^{0}_{u_j,d_j} f^{-1}_{u_j,d_j} r^{H\Phi}_{n0}(c_{Q_i}, c_{u_j,d_j}, \beta) \\ & + \textstyle\sum_{n,m} \psi^{n\dagger}_{Q_i} \psi^{m}_{u_j,d_j} r^{H\Phi}_{nm}(c_{Q_i}, c_{u_j,d_j}, \beta) + \textstyle\sum_{n,m} \psi^{n^{--}}_{Q_i} (\psi^{m^{--}}_{u_j,d_j})^\dagger r^{H\Phi}_{n^- m^-}(c_{Q_i}, c_{u_j,d_j}, \beta) \\ & + \textstyle\sum_{n,m} \psi^{n\dagger}_{Q_i} \psi^{m^{-+}}_{u_j,d_j} r^{H\Phi}_{nm^{-+}}(c_{Q_i}, c_{d_j,u_j}, \beta) + \textstyle\sum_{n,m} \psi^{n^{--}}_{Q_i} (\psi^{m^{+-}}_{u_j,d_j})^\dagger r^{H\Phi}_{n^- m^{+-}}(c_{Q_i}, c_{d_j,u_j}, \beta) \Big] ,\end{aligned} \tag{1}$$

where $h^{(*)}_{0(4D)}$ couples to the down (up) sector, corresponding to the first (second) label in $c_{q_i,q'_i}$, and $f_{Q_i,u_i,d_i} = \sqrt{2k}/\hat{\chi}_{0_{Q_i,u_i,d_i}}$, with $\hat{\chi}_{0_{Q_i,u_i,d_i}}$ the canonically normalized zero mode profile of the corresponding fermion at the IR brane – see Appendix A. With the same convention, all KK wave functions on the IR brane are approximately equal to $\sqrt{2k}$. The $\psi$'s denote the 4D wave functions of the fermion fields in the KK tower. The boundary condition (BC) for each KK mode is also specified. Unless stated otherwise, the BC are of the type (++) on the UV and IR brane, respectively. A single (−) in the overlap subscript stands for (−−), and all other BC are fully specified. In the custodial case, each fermion zero mode, with (++) boundary conditions, is accompanied by three first level KK modes, with (++), (−−) and (+−) (or (−+)) boundary conditions. The quantities $r^{H\Phi}_{nm}$ are the overlap correction factors for the states $n$ and $m$ calculated in appendix A. They are functions of the left-handed (LH) fermion bulk mass parameters $c_{Q_i}$, the right-handed (RH) ones $c_{d_i,u_i}$ and the scalar bulk mass parameter $\beta$ (see appendix A). The Higgs field transforms as a bidoublet under $SU(2)_L \times SU(2)_R$, but contains only two degrees of freedom, $h_0$ and $h_+$

$$\mathcal{H} = \begin{pmatrix} H & \tilde{H} \end{pmatrix} = \begin{pmatrix} h_0^* & h_+ \\ -h_+^* & h_0 \end{pmatrix} \qquad h_0(x,y) = v_H(\beta_H, y) + \sum_n h_0^{(n)}(x)\phi_n(y) . \tag{2}$$

The profile of the Higgs VEV along the fifth dimension (see also [22]) is

$$v_H = H_0 e^{(2+\beta_H)k(|y|-\pi R)}\,, \tag{3}$$

with $\beta_H = \sqrt{4+\mu_H^2}$, and $\mu_H$ the bulk mass of the 5D Higgs field in units of the $AdS_5$ curvature scale $k \approx M_{Pl}$. As in [1], we assume $\beta_H \simeq 2$, which yields $H_0 \simeq 0.39 M_{Pl}^{3/2}$, for $k\pi R \simeq 34.8$ and matching with the measured $W$ boson mass. In addition, the profile of the physical higgs $h_0^{(1)}(y)$ is almost identical to the VEV profile for $m_h << M_{KK}$. The VEV profile for the A$_4$ flavon $\Phi$, peaked towards the IR brane, is of similar structure to the one of the Higgs, with $\beta_\phi \simeq 2$ and $\Phi_0 \simeq 0.577 M_{Pl}^{3/2}$. The VEV profile of the UV peaked A$_4$ flavon, $\chi$, will only enter through the subdominant Yukawa interactions and is approximately

$$v_\chi = \chi_0 e^{(2-\beta_\chi)k|y|}(1 - e^{(2\beta_\chi)k(|y|-\pi R)}), \tag{4}$$

with $\beta_\chi \simeq 2$ and $\chi_0 \simeq 0.155 M_{Pl}^{3/2}$. The leading order 5D and A$_4$-invariant Yukawa lagrangian in [1], consisting of operators of the form $(y_{u_i,d_i,e_i}/M_{Pl}^2)\bar{Q}_L(\bar{L}_L)\Phi H u_{R_i}(d_{R_i}, e_{R_i})$, was shown to induce the same pattern of masses and mixings in the up, down and charged lepton sectors. After spontaneous symmetry breaking of A$_4$, by the VEVs of the $\Phi$ triplet, the leading order 4D Yukawa matrices in these sectors take the form

$$(\hat{Y}_{ij}^{u,d,e})_{LO} = \frac{2v_\Phi^{4D} e^{k\pi R}}{k} \begin{pmatrix} y_{u,d,e} & y_{c,s,\mu} & y_{t,b,\tau} \\ y_{u,d,e} & \omega y_{c,s,\mu} & \omega^2 y_{t,b,\tau} \\ y_{u,d,e} & \omega^2 y_{c,s,\mu} & \omega y_{t,b,\tau} \end{pmatrix} \equiv \frac{2v_\Phi^{4D} e^{k\pi R}}{k} (\hat{y}_{ij}^{u,d,e})_{LO}\,, \tag{5}$$

where $y_{u,d,e}$ are the dimensionless 5D Yukawa couplings and $\omega = e^{2\pi i/3}$. The parameter $v_\Phi^{4D}$ denotes the 4D VEV of $\Phi$ in the IR localized case, and it is given by $\Phi_0 \simeq \sqrt{2k\,(1+\beta_\Phi)} v_\Phi^{4D} e^{k\pi R}$, up to exponentially suppressed contributions – see Appendix A for its exact expression. Notice that, differently from the flavor anarchic case, the overlap factors in Eq. (1) are now functions of the VEV profiles of all scalar fields, $H$ and $\Phi$ at leading order, with $\beta = \beta_H + \beta_\Phi$. The other crucial ingredient of the RS-A$_4$ model is the degeneracy of the LH fermion bulk mass parameters, since the corresponding fermions are unified in triplets of A$_4$; consequently $f_{Q_i} \equiv f_Q$ and $\hat{\chi}_{0_{Q_i}} \equiv \hat{\chi}_{0_Q}$ in Eq. (1).

The Yukawa texture in Eq. (5) was shown [1] to induce the same left-diagonalization matrix

$$V_L^{u,d,e} = U(\omega) = \frac{1}{\sqrt{3}} \begin{pmatrix} 1 & 1 & 1 \\ 1 & \omega & \omega^2 \\ 1 & \omega^2 & \omega \end{pmatrix} \tag{6}$$

for all charged fermions and in particular for the zero modes, identified with the SM fermion content. At leading order, the right diagonalization matrix for all charged fermions is simply the identity. This pattern of the diagonalization matrices, independent of the leading order 5D Yukawa couplings, will be shown not to induce any of the flavor violating interactions we wish to inspect.

The deviation from unity of the CKM matrix, and thus quark mixing, is induced by cross-talk effects [5] in RS-A$_4$ [1]. They mediate between the IR and UV branes and between the

SSB patterns of the neutrino and quark sectors, in the form of higher dimensional operators $(1/M_{Pl}^{7/2})\,\bar{Q}_L\Phi\chi H(u_R, u'_R, u''_R, d_R, d'_R, d''_R)$ and breaking completely the A$_4$ flavor symmetry. Each of these operators turned out to yield two independent contributions to the up- and down-quark mass matrices, for which we label the dimensionless 5D coefficients as $\tilde{x}_i^{u,d}$ and $\tilde{y}_i^{u,d}$. Since the leading order diagonalization matrices are independent of the corresponding Yukawa couplings, the perturbed diagonalization matrices are governed by $\tilde{x}_i^{u,d}$, $\tilde{y}_i^{u,d}$ only. Although we need a specific assignment of these parameters to match the CKM matrix while maintaining the magnitude of all parameters naturally of order one, we will explore the full parameter space of the model to account for the largest possible contributions of new physics to FCNC processes. They will provide the most stringent constraints on the KK mass scale in the RS-A$_4$ setup. The 4D Yukawa matrix induced by the above higher order effects can thus be parameterized as follows

$$(\hat{Y}_{ij}^{u,d})_{NLO} = \frac{2v_\Phi^{4D}v_\chi^{4D}e^{2k\pi R}}{k^2}\begin{pmatrix} \tilde{x}_1^{u,d} & \tilde{x}_2^{u,d} & \tilde{x}_3^{u,d} \\ 0 & 0 & 0 \\ \tilde{y}_1^{u,d} & \tilde{y}_2^{u,d} & \tilde{y}_3^{u,d} \end{pmatrix} \equiv \frac{2v_\Phi^{4D}v_\chi^{4D}e^{2k\pi R}}{k^2}(\hat{y}_{ij}^{u,d})_{NLO}\,. \tag{7}$$

This time the VEV profile of the UV peaked flavon field $\chi$ will also enter all the corresponding overlap correction factors, leading to the NLO 4D lagrangian analogous to Eq. (1), with overlaps $r_{nm}^{H\Phi\chi}$ as defined in appendix A. The modified left- and right-diagonalization matrices for the up and down mass matrix have a simple structure, up to and including linear terms in $\tilde{x}_i^{u,d}$, $\tilde{y}_i^{u,d}$ and working in the zero mode approximation (ZMA)[1]. The left-handed matrix is given by

$$V_L^q = U(\omega)\begin{pmatrix} 1 & f_\chi^{q_2}(\tilde{x}_2^q+\tilde{y}_2^q) & f_\chi^{q_3}(\tilde{x}_3^q+\tilde{y}_3^q) \\ -f_\chi^{q_2}[(\tilde{x}_2^q)^*+(\tilde{y}_2^q)^*] & 1 & f_\chi^{q_3}(\tilde{x}_3^q+\omega\tilde{y}_3^q) \\ -f_\chi^{q_3}[(\tilde{x}_3^q)^*+(\tilde{y}_3^q)^*] & -f_\chi^{q_3}[(\tilde{x}_3^q)^*+\omega^2(\tilde{y}_3^q)^*] & 1 \end{pmatrix}, \tag{8}$$

with $q = u, d$ and $f_\chi^{q_i} = 4C_\chi/(12 - c_q^L - c_{q_i})$, with $C_\chi = \chi_0/k^{3/2} \simeq 0.155$ and $\omega = e^{2\pi i/3}$. In [1], we assigned the degenerate left-handed bulk parameter $c_q^L = 0.4$, and the right-handed parameters $c_u = 0.78$, $c_d = 0.76$, $c_s = 0.683$, $c_c = 0.606$, $c_b = 0.557$ and $c_t = -0.17$, to yield the physical running quark masses at the KK scale of 1.8 TeV and satisfy the stringent constraints coming from $Zb_L\bar{b}_L$. The CKM matrix elements to first order in $f_\chi^{q_i}(\tilde{x}_i^{u,d}, \tilde{y}_i^{u,d})$ are easily obtained from $V_{CKM} = (V_L^u)^\dagger V_L^d$, leading to

$$V_{us} = -V_{cd}^* \simeq \left((\tilde{x}_2^d+\tilde{y}_2^d)f_\chi^s - (\tilde{x}_2^u+\tilde{y}_2^u)f_\chi^c\right), \tag{9}$$

$$V_{cb} = -V_{ts}^* \simeq \left((\tilde{x}_3^d+\omega\tilde{y}_3^d)f_\chi^b - (\tilde{x}_3^u+\omega\tilde{y}_3^u)f_\chi^t\right), \tag{10}$$

$$V_{ub} = -V_{td}^* \simeq \left((\tilde{x}_3^d+\tilde{y}_3^d)f_\chi^b - (\tilde{x}_3^u+\tilde{y}_3^u)f_\chi^t\right). \tag{11}$$

An almost realistic CKM matrix can be obtained with minimal deviations from the universality assumption that all magnitudes of $\tilde{x}_i^{u,d}$, $\tilde{y}_i^{u,d}$ are of $\mathcal{O}(1)$; in particular

$$\tilde{x}_2^u = \tilde{y}_2^u = -\tilde{x}_2^d = -\tilde{y}_2^d = e^{i\delta_2^u}\,,\quad \tilde{x}_3^u \simeq 0.67 - 0.19i\,,\quad \tilde{y}_3^d \simeq 0.59 - 0.23i\,. \tag{12}$$

Considering the global fit of the parameters of the Wolfenstein parametrization [20], we can obtain real $V_{us}$ and consequently real $V_{cd}$ with the choices $\delta_2^u = 0, \pi$. All other $\tilde{x}_i^{u,d}$, $\tilde{y}_i^{u,d}$ parameters are simply set to unity, as explained in [1]. The CKM matrix obtained by this choice has $|V_{us}| = |V_{cd}| = 0.2257$, $|V_{cb}| = |V_{ts}| = 0.0415$, $|V_{ub}| = |V_{td}| = 0.00359$ and $V_{ii} = 1$. The phase of $V_{ub}$ is matched by the same assignments to its experimental value, $\delta \simeq 1.2$, while the other off-diagonal elements are real. This provides an almost realistic CKM matrix. The main deviation from the global fit [20] amounts to the difference in magnitude of $V_{ub}$ and $V_{td}$. In addition, one still has to account for the $\mathcal{O}(\lambda_{CKM}^2)$ deviations from unity of the diagonal elements and match the phases of the CKM elements to the 9 constraints implied by the Jarlskog invariant. All deviations have to come from higher order corrections in the RS-A$_4$ model, rendering the corresponding parameter assignments less appealing.

The right diagonalization matrices do not enter the CKM matrix, however, they are crucial in the evaluation of the Wilson coefficients contributing to the FCNC processes we are interested in. To first order in $f_\chi^{q_i}(\tilde{x}_i^{u,d}, \tilde{y}_i^{u,d})$ one obtains

$$V_R^q = \begin{pmatrix} 1 & \Delta_1^q & \Delta_2^q \\ -(\Delta_1^q)^* & 1 & \Delta_3^q \\ -(\Delta_2^q)^* & -(\Delta_3^q)^* & 1 \end{pmatrix}, \tag{13}$$

where $q = u, d$ and the $\Delta_i^q$ are given by:

$$\Delta_1^q = \frac{m_{q_1}}{m_{q_2}} \left[ f_\chi^{q_1} \left( (\tilde{x}_1^q)^* + \omega^2 (\tilde{y}_1^q)^* \right) + f_\chi^{q_2} \left( \tilde{x}_2^q + \tilde{y}_2^q \right) \right], \tag{14}$$

$$\Delta_2^q = \frac{m_{q_1}}{m_{q_3}} \left[ f_\chi^{q_1} \left( (\tilde{x}_1^q)^* + \omega (\tilde{y}_1^q)^* \right) + f_\chi^{q_3} \left( \tilde{x}_3^q + \tilde{y}_3^q \right) \right], \tag{15}$$

$$\Delta_3^q = \frac{m_{q_2}}{m_{q_3}} \left[ f_\chi^{q_2} \left( (\tilde{x}_2^q)^* + \omega (\tilde{y}_2^q)^* \right) + f_\chi^{q_3} \left( \tilde{x}_3^q + \omega \tilde{y}_3^q \right) \right]. \tag{16}$$

The suppression by quark mass ratios of the off-diagonal elements in $V_R^{u,d}$ will turn out to play an important role in relaxing the flavor violation bounds on the KK mass scale, as compared to flavor anarchic frameworks.

## 2.2 Parameter counting and physical phases

In order to estimate the new physics contributions associated with the imaginary parts of amplitudes, we need to know how many real and imaginary physical parameters are in our model. We start with the 6 leading order Yukawa couplings $y_{q_i}$ and the 12 $\tilde{x}_i^q$ and $\tilde{y}_i^q$ couplings of the cross-talk operators, $\bar{Q}_L \Phi \chi H (u_R, u_R', u_R'', d_R, d_R', d_R'')$. Besides the Yukawas, we have 6 real and 3 imaginary parameters in the spurions $F_{u,d} = diag(f_{u_j,d_j}^{-1})$, and 1 real parameter $F_Q = f_Q^{-1} \mathbb{1}$. Hence, in total, we have 31 real and 24 imaginary parameters in the most general case.

We now consider the flavor symmetry breaking pattern before the SSB of A$_4$, $U(3)_Q \times U(3)_u \times U(3)_d \longrightarrow A_4$, induced by the leading order Yukawa lagrangian and the cross-talk operators in charge of quark mixing. We realize that we can eliminate 17 phases – the baryon number should still be conserved – and 6 real parameters. This leaves us with 25 physical real parameters, that is the 12 mixing angles in $V_{L,R}^{u,d}$, 6 quark masses and the 7 eigenvalues of $F_{Q,u,d}$. In the imaginary sector, we are left with 7 phases, 4 of which are CKM-like phases, one in each of the $V_{L,R}^{u,d}$ matrices, while the other 3 are Majorana-like phases which can be rotated between the left and right diagonalization matrices of both the up and down sectors. We should take these phases into account when evaluating the imaginary parts of amplitudes and we will do so by parametrizing the phase of each element of $V_{L,R}^{u,d}$ in terms of phases of the parameters $\tilde{x}_i^{u,d}$ and $\tilde{y}_i^{u,d}$, which govern the structure of the diagonalization matrices.

# 3 Dipole Operators and helicity flipping FCNCs

FCNC processes are known to provide among the stringest constraints for physics beyond the standard model. This is also the case for flavor anarchic models in warped extra dimensions [10, 15, 16]. In the quark sector, significant bounds on the KK mass scale may typically come from the neutron electric dipole moment (EDM), the CP violation parameters $\epsilon_K$ and $Re(\epsilon'/\epsilon_K)$, and radiative $B$ decays such as $b \to s\gamma$. All these processes are mediated by effective dipole operators. It is also well known [23] that SM interactions only induce, to leading order, the dipole operators $O_{7\gamma}$ and $O_{8g}$

$$O_{7\gamma(8g)} = \bar{d}_R^i \sigma^{\mu\nu} d_L^j F_{\mu\nu}(G_{\mu\nu}), \tag{17}$$

where $F_{\mu\nu}$ and $G_{\mu\nu}$ are the field strength of the electromagnetic and chromomagnetic interactions and $i, j$ are flavor indices. For $i > j$, as $\bar{b}_R \sigma^{\mu\nu} F_{\mu\nu} s$, the SM contribution to the Wilson coefficients of the opposite chirality operators $O'_{7\gamma,8g}$ is suppressed by the corresponding quark mass ratio, and thus negligible. This might turn out to be a unique feature of the SM not shared by NP contributions. It is therefore instructive to study new physics contributions of any flavor model to the operators $O_{7\gamma,8g}$ and to the opposite chirality operators, $O'_{7\gamma,8g}$, and compare with experimental results. In the following we show that, differently from flavor anarchic models, the RS-A$_4$ model shares the SM features, with no enhancement of the opposite chirality operators.

## 3.1 Flavor structure of Dipole operators

The new physics contributions to the FCNC processes we are interested in are generated at one-loop by the Yukawa interactions between SM fermions and their KK excitations, leading to the diagrams shown in Fig. 1 and Fig. 2. To obtain the flavor structure for the Wilson coefficients of the corresponding dipole operators we first recall the spurion analysis in the mass insertion approximation of [10], corresponding to the IR localized Higgs case. The contributions associated with internal KK down quarks in the special interaction basis[1] can

---

[1] The basis in which $F_{Q,u,d}$ are real and diagonal is referred to as the special interaction basis in [10] and the rest of this paper.

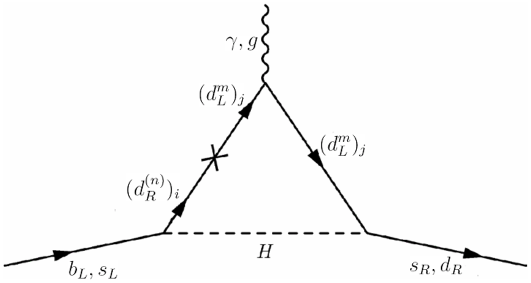

Figure 1: One-loop down-type (neutral Higgs) contribution to $b \to s\gamma$, $\epsilon'/\epsilon_K$ and the neutron EDM (for external $d$ quarks). The analogous one-loop up-type contribution (charged Higgs) contains internal up-type KK modes.

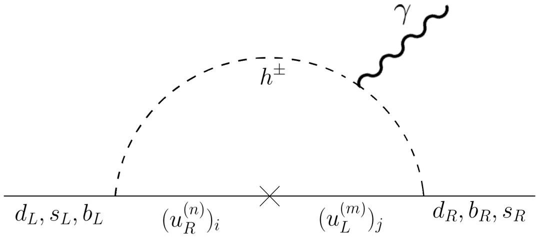

Figure 2: Charged Higgs one-loop contribution to $b \to s\gamma$ and the neutron EDM. The latter has external $d$ quarks.

be written as

$$(C^{d-type}_{7\gamma(8g)})_{ij} = A^{1L}\frac{v}{M_{KK}}\left(F_Q\,\hat{Y}_d\hat{Y}_d^{\dagger}\hat{Y}_d\,F_d\right)_{ij}\,, \tag{18}$$

where $v \equiv v_H^{4D} = 174$ GeV denotes the Higgs VEV, $\hat{Y}_d$ the 5D Yukawa matrices and the fermion profile matrices are $F_{Q,u,d} = diag(f^{-1}_{Q_i,u_j,d_j})$ – see also appendix A. Finally, the factor $A^{1L} = 1/(64\pi^2 M_{KK})$ comes from the one-loop integral for the diagram in Fig. 1[2] and the factor $v/M_{KK}$ comes from the mass insertion approximation. The contributions associated with internal up-type KK quarks (and a charged Higgs) in Fig. 1 will analogously be given by:

$$(C^{u-type}_{7\gamma(8g)})_{ij} = A^{1L}\frac{v}{M_{KK}}\left(F_Q\,\hat{Y}_u\hat{Y}_u^{\dagger}\hat{Y}_d\,F_d\right)_{ij}\,, \tag{19}$$

written again in the special interaction basis. The neutron EDM and $b \to s\gamma$ receive an additional up-type contribution from the diagram in Fig. 2, which carries the same flavor (and overlap) structure of the up-type diagram in Fig. 1 and a one-loop amplitude that differs by a sign to a very good approximation[3]. Hence, the total up-type contribution is obtained by replacing $A^{1L}$ with

$$(\tilde{A}^{1L}_u) = A^{1L}Q_u + A^{1L}_{H\gamma}Q_{h-} = A^{1L}(\frac{2}{3}+1) = \frac{5}{3}\frac{1}{64\pi^2 M_{KK}}, \tag{20}$$

where $Q_u$ and $Q_{h-}$ are the electric charges of an up-type quark and the negatively charged Higgs, respectively.

Thus far we have not considered the modifications of the above spurion structures due to the overlap of internal KK quarks, external fermion zero modes, and bulk scalar fields $\Phi$, $\chi$ and Higgs field, encoded in the various $r_{nm}$ factors in Eq. (1). Since the bulk nature of all

---

[2] Notice that we assumed degenerate KK masses with common mass $M_{KK}$ and the result is valid in the limit $m_H \ll M_{KK}$. We also disregard subdominant W/Z mediated diagrams.

[3] Neglected contributions are suppressed by mass ratios $m_{d_i}/M_{KK}$, see [15] for a derivation of those terms.

5D fields is an essential feature of our model, the effect of all overlaps should be taken into account. In the following section we derive the analogous of Eqs. (18) and (19), corrected by the overlap factors in our model. Subsequently, we show that conservatively reducing the overlap corrections to an overall multiplicative factor will suffice for a conservative estimate of most of the flavor violation bounds on the KK scale in our model, and it will be instructive for the comparison with other flavor scenarios and in particular warped flavor anarchic models.

### 3.2 The spurion-overlap approximation

Observing the Yukawa Lagrangian of Eq. (1), we realize that the spurion analysis in the mass insertion approximation can only directly account for the interactions (and related overlaps) associated with (++) KK modes or a combination of (−+) and (++) KK modes as internal states in the Feynman diagrams of Figs. 1 and 2. However, since the first KK masses of each fermion are nearly degenerate (see appendix B), they almost maximally mix. Therefore, we expect that the contributions of the three distinct KK modes of each given fermion, can be estimated to a good approximation by only considering the modes directly entering the spurion analysis. The corresponding overlap correction factors now enter in the spurion structures of Eqs. (18) and (19) to yield in the special interaction basis

$$\begin{aligned}(C_7^{d,u})_{(++)} &\propto F_Q \hat{Y}_{d,u}\, r_{01}(c_{Q_i}, c_{d_{\ell_1},u_{\ell_1}}, \beta)\, \hat{Y}^\dagger_{d,u}\, r_{11}(c_{d_{\ell_1},u_{\ell_1}}, c_{Q_{\ell_2}}, \beta)\, \hat{Y}_{d,d}\, r_{10}(c_{Q_{\ell_2}}, c_{d_j,d_j}) F_d\,,\\ (C_7^{d,u})_{(-+)} &\propto F_Q \hat{Y}_{u,d}\, r_{01-+}(c_{Q_i}, c_{u_{\ell_1},d_{\ell_1}}, \beta)\, \hat{Y}^\dagger_{u,d}\, r_{1-+1}(c_{u_{\ell_1},d_{\ell_1}}, c_{Q_{\ell_2}}, \beta)\, \hat{Y}_{d,d}\, r_{10}(c_{Q_{\ell_2}}, c_{d_j,d_j}, \beta) F_d\,,\end{aligned} \tag{21}$$

where $\beta = \beta_H + \beta_\Phi$ and $\ell_i$, $i$ and $j$ are flavor indices. Notice that we have omitted the flavor independent prefactor $vA^{1L}/M_{KK}$ to ease the notation. From Eq. (1) and Fig. 1, it is clear that the 4D Yukawa matrices $\hat{Y}$ carry the same flavor indices as the adjacent overlap correction factors. Notice also that the $c_{u_j,d_j}$ dependence of the (−+) overlaps is opposite to the one of the (++) ones. This is not surprising since they arise from the Yukawa interactions with $\tilde{u}_i$ and $\tilde{d}_i$, the first (and higher) level KK excitations of the $SU(2)_R$ partners of $d_{R_i}$ and $u_{R_i}$, respectively.

In this context it is important to mention the work of [16], based on the method developed in [15], which involves the direct diagonalization of the zero modes and first KK modes mass matrix; the latter is a 4×4 matrix for a single generation in our case, and it reduces to a 3×3 matrix when no custodial symmetry is imposed. The interesting result in flavor anarchic models for the one generation case, and to a good approximation for the three generation case, is that the most dominant contributions, in terms of the perturbative parameter $x = vY/M_{KK}$ with generic Yukawa $Y$, solely arise from the (−−) modes. Namely, the dominant contribution turns out to be proportional to the overlap structure $r_{01}r_{1-1-}r_{10}$, and it is not accounted for in the naive spurion analysis. This shows the limits of the spurion analysis in the mass insertion approximation and the need to *a priori* account for the mixing between all KK modes of the same generation, in addition to their intergenerational mixing. This is especially important in the RS-A$_4$ setup, where custodial symmetry also induces an extra degree of freedom for each "RH" 5D fermion.

Nevertheless, because of the relative smallness of $r_{1-1-}$ compared to $r_{11}$ and $r_{11-+}$ in our setup (see appendix A.1), the accuracy of the spurion-overlap approximation is still satisfactory for the purpose of imposing constraints on the KK mass scale and the physical Higgs mass, as long as the corresponding contribution turns out to be non vanishing in this approximation. If vanishing – as it is true for the down type contribution to the neutron EDM [1] – one has to fully account for the flavor structure and mixing of all zero modes and first KK modes in order to provide an estimate of the dominant contributions. This is done in section 4.

## 3.3 Explicit structure of dipole contributions in the spurion-overlap approximation

In this section we analyze in more detail the most general flavor structure of up- and down-type contributions to dipole operators and study the simplifications induced by the RS-A$_4$ setup. We limit the analysis to the first level $n = 1$ KK states, since $n = 2$ states will give rise to $\mathcal{O}(25\%)$ effects and for $n = 3$ and higher the theory is strongly coupled and cannot be treated perturbatively [10]. Inverting the relation $(\hat{m}_{u,d})_{ij} = v\, f_{Q_i}^{-1} \hat{Y}_{ij}^{u,d} f_{u_j,d_j}^{-1} r_{00}(\beta c_{Q_i}, c_{u_j,d_j})$ and rotating the mass matrix (see also Appendix A), we express the Yukawa couplings in terms of the diagonal physical mass matrices

$$\hat{Y}_{ij}^{u(d)} = \frac{1}{v} r_{00}^{-1}(c_{Q_i}, c_{u_j(d_j)}, \beta) \left( F_Q^{-1} V_L^{u(d)} \mathrm{diag}(m_{u,c,t(d,s,b)}) V_R^{u(d)\dagger} F_{u(d)}^{-1} \right)_{ij} . \tag{22}$$

Promoting the overlap corrections to matrices $\hat{r}$ in flavor space, the down-type contributions to the dipole amplitude rotated to the ZMA mass basis can be written as

$$\begin{aligned}
(C_{7\gamma(8g)}^{d-type})_{ij} \;=\; & \frac{A_{1L}}{v^2 M_{KK}} \Big[ (V_L^d)^\dagger_{i\ell} (\hat{r}_{0n}^d)_{\ell\ell_1} (\hat{r}_{00}^d)^{-1}_{\ell\ell_1} \left( V_L^d diag(m_{d,s,b}) (V_R^d)^\dagger \mathrm{diag}(f_{d,s,b}^2) \right)_{\ell\ell_1} \\
& \times (\hat{r}_{nm}^d)_{\ell_2\ell_1} (\hat{r}_{00}^d)^{-1}_{\ell_2\ell_1} \Big( V_R^d diag(m_{d,s,b}) V_L^{d\dagger} diag(f_{Q1,Q2,Q3}^2) \Big)_{\ell_1\ell_2} (\hat{r}_{m0}^d)_{\ell_2\ell_3} \\
& \times (\hat{r}_{00}^d)^{-1}_{\ell_2\ell_3} \left( V_L^d diag(m_{d,s,b}) (V_R^d)^\dagger \right)_{\ell_2\ell_3} (V_R^d)_{\ell_3 j} \Big] ,
\end{aligned} \tag{23}$$

with an implicit sum over all allowed first level KK modes, and where $(\hat{r}_{nm}^{u,d})_{ij} = r_{nm}(c_{Q_i}, c_{u_j,d_j}, \beta)$. In the above equation flavor indices are written explicitly, in order to clarify the exact flavor structure of the overlap matrices. Analogously, we obtain the up-type contributions to dipole operators

$$\begin{aligned}
(C_{7\gamma(8g)}^{u-type})_{ij} \;=\; & \frac{A_{1L}}{v^2 M_{KK}} \Big[ (V_L^d)^\dagger_{i\ell} (\hat{r}_{0n}^u)_{\ell\ell_1} (\hat{r}_{00}^u)^{-1}_{\ell\ell_1} \left( V_L^u diag(m_{u,c,t}) (V_R^u)^\dagger \mathrm{diag}(f_{u,c,t}^2) \right)_{\ell\ell_1} \\
& \times (\hat{r}_{nm}^u)_{\ell_2\ell_1} (\hat{r}_{00}^u)^{-1}_{\ell_2\ell_1} \Big( V_R^u diag(m_{u,c,t}) V_L^{u\dagger} diag(f_{Q1,Q2,Q3}^2) \Big)_{\ell_1\ell_2} (\hat{r}_{m0}^d)_{\ell_2\ell_3} \\
& \times (\hat{r}_{00}^d)^{-1}_{\ell_2\ell_3} \left( V_L^d diag(m_{d,s,b}) (V_R^d)^\dagger \right)_{\ell_2\ell_3} (V_R^d)_{\ell_3 j} \Big] .
\end{aligned} \tag{24}$$

Notice that the IR localized Higgs case can be obtained by simply setting all overlap matrices in Eqs. (23) and (24) to be proportional to the identity matrix. The above equations are valid for generic textures of the Yukawa couplings and patterns of the bulk profiles $c_{Q_i,u_i,d_i}$, rendering the spurion-overlap formulae in Eqs. (23) and (24) directly applicable to generic flavor scenarios.

In the RS-A$_4$ framework, a simplification comes from the degeneracy of left-handed bulk mass parameters, thus $F_Q = diag(f_{Q_i}^{-1}) = f_Q^{-1} \cdot \mathbb{1}$. For the same reason the overlap correction matrices of Eqs. (23) and (24) simplify

$$\begin{aligned} \hat{r}^{u,d}_{00,10,01} &= \mathrm{d}iag(r_{00,10,01}(c^L_q, c_{u_i,d_i}, \beta)) \qquad \hat{r}^{u,d}_{11} = \mathrm{d}iag(r_{11}(c_{u_i,d_i}, c^L_q, \beta)) \\ \hat{r}^{u,d}_{01-+} &= \mathrm{d}iag(r_{01-+}(c^L_q, c_{d_j,u_j}, \beta)) \quad \hat{r}^{u,d}_{1-+1} = \mathrm{d}iag(r_{1-+1}(c_{d_i,u_i}, c^L_q, \beta)). \end{aligned} \tag{25}$$

The resulting structure of the down-type contributions in the mass basis follows straightforwardly

$$\begin{aligned} (C^{d-type}_{7\gamma(8g)})_{ij} &= \frac{m_{d_i} A^{1L} f_Q^2}{v^2 M_{KK}} \Big[ V_R^{d\dagger} \mathrm{d}iag(f^2_{d,s,b}) (\hat{r}^d_{00})^{-1} \tilde{r}^d_{01}\, \tilde{r}^d_{11} (\hat{r}^d_{00})^{-1} V_R^d \,\mathrm{d}iag(m^2_{d,s,b}) \\ &\quad \times V_R^{d\dagger}\, (\hat{r}^d_{00})^{-1} \hat{r}^d_{10}\, V_R^d \,\Big]_{ij}, \end{aligned} \tag{26}$$

where $\tilde{r}^{u,d}_{01} \tilde{r}^{u,d}_{11} = \hat{r}^{u,d}_{01} \hat{r}^{u,d}_{11} + \hat{r}^{u,d}_{01-+} \hat{r}^{u,d}_{1-+1}$ and all overlap matrices are diagonal. Similarly, we obtain the up-type contributions to dipole operators in the mass basis

$$\begin{aligned} (C^{u-type}_{7\gamma(8g)})_{ij} &= \frac{A^{1L} f_Q^2}{v^2 M_{KK}} \Big[ V^\dagger_{CKM} \,\mathrm{d}iag(m_{u,c,t}) V_R^{u\dagger} \mathrm{d}iag(f^2_{u,c,t}) (\hat{r}^u_{00})^{-1}\, \tilde{r}^u_{01} \tilde{r}^u_{11} (\hat{r}^u_{00})^{-1} \\ &\quad \times V_R^u \,\mathrm{d}iag(m_{u,c,t}) V_{CKM} \,\mathrm{d}iag(m_{d,s,b}) V_R^{d\dagger} (\hat{r}^d_{00})^{-1} \hat{r}^d_{10}\, V_R^d \Big]_{ij}\,. \end{aligned} \tag{27}$$

Since all overlap corrections are real and enter through diagonal matrices, the resulting modifications to the IR localized Higgs case are limited, in particular their effect on the imaginary parts relevant for CP violating processes. Qualitatively, this result can be understood from the fact that the new (real valued) overlap correction matrices appear always together with the diagonal $f$'s, with patterns $V^{u,d\dagger}_{L,R} r_1 f_1 r_2 f_2 r_3 V^{u,d}_{L,R}$. Given the structure of $V^{u,d}_{L,R}$ (see Eqs. (8) and (13)), it can be shown that the presence of the $r$'s will have no effect on the cancellation of imaginary parts of diagonal dipole operators to $\mathcal{O}(f_\chi^{u_i,d_i} \tilde{x}_i^{u,d}, f_\chi^{u_i,d_i} \tilde{y}_i^{u,d})$. At the following order, $\mathcal{O}((f_\chi^{u_i,d_i})^2)$, the cancellation pattern of imaginary parts of the diagonal elements of $C_7^{u,d}$ in the IR localized Higgs case will be modified by terms that are suppressed by linear or quadratic quark mass ratios, coming from $V_R^{u,d}$ and proportional to differences between overlap correction factors. We will provide an explicit example in the case of the neutron EDM.

As shown in appendix A.1, the generational flavor dependence of the overlap factors is anyway very small and the largest difference of $\mathcal{O}(5\%)$ is associated with $t_R$ and its $SU(2)_R$ partner $\tilde{b}$. In addition, as will be shown explicitly below, most of the dominant contributions will be proportional to the first generation "inverted" zero mode profiles $f^2_{u,d} \propto (\hat{\chi}^{u,d}_0)^{-2}$, due to the large hierarchy of quark masses. In general, the modifications induced by the slight generational dependence of overlap effects are thus expected to be less significant (numerically) than the ones arising from second order corrections, $\mathcal{O}((f_\chi^{u_i,d_i})^2)$, to the NLO Yukawa matrices, with $f_\chi \approx 0.05$. For this reason, and barring zeros of the amplitudes, one should expect to obtain a fairly conservative estimate of the contributions to the neutron EDM, $\epsilon'/\epsilon$ and $b \to s\gamma$, by parametrizing the effect of the overlap corrections by an overall multiplicative factor for the up- and down-type contributions to the dipole operators. Defining the overall factor $B_P^{u,d}$ as the maximum for each element of the overlap correction matrices

$$B_P^{u,d} = \max\left((\hat{r}_{00}^{u,d})^{-3}(\hat{r}_{01}^{u,d}\hat{r}_{11}^{u,d} + \hat{r}_{01-+}^{u,d}\hat{r}_{1-+1}^{u,d})\,\hat{r}_{10}^{u,d}\right), \tag{28}$$

the down-type contributions reduce to

$$\begin{aligned}(C_{7\gamma(8g)}^{d-type})_{ij} &= \frac{A^{1L} m_{d_i} m_{d_j} B_P^d}{v^2 M_{KK}}\left[V_R^{d\dagger}\mathrm{d}iag(f^2_{d_1,d_2,d_3})V_R^d \mathrm{d}iag(m_{d,s,b})V_L^{d\dagger}\mathrm{d}iag(f^2_{Q_1,Q_2,Q_3})V_L^d\right]_{ij}\\ &= \frac{A^{1L} f_Q^2 m_{d_i} m_{d_j}^2 B_P^d}{v^2 M_{KK}}\sum_{n=1}^{3}(V_R^d)^*_{ni}(V_R^d)_{nj} f^2_{d_n}\,,\end{aligned} \tag{29}$$

while the contributions associated with internal up-type KK quarks have a slightly more complicated structure

$$\begin{aligned}(C_{7\gamma(8g)}^{u-type})_{ij} &= \frac{A^{1L} m_{d_j} B_P^u}{v^2 M_{KK}}\left[V_{CKM}^\dagger \mathrm{d}iag(m_{u,c,t})V_R^{u\dagger}\mathrm{d}iag(f^2_{u_i})V_R^u \mathrm{d}iag(m_{u,c,t})V_L^{u\dagger}\mathrm{d}iag(f^2_{Q_i})V_L^d\right]_{ij}\\ &= \frac{A^{1L} f_Q^2 m_{d_j} B_P^u}{v^2 M_{KK}}\left[V_{CKM}^\dagger \mathrm{d}iag(m_{u,c,t})V_R^{u\dagger}\mathrm{d}iag(f^2_{u_i})V_R^u \mathrm{d}iag(m_{u,c,t})V_{CKM}\right]_{ij}.\end{aligned} \tag{30}$$

It is evident from Eqs. (29) and (30) that, if we restrict ourselves to the LO Yukawa interactions in Eq. (5), we have $V_L^{u,d} = U(\omega)$ and $V_R^{u,d} = \mathbb{1}$. Hence, both up- and down-type NP contributions to $C_{7ij}$ reduce to real diagonal matrices and generate no corrections to the processes we are interested in, as already anticipated in [1]. This situation typically changes when we also consider the NLO Yukawa interactions in Eq. (7) and the corresponding diagonalization matrices in Eqs. (8) and (13). As we said, small additional corrections can also be induced at leading order by the slight generational non degeneracy of overlap factors. In principle, both sources have to be taken into account when estimating deviations from zero of the NP contributions. In practice, the latter source is typically suppressed by roughly an order of magnitude in comparison with the corrections generatd by NLO Yukawa interactions. This can also be inferred from Eqs.(26) and (27), where the terms generated by LO Yukawa interactions in RS-A$_4$ carry through a systematic cancellation pattern of the form $1 + \omega + \omega^2$ between nearly degenerate quadratic functions of the overlap correction factors, which originates from $U(\omega)$.

In the flavor anarchic case, a direct diagonalization of the one generation KK mass matrix, augmented with generational mixing factors derived in the mass insertion approximation, yields reliable predictions due to the lack of structure of the Yukawa couplings and the bulk mass parameters, as shown in [15]. On the other hand, when considering flavor symmetries we particularly care for the three-generation structure. To go beyond the mass insertion approximation and the one-generation case requires diagonalizing a $9 \times 9$ mass matrix in the non custodial setup and a $12 \times 12$ mass matrix in the custodial one, leaving limited space for a fully analytical description. For this reason the spurion-overlap analysis remains an appealing tool for understanding the cancellation mechanisms induced by a particular flavor pattern, as is the case when a discrete flavor symmetry such as $\mathrm{A}_4$ is imposed.

# 4 Beyond the mass insertion approximation

To go beyond the mass insertion approximation and account for the complete generational mixing requires the direct diagonalization of the full $12 \times 12$ KK mass matrix in the custodial case. The mass matrix can be perturbatively diagonalized to first order in the parameter $x = vY/M_{KK}$, which measures the relative strength of Yukawa interactions with the Higgs compared to the masses of the first level KK modes. A lower level of approximation is obtained by disregarding the mixing among generations and work with one-generation mass matrices. This was done in [15] and [16] for the flavor anarchic non-custodial case. Already at this level, the diagonalization of the one-generation mass matrix enables one to account for the contribution of the $(--)$ KK modes to the dipole operators, not realized in the spurion-overlap analysis within the mass insertion approximation. In addition, it was numerically verified [15] that within the flavor anarchic non-custodial framework of [10] the difference between the results in the one-generation and the three-generation case is rather mild. This is expected, and stems from the fact that all Yukawa couplings are $\mathcal{O}(1)$ and no pattern is present in the phases of these couplings. Consequently, the structure of each diagonal and off-diagonal block in the full $9 \times 9$ mass matrix is identical up to the profiles $f_{q,u,d}$'s and the slight variation of the overlap corrections over the three generations. The texture of Yukawa couplings and bulk profiles in RS-$\mathrm{A}_4$ induces different patterns of the results and gives more significance to the comparison between the one-generation and three-generation analysis.

## 4.1 Direct diagonalization of the one-generation mass matrix

The study described in this section is also instructive for flavor anarchic models with custodial symmetry, which contain a separate $SU(2)_R$ doublet for each 5D fermion with a RH zero mode. This case was not considered in [10, 15, 16]. The LO mass matrix for the first generation in the down-type sector, including the zero modes and first level KK modes, is of the form

$$\frac{\hat{\mathbf{M}}_d^{KK}}{(M_{KK})} = \begin{pmatrix} \bar{Q}_L^{d(0)} \\ \bar{d}_L^{(1--)} \\ \bar{Q}_L^{d(1)} \\ \bar{\tilde{d}}_L^{(1+-)} \end{pmatrix}^T \begin{pmatrix} \breve{y}_d f_Q^{-1} f_d^{-1} r_{00} x & 0 & \breve{y}_d f_Q^{-1} r_{01} x & \breve{y}_u f_Q^{-1} r_{101} x \\ 0 & \breve{y}_d^* r_{22} x & 1 & 0 \\ \breve{y}_d f_d^{-1} r_{10} x & 1 & \breve{y}_d r_{11} x & \breve{y}_u r_{111} x \\ 0 & \breve{y}_u^* r_{222} x & 0 & 1 \end{pmatrix} \begin{pmatrix} d_R^{(0)} \\ Q_R^{d(1--)} \\ d_R^{(1)} \\ \tilde{d}_R^{(1-+)} \end{pmatrix}, \tag{31}$$

where we factorized a common KK mass scale $M_{KK}$, $\breve{y}_{u,d} \equiv (\hat{Y}^{u,d}_{LO})_{11} = 2y_{u,d} v_\Phi^{4D} e^{k\pi R}/k$ and the perturbative expansion parameter is defined as $x \equiv v/M_{KK}$. In the above equation $r_{111} \equiv r_{11^{-+}}$, $r_{101} \equiv r_{01^{-+}}$, $r_{22} \equiv r_{1^{-}1^{-}}$, $r_{222} \equiv r_{1^{-}1^{+-}}$ and the notation for the rest of the overlaps is the same as in Eq. (1). The $c$ dependence of the overlap corrections was suppressed to ease the notation and can be inferred from the labelling of the rows and columns. Since the overlaps vary little among generations, the structure of the mass matrix will be almost identical for all three generations of the up and down sectors, up to the zero mode profiles denoted by the $f_{q,u,d}$ and the Yukawa couplings, $\breve{y}_{u,d}$. Notice that the NLO Yukawa interactions are suppressed by $f_\chi^{u_i,d_i}$ compared to the LO contributions, rendering them to be approximately $\mathcal{O}(x^2)$ numerically and thus in principle safe to neglect when working to $\mathcal{O}(x)$. In order to include NLO Yukawa interactions in the above matrix one should simply replace $y_{u,d} \to y_{u,d} + f_\chi^{u,d}(\tilde{x}_1^{u,d} + \tilde{y}_1^{u,d})$ in $\breve{y}_{u,d}$, following Eqs. (5) and (7), and analogously for the other matrices. Despite their relative smallness, it is still important to study the generational modifications associated with NLO Yukawa interactions, which are essential for matching the quark mixing data in the ZMA.

Notice that the anarchic case is simply obtained from Eq. (31) by setting $\breve{y}_{u,d} = Y$ for all generations, where $Y$ is a $\mathcal{O}(1)$ Yukawa coupling which can be absorbed in $x$. In RS-A$_4$, when considering the mass matrices for the second and third generation, we encounter additional $\omega$ factors coming from the LO Yukawa matrix of Eq. (5). In addition, the approximation of degenerate KK masses will turn out to be fair only for two out of the three KK masses in Eq. (31), given the bulk mass assignments of the RS-A$_4$ setup. In appendix B.1 we perform the diagonalization of each of the one-generation mass matrices for the up and down sectors to first order in $x$, before proceeding to the approximate analytical diagonalization of the full $12 \times 12$ up and down mass matrices in appendix B.3.

The $4 \times 4$ one-generation diagonalization matrices, $O_L^{(u,c,t,d,s,b)_{KK}}$ and $O_R^{(u,c,t,d,s,b)_{KK}}$, are defined as follows

$$(O_L^{(u_i,d_i)_{KK}})^\dagger\, \hat{\mathbf{M}}^{KK}_{u_i,d_i}\, (O_R^{(u_i,d_i)_{KK}}) = \hat{\mathbf{M}}^{KK_{diag}}_{u_i,d_i}\,. \tag{32}$$

Once the above diagonalization matrices are obtained, the ground is set for the estimation of physical couplings between light and heavy modes in the flavor anarchic custodial case. This is done by simply transforming the charged and neutral Higgs Yukawa interaction matrices to the mass basis using $O_{L,R}^{(u_i,d_i)_{KK}}$, while the generational mixing factors can be estimated in the mass insertion approximation, as also done in [15, 16].

In the RS-A$_4$ setup we can extract the overlap dependence of the coupling between the zero mode and the three first level KK modes of each generation in the same way. Then, to account for generational mixing and the underlying flavor pattern, this information is combined with the spurion-overlap analysis in the mass insertion approximation of Eqs. (29) and (30), where it provides a redefinition of the overall overlap factors $B_P^{u,d}$. As already noticed, the latter approximation of reducing the overlap structure to a common overall factor, is justified since the almost degenerate KK modes mix almost maximally and are hence well approximated by one representative for each type of BC. The new down-type $B_P^d$ factors for the dipole operators, corresponding to the process in Fig. 1 with a neutral Higgs, will thus be extracted from

$$(\mathcal{A}_{ij})_D^{overlap} = \left. \frac{\sum_n ((O_L^{(d_i)KK})^\dagger \hat{Y}_{KK}^{d_i} O_R^{(d_i)KK})_{1n} ((O_L^{(d_i)KK})^\dagger \hat{Y}_{KK}^{d_j} O_R^{(d_i)KK})_{n1}}{\left( M_{KK}^{d_i\,(n)} / M_{KK} \right)} \right|_{overlap} , \tag{33}$$

where $|_{overlap}$ denotes taking the overlap part of the corresponding expression by assigning all Yukawas to one. The indices $i, j$ denote the flavor of the external SM physical zero modes, while $n$ runs over the three KK states for the given generation. The components (1n), (n1) of the Yukawa matrices rotated to the mass basis indicate the coupling between a zero mode and the n-th KK mode of the same generation. The new $B_P^u$ factors, corresponding to the amplitudes in Fig. 1 and Fig. 2 with a charged Higgs, will analogously be extracted from

$$(\mathcal{A}_{ij})_U^{overlap} = \left. \frac{\sum_n ((O_L^{(d_i)KK})^\dagger \hat{Y}_{KK}^{(h_-)d_i} O_R^{(u_i)KK})_{1n} ((O_L^{(u_i)KK})^\dagger \hat{Y}_{KK}^{(h_+)d_j} O_R^{(d_i)KK})_{n1}}{\left( M_{KK}^{u_i\,(n)} / M_{KK} \right)} \right|_{overlap} . \tag{34}$$

Notice that the one-loop factor $A^{1L}$ in Eqs. (29) and (30) is calculated at the reference KK mass $M_{KK} \simeq 2.55\,(R')^{-1}$, while the non-degeneracy of KK states is taken into account by the rescaling $(M_{KK}^{d_i,u_i\,(n)}/M_{KK})$. It is useful to mention the explicit structure of the down-type Yukawa couplings with a neutral Higgs in the interaction basis

$$\hat{Y}_{KK}^{d} = \begin{pmatrix} \bar{Q}_L^{d(0)} \\ \bar{d}_L^{(1--)} \\ \bar{Q}_L^{d(1)} \\ \bar{\tilde{d}}_L^{(1+-)} \end{pmatrix}^T \begin{pmatrix} \breve{y}_d f_Q^{-1} f_d^{-1} r_{00} & 0 & \breve{y}_d f_Q^{-1} r_{01} & \breve{y}_u f_Q^{-1} r_{101} \\ 0 & \breve{y}_d^* r_{22} & 0 & 0 \\ \breve{y}_d f_d^{-1} r_{10} & 0 & \breve{y}_d r_{11} & \breve{y}_u r_{111} \\ 0 & \breve{y}_u^* r_{222} & 0 & 0 \end{pmatrix} \begin{pmatrix} d_R^{(0)} \\ Q_R^{d(1--)} \\ d_R^{(1)} \\ \tilde{d}_R^{(1-+)} \end{pmatrix} . \tag{35}$$

Similarly, the Yukawa interactions with the charged Higgs $h^-$ are

$$\hat{Y}_{KK}^{(h_-)d} = \begin{pmatrix} \bar{Q}_L^{d(0)} \\ \bar{d}_L^{(1--)} \\ \bar{Q}_L^{d(1)} \\ \bar{\tilde{d}}_L^{(1+-)} \end{pmatrix}^T \begin{pmatrix} -\breve{y}_u f_Q^{-1} f_u^{-1} r_{00} & 0 & -\breve{y}_u f_Q^{-1} r_{01} & -\breve{y}_d f_Q^{-1} r_{101} \\ 0 & \breve{y}_d^* r_{22} & 0 & 0 \\ -\breve{y}_u f_u^{-1} r_{10} & 0 & -\breve{y}_u r_{11} & -\breve{y}_d r_{111} \\ 0 & \breve{y}_u^* r_{222} & 0 & 0 \end{pmatrix} \begin{pmatrix} u_R^{(0)} \\ Q_R^{u(1--)} \\ u_R^{(1)} \\ \tilde{u}_R^{(1-+)} \end{pmatrix} , \tag{36}$$

and for $h^+$ they are given by the replacement $\breve{y}_{u,d} \to -\breve{y}_{d,u}$ and $f_{u,d} \to f_{d,u}$

$$\hat{Y}_{KK}^{(h_+)d} = \begin{pmatrix} \bar{Q}_L^{u(0)} \\ \bar{u}_L^{(1--)} \\ \bar{Q}_L^{u(1)} \\ \bar{\tilde{u}}_L^{(1+-)} \end{pmatrix}^T \begin{pmatrix} \breve{y}_d f_Q^{-1} f_d^{-1} r_{00} & 0 & \breve{y}_d f_Q^{-1} r_{01} & \breve{y}_u f_Q^{-1} r_{101} \\ 0 & -\breve{y}_u^* r_{22} & 0 & 0 \\ \breve{y}_d f_d^{-1} r_{10} & 0 & \breve{y}_d r_{11} & \breve{y}_u r_{111} \\ 0 & -\breve{y}_d^* r_{222} & 0 & 0 \end{pmatrix} \begin{pmatrix} d_R^{(0)} \\ Q_R^{d(1--)} \\ d_R^{(1)} \\ \tilde{d}_R^{(1-+)} \end{pmatrix} . \tag{37}$$

The physical Yukawa couplings between zero modes and KK modes are then obtained by the $O^{u,d}_{L,R}$ rotations. Once inserted in Eqs. (33) and (34), they provide the new overlap factors $B^{u,d}_{P}$ to be inserted in the spurion-overlap formulae Eqs. (29) and (30), for each dipole operator. The results of this analysis – diagonalization of the one-generation mass matrices combined with the spurion-overlap procedure – will be considered separately for each process, while the details of the derivation and the $B^{u,d}_{P}$ factors can be found in appendices B.1 and B.2.
It is however important to recall that the complete $\mathrm{A}_4$ flavor structure in the full $12 \times 12$ up and down mass matrices may still induce deviations from the approximations considered till now. Differences may arise from inter- and intra-generational mixing, non-degeneracy of KK states and overlaps. All these effects are numerically more significant when involving the third generation. On the other hand, the drawback of a fully numerical treatment of the 12x12 mass matrix is that it does not allow to easily discriminate among different orders in the $x$-parameter expansion, and it fails to provide insightful information on the flavor patterns and cancellation mechanisms of the numerical results. Eventually, such a numerical treatment will turn out to induce more sizable contributions to the neutron EDM and less significantly so for other processes. This situation illustrates the importance of a full three-generation diagonalization and its comparison with approximate analytical estimates when a flavor texture is present in the Yukawa matrices.

## 4.2 Approximate analytical diagonalization of the $12 \times 12$ mass matrix

It is clear that a complete description of the contributions to physical processes in the three-generation RS-$\mathrm{A}_4$ can only be achieved by a direct diagonalization of the full $12 \times 12$ up and down mass matrices, including first level, $n = 1$, KK modes. Using the $12 \times 12$ rotation matrices we can obtain all the couplings between each zero mode and KK modes of all generations, thus establishing an a priori more reliable way to describe the flavor patterns of $\mathrm{A}_4$. However, the size of the matrices, the large number of parameters even in the minimal case and the near degeneracy of most of the KK masses, render the diagonalization hard to perform analytically. For this reason the three-generation case was considered only numerically in [15], for flavor anarchic models. A fully numerical diagonalization of the $12 \times 12$ mass matrices in RS-$\mathrm{A}_4$ may provide an estimate of contributions possibly missed by other approximations, but fails to give us insight on the flavor pattern of the three-generation $\mathrm{A}_4$ case. In addition, since the one-generation 4D mass matrices have been themselves derived and diagonalized linearly in the $\mathrm{A}_4$ parameters $\tilde{x}^{u,d}_i$, $\tilde{y}^{u,d}_i$, the most appropriate diagonalization should always be performed to the same order. Instead, a numerical treatment will inevitably include higher order contributions in an a priori uncontrolled way.
Given all the above reasons, one should still attempt an approximate analytical diagonalization, as described below. We first decompose the $12 \times 12$ mass matrix of the RS-$\mathrm{A}_4$ down

sector in terms of the one-generation matrices in Eq. (31)

$$\hat{\mathbf{M}}^D_{Full} = M_{KK} \left( \begin{array}{ccc} \hat{\mathbf{M}}^{KK}_d/M_{KK} & x\hat{Y}^s_{KK}(\hat{y}^{LO}_{12}, f_s) & x\hat{Y}^b_{KK}(\hat{y}^{LO}_{13}, f_b) \\ x\hat{Y}^d_{KK}(\hat{y}^{LO}_{21}, f_d) & \hat{\mathbf{M}}^{KK}_s/M_{KK} & x\hat{Y}^b_{KK}(\hat{y}^{LO}_{23}, f_b) \\ x\hat{Y}^d_{KK}(\hat{y}^{LO}_{31}, f_d) & x\hat{Y}^s_{KK}(\hat{y}^{LO}_{32}, f_s) & \hat{\mathbf{M}}^{KK}_b/M_{KK} \end{array} \right) , \tag{38}$$

where the expression in brackets of each off-diagonal element denotes the replacements to be made in Eq. (35). The $s$ and $b$ one-generation mass matrices $\hat{\mathbf{M}}^{KK}_{s,b}$ are obtained by obvious replacements in Eq. (31). To account for NLO Yukawa interactions, the replacement $\hat{y}^{LO}_{ij} \to \hat{y}^{LO}_{ij} + \hat{y}^{NLO}_{ij}$ applies. In the above equation, $M_{KK}$ is the KK mass corresponding to the degenerate left-handed bulk mass parameter, $c^L_q$, and we normalize all matrices accordingly while keeping non-degenerate KK modes. The only significant deviations from degeneracy lie in the third generation mass matrix due to $\tilde{b}$, the $SU(2)_R$ partner of $t_R$ .
Using the $4 \times 4$ diagonalization matrices for each generation, we construct the matrices $\hat{\mathbf{O}}^{D_{KK}}_{L,R} = \mathrm{d}iag(O^{d_{KK}}_{L,R}, O^{s_{KK}}_{L,R}, O^{b_{KK}}_{L,R})$ to first diagonalize the diagonal entries of $\hat{\mathbf{M}}^D_{Full}$. The main difficulty in achieving the diagonalization of the full mass matrix in Eq. (38) is the near degeneracy of 6 out of 9 KK masses which also survives the $(\hat{\mathbf{O}}^{D_{KK}}_L)^\dagger \hat{\mathbf{M}}^D_{Full} \hat{\mathbf{O}}^{D_{KK}}_R$ rotation, rendering non degenerate perturbation theory useless in the corresponding subspace. Therefore, the nearly degenerate subspace is first diagonalized non perturbatively to find a new basis, in which non-degenerate perturbation theory can be used. Off-diagonal elements in the non-degenerate subspaces can obviously be treated in the conventional way. Since this task is hard to perform analytically when all parameters are unassigned, we look for some symmetry property of the A$_4$ structure in $\hat{\mathbf{M}}^D_{Full}$ that might supplement us with a shortcut. Given the structure of Eq. (38), we then construct new rotation matrices using $V^{u,d}_{L,R}$ from Eq. (13). The new A$_4$ rotation matrices are thus defined as the direct product

$$\hat{\mathbf{O}}^{(U,D)_{A_4}}_{L,R} = V^{u,d}_{L,R} \otimes \tilde{\mathbb{1}}_{4\times 4} , \tag{39}$$

where $\tilde{\mathbb{1}}_{4\times4} = \mathrm{d}iag(1, 1()^*, 1, 1()^*)$ and $()^*$ denotes complex conjugation of the coefficient that multiplies the corresponding element, namely $(V^{u,d}_{L,R})_{ij}$. In appendix B.3 we show that using $\hat{\mathbf{O}}^{(U,D)_{A_4}}_{L,R}$ and $\hat{\mathbf{O}}^{D_{KK}}_{L,R}$ to rotate $\hat{\mathbf{M}}^D_{Full}$, one obtains an approximately diagonalized degenerate subspace, which in turn enables to generate the remnant rotation by acting with non-degenerate perturbation theory on $(\hat{\mathbf{O}}^{D_{A_4}}_L)^\dagger (\hat{\mathbf{O}}^{D_{KK}}_L)^\dagger \hat{\mathbf{M}}^D_{Full} \hat{\mathbf{O}}^{D_{KK}}_R \hat{\mathbf{O}}^{D_{A_4}}_R$. The analogous procedure is followed in the up sector. More details are collected in appendix B.3. Once the diagonalization matrices are obtained, the contribution to the Wilson coefficient of a given dipole operator will be a generalization of the one-generation case and can generically be written as follows

$$\left(C^{d-type}_{7\gamma(8g)}\right)_{ij} = A^{1L}(M_{KK}) \frac{\sum_n ((O^{(d_i)}_L)^\dagger \hat{Y}^{d_i}_{KK} O^{(d_i)}_R)_{(4i-3)\,n} ((O^{(d_i)}_L)^\dagger \hat{Y}^{d_j}_{KK} O^{(d_i)}_R)_{n\,(4j-3)}}{(M^{(n)}_{KK}/M_{KK})}, \tag{40}$$

for down-type contributions, and

$$\left(C^{u-type}_{7\gamma(8g)}\right)_{ij} = \tilde{A}^{1L}_u(M_{KK}) \frac{\sum_n ((O^{(d_i)}_L)^\dagger \hat{Y}^{d_i}_{KK} O^{(d_i)}_R)_{(4i-3)\,n} ((O^{(d_i)}_L)^\dagger \hat{Y}^{d_j}_{KK} O^{(d_i)}_R)_{n\,(4j-3)}}{(M^{(n)}_{KK}/M_{KK})}, \tag{41}$$

for up-type contributions. The matrices $O_{L,R}^{(u_i,d_i)}$ diagonalize the $12 \times 12$ mass matrices. The index $n$ runs over the KK modes of the three generations, thus $n \neq 1, 5, 9$, and the indices $(4i-3)\,n$ and $n\,(4j-3)$ select the couplings of the external zero mode to the internal KK states. The one-loop factors are calculated at the reference KK mass $M_{KK} \simeq 2.55\,(R')^{-1}$, while the non-degeneracy of KK states is taken into account by the rescaling $(M_{KK}^{(n)}/M_{KK})$. However, as expected, the resulting expressions for the physical couplings between zero modes and KK modes are long functions of all overlap correction factors and are therefore not stated explicitly. Instead, we explore the couplings and the resulting predictions for assigned values of the parameters, and compare them with the results of a fully numerical diagonalization for varying values of the KK scale, $M_{KK}$. This will be done separately for each process in section 5.

# 5 Numerical Results and Experimental Bounds for Dipole Operators

In this section we analyze FCNC processes in the RS-A$_4$ model, using the approximations described in sections 3 and 4, and compare them with a fully numerical analysis based on the diagonalization of the $12 \times 12$ mass matrices for the zero modes and first level KK modes. We focus on those processes mediated by dipole operators and known to provide the most stringent constraints on new physics contributions, and thus the KK scale, in the context of flavor models in warped geometry: these are the neutron EDM in section 5.1, $\epsilon'/\epsilon_K$ in section 5.2 and the radiative decay $b \to s\gamma$ in section 5.3. Finally, tree level Higgs mediated FCNC contributions are considered in section 6.

## 5.1 New physics contributions to the neutron EDM

The new physics contributions to the neutron EDM are mediated by the dipole operator $e\bar{d}_L\sigma^{\mu\nu}F_{\mu\nu}d_R$. In particular, we need to compute the imaginary part of the $i = j = 1$ component of the Wilson coefficients defined in Eqs. (29) and (30). They are of dimension $[mass]^{-1}$ and can thus be directly compared to the experimental bound $|d_n| < 3 \times 10^{-26} e \cdot cm$ [24]. We have already anticipated in [1] that the down-type contribution to the EDM is vanishing in RS-A$_4$, due to the fact that $V_L^d$ disappears from the down-type contributions. This conclusion can also be reached by inspecting Eq. (26). This leaves us with the up-type contributions encoded in $\mathrm{I}m[(C_7^{u-type})_{11}]$. In order to isolate the dominant terms in Eq. (30), where we approximate the overlap factors with an overall constant, we recall that the hierarchy of quark masses is translated into the inverse hierarchy of the right-handed profiles $f_{q_i}$, since there is only one left-handed bulk mass parameter. More specifically, $f_u \simeq 4.48 \times 10^4$, $f_d \simeq 2.25 \times 10^4$, $f_s \simeq 1.36 \times 10^3$, $f_c \simeq 1.22 \times 10^2$, $f_b \simeq 28.8$, $f_t \simeq 1.22$ and $f_Q \simeq 3.14$. In addition, we recall that the off-diagonal elements of $V_R^u$ in Eqs. (14)-(16) are suppressed by up-type quark mass ratios. Hence, the most dominant contribution to the neutron EDM from Eq. (30) turns out to be

$$\mathrm{Im}[(C_7^{u-type})_{11}] \simeq \mathrm{Im}\left[\frac{5B_P^u A^{1L} m_d f_Q^2 F^u_{EDM}}{3v^2 M_{KK}}\right], \tag{42}$$

where the factor 5/3 comes from the electric charge of an up-type quark and a charged Higgs from Eq. (20). The factor $F^u_{EDM}$ is obtained from Eq. (30) and given by

$$\begin{aligned} F^u_{EDM} &= \left[V^\dagger_{CKM} diag(m_{u,c,t}) V_R^{u\dagger} diag(f^2_{u_i}) V_R^u diag(m_{u,c,t}) V_{CKM}\right]_{11} \\ &= \sum_{k,l=1}^{3} (V^\dagger_{CKM})_{1k} (\tilde{R}_u)_{k\ell} (V_{CKM})_{\ell 1} \;\Rightarrow\; \mathrm{Im}(F^u_{EDM}) = 0, \end{aligned} \tag{43}$$

with

$$(\tilde{R}_u)_{ij} = \Big(diag(m_{u,c,t}) V_R^{u\dagger} diag(f^2_{u_i}) V_R^u diag(m_{u,c,t})\Big)_{ij} = \sum_{n=1}^{3} m_i m_j (V_R^u)^*_{ni} (V_R^u)_{nj} f^2_{u_n}\,. \tag{44}$$

Given that the matrix $\tilde{R}_u$ is hermitian and that in RS-A$_4$ to $O(\tilde{x}_i^{u,d}, \tilde{y}_i^{u,d})$ one has $(V_{CKM})_{ii} = 1$, and $(V_{CKM})_{ij} = -(V_{CKM})^*_{ji}$ for $i \neq j$ (see Eqs. (8) − (11)), we conclude that $F^u_{EDM}$ has no imaginary part if we disregard the tiny non-degeneracy of overlap factors by replacing them with the overall coefficient $B_P^u$. For later convenience we anyway look at what terms are dominant in the cancellation pattern; they are proportional to $f_u^2$ or $f_c^2$

$$\begin{aligned} F^u_{EDM} &= f_u^2 [m_u^2 - m_u m_c V_{us} (\Delta_1^u)^* - m_u m_c V^*_{us} \Delta_1^u \\ &- (f_c^2/f_u^2) m_c^2 V_{us} V^*_{us} - m_u m_t V^*_{ub} \Delta_2^u - m_u m_t V_{ub} (\Delta_2^u)^*]\,. \end{aligned} \tag{45}$$

The first and fourth terms are real, while the second and third terms and the fifth and sixth terms cancel each other's imaginary parts. All other contributions to $F^u_{EDM}$ are suppressed by at least two orders of magnitude, and exhibit the same cancellation pattern of imaginary parts. Thus, in order to obtain a conservative estimate of the contribution to the neutron EDM in our setup, we must fully account for non degeneracies and possibly go beyond the mass insertion approximation.

It is also important to recall that $V^{u,d}_{L,R}$ have been determined [1] to linear order in the Yukawa parameters $\tilde{x}_i^{u,d} f_\chi^{u,d}$, $\tilde{y}_i^{u,d} f_\chi^{u,d}$ and that the neglected $\mathcal{O}((x_i^{u,d} f_\chi^{u,d})^2, (y_i^{u,d} f_\chi^{u,d})^2)$ corrections can also a priori modify the cancellation pattern of imaginary parts for up- and down-type contributions to the neutron EDM. However, a realistic estimate of these corrections would require to perform a new matching with the experimentally determined CKM matrix. We can still provide a conservative order of magnitude estimate of these effects by evaluating the size of a generic term in Eq. (45). In particular, labelling the second (or third) term, proportional to the largest CKM element $V_{us}$, as $\Delta F^u_{EDM}$ one obtains

$$\begin{aligned} \Delta F^u_{EDM} = f_u^2 m_u m_c V_{us} (\Delta_1^u)^* \Rightarrow d_n &\approx \mathrm{Im}\left[\frac{5B_P^u A^{1L} m_d f_Q^2 \Delta F^u_{EDM}}{3v^2 M_{KK}}\right] \\ &\approx 4.1 \times 10^{-27} \left(\frac{3\,\mathrm{TeV}}{M_{KK}}\right)^2 Y^2\, e \cdot cm, \end{aligned} \tag{46}$$

for $B_P^u \simeq 1.5$ and assuming $|\Delta_1^u| \approx |V_{us}| m_u/m_c$, with maximal phase for $\Delta F_{EDM}^u$. The symbol $Y$ denotes the overall scale of the 5D Yukawa couplings, defined as $y_{u,d,c,s,t,b} \to Y\, y_{u,d,c,s,t,b}$ with reference values $y_{u,d,c,s,b} = 1$ and $y_t = 2.8$. The predicted contribution is suppressed by one order of magnitude compared to the experimental bound, however, an enhancement induced by a coherent sum of many higher order terms in $\tilde{x}_i^{u,d}, \tilde{y}_i^{u,d}$ cannot be excluded at this level. Translating the above result into a conservative constraint on the KK mass scale yields

$$(M_{KK}^{EDM})_{cons.}^{spur.} \gtrsim 1.1\, Y\, \mathrm{TeV}\,. \tag{47}$$

When taking into account the non-degeneracy of the overlap factors in the spurion-overlap approximation of Eqs. (26) and (27), the contributions to the EDM are still vanishing to $O(C_\chi f_\chi)$ – corresponding to $O(\lambda)$ of the Wolfenstein parametrization of the CKM matrix. Negligible non vanishing contributions appear in the up sector at $O(\lambda^2)$. The most dominant non vanishing contribution in the up sector, together with its exact generational dependence of the overlap correction factors is as follows

$$F_{EDM}^u = ((r_{00}^b)^{-1} r_{10}^b - (r_{00}^d)^{-1} r_{10}^d)(r_{00}^t)^{-2}(r_{01}^t r_{11}^t + r_{101}^t r_{111}^t) f_t^2 m_t^2 V_{ub} (\Delta_2^u)^*\,. \tag{48}$$

It provides the estimate

$$(d_n)_{RS-A_4}^{\mathrm{Spurion}} \approx 2 \times 10^{-29} \left(\frac{3\,\mathrm{TeV}}{M_{KK}}\right)^2 Y^2\, e \cdot cm\,,$$

and a lower bound on the KK mass scale $M_{KK} \gtrsim 0.07\, Y$ TeV, when comparing with the experimental result.

We can improve upon the previous estimate by directly diagonalizing the mass matrices and work with KK mass eigenstates. In the estimates below, the effects of generational mixing, non-degeneracy of overlaps and KK states are described to various degrees of approximation. We first state the results obtained by the procedure of section 4.1, where we use the diagonalization of the one-generation mass matrices combined with the spurion-overlap analysis to account for generational mixing. The contribution from $\Delta F_{EDM}^u$ in Eq. (46) to the neutron EDM will be obtained by the replacement $B_P^u \to (B_P^u)_{EDM}^{KK(1gen)}$, see appendix B.2). Using $(B_P^u)_{EDM}^{KK(1gen)} \simeq 5.2$, we obtain:

$$(d_n)_{RS-A4}^{1-gen(cons.)} \simeq 1.42 * 10^{-26} \left(\frac{3TeV}{M_{KK}}\right)^2 Y^2\, e \cdot cm\,, \tag{49}$$

which implies the bound $M_{KK} \gtrsim 2.1\, Y$ TeV. The modification of the contribution in Eq. (48) will be obtained by the same replacement and leads to

$$(d_n)_{RS-A_4}^{1-gen} \simeq 8 \times 10^{-29} \left(\frac{3\,\mathrm{TeV}}{M_{KK}}\right)^2 Y^2\, e \cdot cm\,, \tag{50}$$

implying a weak lower bound on the KK mass scale $M_{KK} \gtrsim 0.15\, Y$ TeV, when comparing with the experimental result.

Secondly, we consider the three-generation case, where the $12 \times 12$ mass matrices can be approximately diagonalized analytically as described in section 4.2, or they can be diagonalized numerically. In both cases we assign the bulk masses and Yukawa couplings according to Eq. (12) and the assignments in Appendix A and use the corresponding values of the overlap correction factors obtained in Appendix A.1. In the numerical case, we perform a scan in the KK mass scale $M_{KK}$ in the range $1 - 10$ TeV and $Y$ in the range $[0.3, 5]$. We have also verified the stability of the results against modifications of the phases of the NLO Yukawa couplings and in particular for the assignments of Eqs. (72), (60) and (77). Notice that differences with the previous estimates can be attributed to the presence of higher order corrections in the perturbative parameter $x$ (beyond the mass insertion approximation) and to the partial, and a priori uncontrolled, contamination of higher order terms in $\tilde{x}_i^{u,d}$, $\tilde{y}_i^{u,d}$. The first source can be estimated by performing a scan over the values of $x$ and match the dominant linear behavior in the vicinity of $x = 0.037$. We recall [1] that the latter value corresponds to $(R')^{-1} \simeq 1.8$ TeV and $M_{KK} \simeq 2.55\,(R')^{-1} \simeq 4.6$ TeV, the value for which RS-$A_4$ predicts a NP correction to the $Zb_L\bar{b}_L$ coupling within 67% CL for the bulk parameters in Eq. (110).

To obtain the explicit contributions for each of the processes of interest, we use the $12 \times 12$ analogues of Eqs. (33) and (34). The fully numerical diagonalization procedure, and without truncation in the $x$-parameter expansion, leads to the prediction for the neutron EDM

$$\mathrm{I}m\left[(C_7^d)^{Num}_{EDM}\right] \simeq 3.1 \times 10^{-29} e \cdot cm \qquad \mathrm{I}m\left[(C_7^u)^{Num}_{EDM}\right] \simeq -1.66 \times 10^{-28} e \cdot cm, \tag{51}$$

$$(d_n)^{Num}_{RS-A_4} \simeq 1.65 \times 10^{-28} e \cdot cm\,,$$

while a scan in $x$ and matching to the linear behavior leads to

$$\mathrm{I}m\left[(C_7^d)^{Num}_{EDM}\right] \simeq 3.3 \times 10^{-29} e \cdot cm \qquad \mathrm{I}m\left[(C_7^u)^{Num}_{EDM}\right] \simeq -1.75 \times 10^{-28} e \cdot cm, \tag{52}$$

$$(d_n)^{Num}_{RS-A_4} \simeq 1.7 \times 10^{-28} e \cdot cm\,,$$

where the up- and down-type contributions were summed in quadrature. Both results saturate the experimental bound for $M_{KK} \approx 0.3$ TeV. For $M_{KK} \simeq 4.6$ TeV the neutron EDM is smaller than the experimental bound by two orders of magnitude. What is also relevant is that the resultant constraint on $M_{KK}$ deviates by a $O(1)$ factor from the constraint implied by Eq. (48). The characteristic strength of the numerical results is rather stable against modifications of $\tilde{y}_i^{u,d}$, $\tilde{x}_i^{u,d}$, $f_{Q,u_i,d_i}$ and $y_{u_i,d_i}$ that still yield physical quark masses and CKM elements. In addition, when varying the parameters up to $O(3)$ in magnitude away from their CKM values, the variation of the predicted neutron EDM and all other observables stays within a factor two.

The contributions predicted by the approximate analytical diagonalization procedure described in Sec. 4.2 consist of extremely long expressions, which we do not state explicitly. Instead, we study them as a function of $x = v/M_{KK}$ only, with all other parameters assigned to yield the physical quark masses and CKM matrix elements. Finally, we can compare the resulting predictions with the results of the fully numerical analysis. The approximate analytical diagonalization for the neutron EDM provides

$$\mathrm{Im}\left[(C_7^d)_{EDM}^{12\times 12th})\right] \simeq -2.5\times 10^{-9} A_{1L} \qquad \mathrm{Im}\left[(C_7^u)_{EDM}^{12\times 12th})\right] \simeq -2\times 10^{-9} \tilde{A}_{1L}^u \tag{53}$$

and

$$(d_n)_{RS-A_4}^{12\times 12th} \simeq 1.6\times 10^{-28}\left(\frac{4.3\,\mathrm{TeV}}{M_{KK}}\right)^2 Y^2\, e\cdot cm\,,$$

in good agreement with the estimate of Eq. (48) and the numerical results in Eqs. (51) and (52). The discrepancy between the numerical and the semianalytical approach for the three-generation case will turn out to be larger for other observables. This is due to the fact that the semianalytical diagonalization described in Sec. 4.2 works better within the first generation, while more significant off-diagonal terms still appear in the second and third generation. In the case of the EDM, a cancellation mechanism at leading order is indeed in place.

## 5.2 New physics and $(\epsilon'/\epsilon)$

In this section we derive the new physics contributions to $\mathrm{Re}(\epsilon'/\epsilon)$ in RS-$A_4$, generalizing the flavor anarchic analysis of [16] to our setup. We show that the bound induced on the KK mass scale by this quantity is relaxed even below the bounds obtained from EWPM, differently from what happens in the flavor anarchic case. The current experimental average, measured by KTeV and the NA48 collaborations, is $\mathrm{R}e(\epsilon'/\epsilon)_{exp} = (1.65\pm 0.26)\times 10^{-3}$ [20]. Given the uncertainties still affecting the standard model prediction $\mathrm{R}e(\epsilon'/\epsilon)_{SM}$ [25], we adopt the most conservative approach as also done in [16] and assume $0 < \mathrm{R}e(\epsilon'/\epsilon)_{SM} < 3.3\times 10^{-3}$.
The potentially large new physics contributions to $\mathrm{R}e(\epsilon'/\epsilon)$ in the RS setup are induced by the two effective chromomagnetic operators with opposite chirality

$$O_g = g_s H^\dagger \bar{s}_R \sigma^{\mu\nu} T^a G^a_{\mu\nu} d_L\,, \qquad O'_g = g_s H \bar{s}_L \sigma^{\mu\nu} T^a G^a_{\mu\nu} d_R\,, \tag{54}$$

generated by the one-loop amplitude in Fig. 1[4]. The imaginary part of the corresponding Wilson coefficients $C_g$ and $C'_g$ contributes to $\mathrm{R}e(\epsilon'/\epsilon) \propto Im(C_g - C'_g)$.
In the spurion-overlap analysis and neglecting the generational dependence of the overlap functions, we need to compute the (12) and (21) elements in Eqs. (29) and (30), respectively. Again, given the dominance of terms proportional to $f^2_{u,d}$ and the suppressions by mass ratios in $V_R^{u,d}$, there are only a few dominant contributions for each of the above elements in the up and down sectors, while all other contributions are suppressed by at least an order of magnitude. However, since the dominant contributions to $(C_{8g}^{up-type})_{12(21)}$ are proportional

---

[4] The presence of $H$ in the definition of the 4D effective operators in Eq. (54), tells us that the Wilson coefficients $C_g$ and $C'_g$ for these operators should be obtained by dividing the spurion analysis result by the Higgs VEV $v$ , thus obtaining Wilson coefficients of mass dimension -2.

to $V_{us}(V_{us}^*)$ and they are real if $\tilde{x}_2^{u,d}$ and $\tilde{y}_2^{u,d}$ are assigned according to Eq. (12), we also consider the leading sub-dominant contributions in the up and down sectors. We obtain

$$\begin{aligned} \mathrm{I}m(C_g - C_g') &= \mathrm{I}m\left[(C_{8g}^{u-type} + C_{8g}^{d-type})_{12} - (C_{8g}^{u-type} + C_{8g}^{d-type})_{21}\right] \qquad (55) \\ &\simeq \frac{A^{1L} f_Q^2}{v^3 M_{KK}} \mathrm{I}m\left[B_P^u\left(m_s F^u_{\epsilon_{12}} - m_d F^u_{\epsilon_{21}}\right) + B_P^d m_d m_s\left((F^d_{\epsilon_{12}} - F^d_{\epsilon_{21}})\right)\right] , \\ &\simeq \frac{1}{4.3\pi^2 v^3 M_{KK}^2} \mathrm{I}m\left[\left(m_s F^u_{\epsilon_{12}} - m_d F^u_{\epsilon_{21}}\right) + m_d m_s\left(F^d_{\epsilon_{12}} - F^d_{\epsilon_{21}}\right)\right] , \end{aligned}$$

where in the last line we used $A_{1L} = 1/(64\pi^2 M_{KK})$, $f_Q^2 \simeq 9.9$ and $B_P^{u,d} \simeq 1.5$. The dominant contributions to the functions $F^{u,d}_{\epsilon_{12,21}}$ are

$$F^d_{\epsilon_{12}} = m_s(f_d^2 - f_s^2)\Delta_1^d \qquad F^d_{\epsilon_{21}} = m_d(f_d^2 - f_s^2)(\Delta_1^d)^*, \qquad (56)$$

in the down sector and

$$F^u_{\epsilon_{12}} \simeq (f_u^2 m_u^2 - f_c^2 m_c^2)V_{us} + (f_u^2 - f_c^2)m_u m_c \Delta_1^u + f_c^2 m_c^2 V_{us}\left((\tilde{x}_3^u + \omega\tilde{y}_3^u)f_\chi^t + ((\tilde{x}_2^u)^* + \omega(\tilde{y}_2^u)^*)f_\chi^c\right) , \qquad (57)$$

$$F^u_{\epsilon_{21}} \simeq (f_u^2 m_u^2 - f_c^2 m_c^2)V_{us}^* + (f_u^2 - f_c^2)m_u m_c (\Delta_1^u)^* + f_c^2 m_c^2 V_{us}^*\left(((\tilde{x}_3^u)^* + \omega^2(\tilde{y}_3^u)^*)f_\chi^t + (\tilde{x}_2^u + \omega^2\tilde{y}_2^u)f_\chi^c\right) \qquad (58)$$

in the up sector. It is evident from Eqs. (55) – (58) that the contributions associated with $F^u_{\epsilon_{21}}$ are suppressed by $m_d/m_s$ compared to those arising from $F^u_{\epsilon_{12}}$, and the contributions from $F^d_{\epsilon_{21}}$ are similarly suppressed compared to those from $F^d_{\epsilon_{12}}$. This is analogous to the standard model pattern and opposite to what happens in flavor anarchic models. Therefore, to a good approximation, we only need to estimate the imaginary parts of $F^{u,d}_{\epsilon_{12}}$ as functions of the input parameters, in order to obtain bounds on the KK mass scale in RS-A$_4$. Since $f_c^2 m_c^2 \simeq f_u^2 m_u^2$, and more precisely $f_c^2 m_c^2/(f_u^2 m_u^2) - 1 \simeq O(10^{-4})$, the first term of $F^u_{\epsilon_{12}}$ in Eq. (57) approximately vanishes, and the third term is roughly suppressed by $|V_{us}| = 0.2257$ compared to the second term. Consequently, the imaginary part of $F^{u,d}_{\epsilon_{12}}$ is largest for $\Delta_1^d$ and $\Delta_1^u$ pure imaginary. We first find the maximal possible contributions by spanning the $(\tilde{x}_i^{u,d}, \tilde{y}_i^{u,d})$ parameter space, and only later we impose the constraints arising from matching the CKM matrix. Denoting the magnitude of all $\tilde{x}_i^{u,d}$ and $\tilde{y}_i^{u,d}$ parameters collectively by $\tilde{y}_{U,D}$ we obtain

$$max\left[|\mathrm{I}m(\Delta_1^d)|\right] = 2\frac{m_d}{m_s}(f_\chi^d + f_\chi^s)\tilde{y}_D \qquad max\left[|\mathrm{I}m(\Delta_1^u)|\right] = 2\frac{m_u}{m_c}(f_\chi^u + f_\chi^c)\tilde{y}_U , \qquad (59)$$

with the assignment

$$(\tilde{x}_1^{u,d})^* = \omega^2(\tilde{y}_1^{u,d})^* = \pm i\tilde{y}_{U,D} \qquad \tilde{x}_2^{u,d} = \tilde{y}_2^{u,d} = \pm i\tilde{y}_{U,D} . \qquad (60)$$

From Eq. (12), in order to get $|V_{us}| = |V_{cd}| = 0.2257$, we must require $\tilde{x}_2^d = \tilde{y}_2^d = -\tilde{x}_2^u = -\tilde{y}_2^u$ and $\tilde{y}_{U,D} = 1$. The resulting maximal imaginary parts in Eq. (59) will then be reduced by a factor 2 for realistic CKM assignments, due to the exact cancellation of terms proportional to

$\tilde{x}_2^{u,d}$ and $\tilde{y}_2^{u,d}$. For $\tilde{y}_{U,D} \neq 1$, we should correspondingly rescale the $\chi$ VEV to maintain $|V_{us}| = 0.2257$. However, this will have significant implications on the neutrino mass spectrum even for $\mathcal{O}(1)$ rescaling, as was shown in [1]. The two (dominant) terms in Eq. (59) will add up maximally for $\tilde{x}_2^d = \tilde{y}_2^d = \tilde{x}_2^u = \tilde{y}_2^u$, which corresponds to a vanishing $V_{us}$ according to Eq. (9). Focusing now on the third term in Eq. (57), and considering the assignment of Eq. (60), we realize that for $V_{us}$ pure imaginary we should maximize the real part of the expression adjacent to it. The only parameters left to be assigned are $\tilde{x}_3^{u,d}$ and $\tilde{y}_3^{u,d}$ leading to

$$max[|\mathrm{Re}\left((\tilde{x}_3^u + \omega\tilde{y}_3^u) f_\chi^t + ((\tilde{x}_2^u)^* + \omega(\tilde{y}_2^u)^*) f_\chi^c\right)|] = (2f_\chi^t - (\sqrt{3}/2) f_\chi^c)\tilde{y}_U, \tag{61}$$

for the parameter choice $\tilde{x}_3^u = \omega\tilde{y}_3^u = \tilde{y}_U$. Notice that this contribution, proportional to $V_{us}$, will vanish for the choice $V_{us} = 0$ that maximizes the sum of the terms in Eq. (59). Instead, for the assignments that lead to a realistic CKM matrix such as the one in Eq. (12), the contribution of the above terms will be suppressed by roughly an order of magnitude compared to the $(\Delta_1^{u,d})$ terms, and can be safely neglected.
From Eq. (57), using $f_c \ll f_u$ and $B_P^{u,d} \simeq 1.5$, we obtain the following upper bound on the up-type contribution to $\epsilon'/\epsilon$

$$\mathrm{I}m(C_g - C_g')^u \simeq \frac{Y^2 f_u^2 m_u^2 m_s}{11.5\pi^2 v^3 M_{KK}^2} 2(f_\chi^u + f_\chi^c)\tilde{y}_U. \tag{62}$$

It scales with $Y^2$, where $Y$ generically denotes the overall scale of the 5D LO Yukawa couplings associated with the $H\Phi$ interactions. Using again the assignment in Eq. (60) the down type contribution is given by

$$\mathrm{I}m(C_g - C_g')^d \simeq \frac{Y^2 f_d^2 m_d^2 m_s}{11.5\pi^2 v^3 M_{KK}^2} 2(f_\chi^d + f_\chi^s)\tilde{y}_D\,. \tag{63}$$

The NP contributions to $\mathrm{R}e(\epsilon'/\epsilon)$ are directly constrained by the experiment. In order to extract such a constraint we construct the difference $\delta'_\epsilon = (\mathrm{R}e(\epsilon'/\epsilon)_{NP} - \mathrm{R}e(\epsilon'/\epsilon)_{SM})/\mathrm{R}e(\epsilon'/\epsilon)_{exp}$, as done in [16]. Assuming $\mathrm{R}e(\epsilon'/\epsilon)_{SM} = 0$ one can write

$$\delta'_\epsilon = \frac{\omega_\epsilon \langle (2\pi)_{I=0} | \lambda_s O_g | K^0 \rangle)}{\sqrt{2}\mathrm{R}eA_0 \mathrm{R}e(\epsilon'/\epsilon)_{exp} |\epsilon|_{exp}} \left[\frac{\mathrm{I}m(C_g - C_g')}{\lambda_s}\right] \simeq (58\mathrm{T}eV)^2 B_G \left[\frac{\mathrm{I}m(C_g - C_g')}{\lambda_s}\right], \tag{64}$$

where $B_G$, the hadronic bag parameter [26], is given by

$$\langle (2\pi)_{I=0} | \lambda_s O_g | K^0 \rangle = \sqrt{\frac{3}{2}} \frac{11}{4} \frac{m_\pi^2 m_K^2}{F_\pi} B_G, \tag{65}$$

and we set $B_G = 1$ as in [16]. The parameter $\lambda_s$ is the SM Yukawa coupling of the $s$ quark, namely $\lambda_s \times 174\,\mathrm{G}eV = m_s \simeq 50\,\mathrm{M}eV$. The quantities $A_0$ and $A_2$ denote the amplitudes for the $(2\pi)_{I=0}$ and $(2\pi)_{I=2}$ decay channels of the $K^0$ meson, respectively. We take $F_\pi = 131\,\mathrm{M}eV$, $\mathrm{Re}(A_0) = 3.3\times 10^{-4}\mathrm{MeV}$, $\omega_\epsilon = |A_2/A_0| = 0.045$ and $|\epsilon_{exp}| = 2.23\times 10^{-3}$. Imposing $|\delta'_\epsilon| < 1$ and using Eqs. (62) and (63) directly leads to a bound for the KK scale

$$(M_{KK})_{\epsilon'/\epsilon}^{Spurion-overlap} \gtrsim 1.4\,Y\ \mathrm{T}eV. \tag{66}$$

Using the results for the overlap dependence of the up- and down-type contributions to $\epsilon'/\epsilon$ from the one-generation KK diagonalization scheme in Eq. (151), the up- and down-type contributions get enhanced and suppressed respectively and the resulting bound on $M_{KK}$ is

$$(M_{KK})^{KK(1gen)}_{\epsilon'/\epsilon} \gtrsim 1.25\,Y\ \mathrm{T}eV. \qquad (67)$$

This bound is the most stringent in the $(\tilde{x}_i^{u,d}, \tilde{y}_i^{u,d})$ parameter space and corresponds to an highly unnatural set of parameter assignments, for which $V_{us} = 0$, and maximize the sum of up and down imaginary parts. Nevertheless, this bound is still less stringent than the one in the flavor anarchic case considered in [16], and it allows for $O(1\,\mathrm{Te}V)$ KK masses for $O(1)$ Yukawa couplings $Y \approx 1$, $\tilde{y}_{U,D} \simeq 1$. The latter values correspond to $\chi_0 = 0.155 M_{Pl}^{3/2}$, a value allowed by the neutrino oscillation data [1]. Notice also that in the flavor anarchic case [16] the most stringent bound on the KK scale arises from the combined Yukawa coupling dependence of the new physics contributions to $\epsilon'/\epsilon_K$ and $\epsilon_K$. The latter contribution comes from the tree level KK gluon exchange, it is inversely proportional to the Yukawa coupling, and provides the most stringent bound on the KK scale for $O(1)$ Yukawas. The combined bound on $M_{KK}$ in [16] has been obtained for Yukawa couplings of $\mathcal{O}(6)$, implied by the constraint from the tree level KK gluon exchange contribution to $\epsilon_K$. This contribution vanishes identically in RS-A$_4$ [1], thus relaxing one of the most stringent constraints of flavor anarchic models.

A more natural bound on the KK mass scale is obtained for the parameters assignment of Eq. (12) that provides an almost realistic CKM matrix, while still choosing $\tilde{x}_1^{u,d}$ and $\tilde{y}_1^{u,d}$ to maximize the imaginary parts of up- and down-type contributions according to Eq. (60). The resulting bound on $M_{KK}$ will be further suppressed by at most a factor of $\sqrt{2}$ compared to the one in Eq. (67). This bound (for $Y = 1$) is again significantly lower than the one implied by constraints arising from EWPM [1], in particular the $Zb_L\bar{b}_L$ coupling. This is a pleasing result in RS-A$_4$, indicating that constraints arising from new physics contributions to FCNC processes tend to be weaker than in flavor anarchic models, see for example [10, 14, 16] and references therein. Another important difference between RS-A$_4$ and anarchic frameworks stems from the dominance of SM-like dipole operators, and the lack of enhancement of the opposite chirality operators.

To conclude the analysis of the constraints arising from $\epsilon'/\epsilon$ we state the results from the numerical and semianalytical diagonalization of the three-generation $12 \times 12$ mass matrices. For $x = 0.037$ the numerical result is

$$(\delta_{\epsilon'})^{Num.}_{RS-A4} \simeq 0.1 \quad (M_{KK})^{Num.}_{RS-A4} \gtrsim 0.98\,\mathrm{Te}V\,, \qquad (68)$$

close to the spurion-overlap and the one-generation mass-matrix diagonalization approximations. The results of the semianalytical diagonalization for the RS-A$_4$ contributions to $\epsilon'/\epsilon$ are given by

$$(\delta_{\epsilon'})^{12\times12th}_{RS-A4} \simeq 0.3 \qquad (M_{KK})^{12\times12th}_{RS-A4} \simeq 2.5\,Y\,\mathrm{Te}V\,. \qquad (69)$$

As anticipated, the deviation of the semianalytical $12 \times 12$ estimate from the numerical one can be attributed to the fact that the mass matrices in the first case are only approximately diagonalized, and a residual contamination of $\mathcal{O}(x)$ is noticed to be still present in the second- and third-generation off-diagonal blocks of the approximately diagonalized mass matrix. Nonetheless, the importance of the semianalytical method stays in providing some insight into the way the $\mathrm{A}_4$ flavor structure induces cancellation patterns, due to the explicit phase structure of the LO Yukawa interactions in Eq. (5).

## 5.3 How stringent is the constraint from $b \to s\gamma$?

Measurements of the branching ratio $\mathrm{BR}(B \to X_s\gamma)$ are already accurate enough to provide stringent constraints on new physics contributions to $b \to s\gamma$. It is thus instructive to obtain the NP physics contributions to $b \to s\gamma$ in RS-$\mathrm{A}_4$, derive the corresponding bound on the KK mass scale and compare with the flavor anarchic results of [16] and [15].
As it is also true for $\epsilon'/\epsilon$, and in contrast to flavor anarchic models, the largest contribution to $b \to s\gamma$ in RS-$\mathrm{A}_4$ is generated by the single-chirality effective dipole operator

$$O_7 = \frac{e m_b}{8\pi^2} \bar{b}_R \sigma^{\mu\nu} F_{\mu\nu} s_L \,, \tag{70}$$

while the contribution arising from the opposite chirality operator $O_7'$ is suppressed by $m_s/m_b$ as in the SM. This can easily be inferred by looking at the $i = 2, j = 3$ (for $O_7$) and $i = 3, j = 2$ (for $O_7'$) components of the Wilson coefficients defined in Eqs. (29) and (30).
The Wilson coefficient $C_7$ for $O_7$ is generated by the loop amplitudes in Figs. 1 and 2 and we follow the same procedure as for $\epsilon'/\epsilon$ to estimate the dominant contributions to $C_7$[5]. For the down-type contributions we obtain the following dominant terms

$$(C_7)^{d-type} \simeq -\frac{1}{3}\frac{B_P^d f_Q^2 m_s m_b}{8v^2 M_{KK}^2}\left(f_d^2 (\Delta_1^d)^* \Delta_2^d + f_s^2 (\Delta_3^d)\right) , \tag{71}$$

where the factor $-1/3$ comes from the charge of a down-type quark. Considering Eqs. (14)–(16), it is clear that the second term in Eq. (71) is dominant, despite the presence of $f_d^2$ in the first one. As before, we assign a collective magnitude to the $\tilde{x}_i^{u,d}$, $\tilde{y}_i^{u,d}$ parameters in terms of $\tilde{y}_{U,D}$ and look for the phase assignments that maximize the total contribution. We thus first rewrite the maximal magnitudes of $\Delta_{1,2,3}^d$, defined in Eqs. (14)–(16), in terms of $\tilde{y}_D$. It is straightforward to obtain

$$\begin{aligned} max(|\Delta_1^d|) &= \frac{m_d}{m_s}\left(2f_\chi^d + 2f_\chi^s\right)\tilde{y}_D \quad max(|\Delta_2^d|) = \frac{m_d}{m_b}\left(2f_\chi^d + 2f_\chi^b\right)\tilde{y}_D \\ max(|\Delta_3^d|) &= \frac{m_s}{m_b}\left(2f_\chi^s + 2f_\chi^b\right)\tilde{y}_D, \end{aligned} \tag{72}$$

and similar bounds for the up-type right-handed diagonalization matrices are obtained via the replacement $(d, s, b, \tilde{y}_D) \to (u, c, t, \tilde{y}_U)$ in the above equation. In particular, the bound in Eq. (72) on $\Delta_3^d$, to which the dominant term in Eq. (71) is proportional, is obtained with the assignment

---

[5] Considering the definition of $O_7$, we should correspondingly rescale the contributions coming from Eqs. (29) and (30) by $(8\pi^2/m_b)$, supplementing us again with a coefficient of dimension $[mass]^{-2}$.

$$\tilde{x}_2^d = \omega \tilde{y}_2^d = \tilde{x}_3^d = \omega \tilde{y}_3^d = \tilde{y}_D e^{i\delta_{bsD}} . \tag{73}$$

The above bounds can now be used to estimate the down-type contribution to $O_7$ leading to

$$(C_7)^{d-type} \simeq -\frac{Y^2 \tilde{y}_D}{4v^2 M_{KK}^2} \left( m_s^2 f_s^2 (f_\chi^s + f_\chi^b) + 2 m_d^2 f_d^2 (f_\chi^d + f_\chi^b)(f_\chi^d + f_\chi^s) \right) , \tag{74}$$

where we used $f_Q^2 \simeq 9.9$, and $B_P^d \simeq 1.5$ and made explicit the $Y^2$ scaling behavior. In the up sector, we learn from Eq. (30) that there are two dominant contributions to the effective coupling of $O_7$, leading to

$$(C_7)^{u-type} \simeq \frac{5}{3} \frac{B_P^u f_Q^2}{8v^2 M_{KK}^2} \left( (f_c^2 m_c^2 - f_t^2 m_t^2) V_{cb} + f_c^2 m_c^2 (f_\chi^c ((\tilde{x}_2^u)^* + \omega (\tilde{y}_2^u)^*) + f_\chi^t (\tilde{x}_3^u + \omega \tilde{y}_3^u) \right) , \tag{75}$$

where the factor 5/3 comes from the electric charge of an internal up-type quark in Fig. 1 and a negatively charged Higgs in Fig. 2. All the other up-type contributions to $C_7$ are suppressed by at least another order of magnitude. To obtain a conservative bound on NP contributions to $b \to s\gamma$, we can again find the maximal values of the combined up and down contributions in the model parameter space. We first use Eq. (10) to rewrite the up-type contribution as

$$\begin{aligned} (C_7)^{u-type} \simeq \frac{5}{3} \frac{B_P^u f_Q^2}{8v^2 M_{KK}^2} \Bigg[ & - f_t^2 m_t^2 \left( f_\chi^b (\tilde{x}_3^d + \omega \tilde{y}_3^d) - f_\chi^t (\tilde{x}_3^u + \omega \tilde{y}_3^u) \right) \\ & + f_c^2 m_c^2 \left( f_\chi^c ((\tilde{x}_2^u)^* + \omega (\tilde{y}_2^u)^*) + f_\chi^b (\tilde{x}_3^d + \omega \tilde{y}_3^d) \right) \Bigg] , \end{aligned} \tag{76}$$

where we use $f_c^2 m_c^2 \ll f_t^2 m_t^2$, and in particular $f_t^2 m_t^2 = (y_t^2/y_c^2)(r_{00}^t/r_{00}^c)^2 f_c^2 m_c^2 \simeq 6.35\, f_c^2 m_c^2$, so that the first term in Eq. (76) is dominant for $\mathcal{O}(1)$ parameter assignments.
The maximal combined up and down contributions to $C_7$ would be realized when both are real and negative. This corresponds to $\delta_{bsD} = 0$ in Eq. (73) and for the up sector:

$$\tilde{x}_3^u = \omega \tilde{y}_3^u = \tilde{x}_2^u = \omega \tilde{y}_2^u = -\tilde{y}_U . \tag{77}$$

With this assignment the second (subdominant) term in Eq. (76) vanishes. Using $B_P^u \simeq 1.5$ and $f_Q^2 \simeq 9.9$ we obtain

$$(C_7)^{u-type} \simeq -\frac{5 Y^2 \tilde{y}_U}{4v^2 M_{KK}^2} \left( f_t^2 m_t^2 (f_\chi^t + f_\chi^b) \right) . \tag{78}$$

It thus turns out that the up-type contribution to $b \to s\gamma$ dominates over the down-type by roughly an order of magnitude.
A bound on the KK mass scale can be extracted by comparing with the SM contribution to $b \to s\gamma$ and the corresponding experimental bound. Contrary to flavor anarchic models,

the dominant contributions from NP and SM both come from the single chirality Wilson coefficient $C_7$. The SM contribution evaluated at the $W$ scale can be written as follows [23]

$$C_7^{SM}(\mu_W) \simeq \frac{g^2|V_{tb}V_{ts}^*|D_0'(m_t)}{M_W^2} \simeq 1.06 \times 10^{-7}(\mathrm{Ge}V)^{-2}, \tag{79}$$

where $D_0'(m_t) \sim 0.4$, $M_W = 80.4$ GeV and $g \simeq 0.65$. Following the analysis in [15] we conveniently define the ratio between the NP and SM contributions as

$$\delta_7 \equiv \frac{C_7^{RS-A_4}(M_{KK})}{C_7^{SM}(\mu_W)} \simeq \frac{1.3 \times 10^{-7}(GeV)^{-2}}{1.06 \times 10^{-7}(GeV)^{-2}} \times \frac{(1\,\mathrm{TeV})^2}{M_{KK}^2} Y^2 \tilde{y}_U \,, \tag{80}$$

which is thus a function of $\tilde{y}_U$ and $M_{KK}$. An analogous definition holds for $C_7'$. We realize that, even for KK masses as low as 3 TeV and for the largest Yukawa allowed by perturbativity bounds $Y = 4\pi/\sqrt{N_{KK}} \sim 9$, the RS-A$_4$ new physics contribution predicted in the spurion-overlap approximation is at most comparable to the SM one, and it is suppressed by roughly an order of magnitude for the parameter assignments that yield a realistic CKM matrix. To impose a conservative bound on the KK mass scale we proceed as in the analysis of flavor anarchic models [15, 16]. To compare with the experiment, we use the model independent ratio [15] $\Gamma^{total}(b \to s\gamma)/\Gamma^{SM}(b \to s\gamma) \approx 1 + 0.68Re(\delta_7) + 0.11|\delta_7'|$ which takes into account the running from $M_{KK}$ down to $\mu_b$, with $\Gamma^{total} \propto |C_7(\mu_b)|^2 + |C_7'(\mu_b)|^2$. Given that the running of the Wilson coefficients from the KK scale down to $\mu_b$ remains an $\mathcal{O}(1)$ suppression effect, and using the experimental value for $BR(b \to s\gamma)$ affected by $\sim 10\%$ uncertainty, a $\mathcal{O}(20\%)$ departure of NP contributions from the SM prediction is still allowed. Considering separately the contributions from $C_7$ and $C_7'$, the allowed window translates into [15] $Re(\delta_7) \lesssim 0.3$ and $|\delta_7'| \lesssim 1.4$. Since the contribution to $C_7'$ in our setup is further suppressed by $m_s/m_b$ compared to the one of $C_7$ and the bound on $\delta_7'$ is far less stringent, the constraint on the KK mass scale will come from $\delta_7$. Substituting in Eq. (80), we obtain a conservative bound, which do not correspond to a realistic CKM matrix

$$(M_{KK})^{cons.}_{b\to s\gamma} \gtrsim 2.1\, Y \sqrt{\tilde{y}_U}\, \mathrm{Te}V\,. \tag{81}$$

Using instead the parameter assignment of Eq. (12) to obtain a realistic CKM matrix, leads to the more realistic constraint

$$(M_{KK})^{CKM}_{b\to s\gamma} \gtrsim 1.4\, Y \sqrt{\tilde{y}_U}\, \mathrm{Te}V\,. \tag{82}$$

One important difference between RS-A$_4$ and flavor anarchic models resides in the dominance of $C_7$ in the new physics contributions. This can obviously lead to different patterns of interference between NP and SM contributions in direct CP asymmetries. Hence, a study of the latter might discriminate among NP models more efficiently than the measure of branching ratios. In RS-A$_4$, a non trivial pattern of interference between $C_7^{RS-A_4}$ and $C_7^{SM}$ might be in place.

Since the above constraint is the most significant we have encountered so far, we go beyond the spurion-overlap approximation and use the results of the analytical diagonalization of

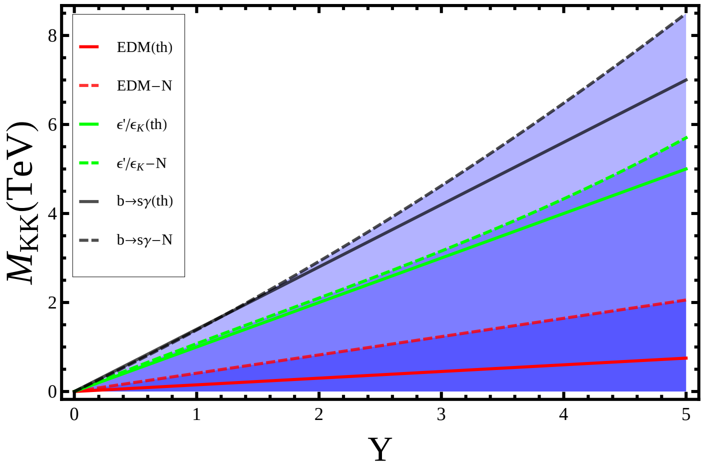

Figure 3: Bounds on the KK mass scale $M_{KK}$ as a function of the overall Yukawa scale $Y$ for the neutron EDM (bottom, red) $\epsilon'/\epsilon$ (centre, green) and $b \to s\gamma$ (top, black). The analytical (th) results (solid lines) are obtained within the one-generation approximation combined with the spurion-overlap analysis and compared with the numerical (N) results (dashed lines) of the three-generation case. In both cases, predictions are obtained for the model parameters that lead to a realistic CKM matrix.

the one-generation mass matrices. In this way we are able to obtain a better description of the overlap dependence of the above process. The modifications to the overlap factor $B_P^u$ for $b \to s\gamma$ are obtained in appendix B.2 and the resulting new overall correction factor is $(B_P^u)_{b\to s\gamma}^{KK(1gen)} \simeq -1.54$, which has a very moderate effect on the KK mass scale bound. The dependence of the resulting constraint on the size of Yukawa couplings is illustrated together with the constraints from $\epsilon'/\epsilon$ and the neutron EDM, in Fig. 3. Finally, we state the results of the numerical and semianalytical approach to the three-generation case. Numerically, and by adding up- and down-type contributions in quadrature, we obtain

$$(\delta_7)_{RS-A4}^{Num.} \simeq 0.03 \qquad (M_{KK})_{RS-A4}^{b\to s\gamma(Num.)} \gtrsim 1.27\,\mathrm{TeV}\,, \tag{83}$$

while the semianalytical diagonalization scheme leads to

$$(\delta_7)_{RS-A4}^{12\times 12th} \simeq 0.06 \qquad (M_{KK})_{RS-A4}^{12\times 12th} \gtrsim 1.8\,Y\,\mathrm{TeV}\,. \tag{84}$$

Fig. 3 provides a summary of the results obtained in this section. We compare the bounds on the KK mass scale $M_{KK}$ as a function of the Yukawa coupling for the neutron EDM, $\epsilon'/\epsilon$ and $b \to s\gamma$. Differently from flavor anarchic models, the most stringent constraint eventually comes from $b \to s\gamma$. For an overall Yukawa scale $Y \simeq 1$[6] all constraints are weaker than the one implied by EWPM, in particular $Zb_L\bar{b}_L$. In Fig. 3 we also compare the analytical prediction ($th$), obtained in the combined spurion-overlap and one-generation diagonalization scheme described in Sec. 4.1, with the *exact* numerical analysis ($N$) of all three generations. Both predictions are obtained for the model parameters that lead to a realistic CKM matrix. It is worth to recall that the analytical prediction for the neutron EDM reported in Fig. 3 and Eq. (50), represents a very conservative estimate coming from the up sector contribution in Eq. (48) and entirely due to the non degeneracy of overlap factors. Differently from other quantities, the neutron EDM identically vanishes in the spurion-overlap approximation with degenerate overlap factors.

---

[6] We recall that the overall Yukawa scale is defined as $y_{u,d,c,s,t,b} \to Y\, y_{u,d,c,s,t,b}$, with reference values $y_{u,d,c,s,b} = 1$ and $y_t = 2.8$.

We conclude that the constraints on new physics contributions from the neutron EDM, $(\epsilon'/\epsilon)$ and $b \to s\gamma$ are relaxed in our setup compared to generic warped flavor anarchic models. In order to impose significant bounds on the KK mass scale in RS-A$_4$ using the above processes we must wait for more precise measurements of these observables. This might not be the situation with Higgs mediated FCNCs, considered in the next section.

# 6 New physics from Higgs mediated FCNCs

It has been pointed out, both in the context of a composite Higgs sector of strong dynamics [18] and warped extra dimensions [19], that higher dimensional operators in the low energy 4D effective theory with extra insertions of a Higgs field generally leads to a misalignment between mass and Yukawa matrices and consequently to tree level Higgs mediated FCNCs. The presence of a misalignment is a quite general and model independent result.

In the RS-A$_4$ framework, once A$_4$ is completely broken by "cross-talk" interactions, the 4D effective Yukawa couplings originate from 5D Yukawa operators that involve the Higgs, and one or both flavons $\Phi$ and $\chi$. This is relevant to determine the typical strength of the effective 4D interactions. The operators that generate the misalignment between the Higgs Yukawa couplings and SM fermion mass matrices in the 4D effective theory, are of dimension six and can be written in terms of the 4D fields as follows [19]:

$$A^{u,d}_{ij}\frac{H^2}{\Lambda^2}H\bar{Q}_{L_i}(U_{R_j},D_{R_j}), \qquad B_{ij}\frac{H^2}{\Lambda^2}\bar{D}_{R_i}\not{\partial}D_{R_j}, \qquad C_{ij}\frac{H^2}{\Lambda^2}\bar{U}_{R_i}\not{\partial}U_{R_j}, \qquad K_{ij}\frac{H^2}{\Lambda^2}\bar{Q}_{L_i}\not{\partial}Q_{L_j}, \tag{85}$$

where $Q_{L_i}$ and $D_{R_i}(U_{R_i})$ are the $SU(2)_L$ SM fermion doublets and singlets, respectively, and the Higgs field $H = v + h$ is a 4D field containing the physical Higgs $h$. The scale $\Lambda$ is the 4D cutoff and the coefficients $A_{ij}$, $B_{ij}$, $C_{ij}$ and $K_{ij}$ are in general complex. The indices $i, j$ denote flavors of the SM quarks. Once the electroweak symmetry is broken at the Higgs VEV scale, $v = 174\,\text{GeV}$, the above operators will induce corrections to the fermion masses, Yukawa couplings and kinetic terms. The corrected mass and kinetic terms can be generically parametrized as [19]

$$v\left(\hat{y}^{SM}_{ij_d} + A^d_{ij}\frac{v^2}{\Lambda^2}\right)\bar{Q}_{L_i}D_{R_j}\,, \qquad \left(\frac{\delta_{ij}}{2} + K_{ij}\frac{v^2}{\Lambda^2}\right)\bar{Q}_{L_i}\not{\partial}Q_{L_j}\,, \qquad \left(\frac{\delta_{ij}}{2} + B_{ij}\frac{v^2}{\Lambda^2}\right)\bar{D}_{R_i}\not{\partial}D_{R_j}\,, \tag{86}$$

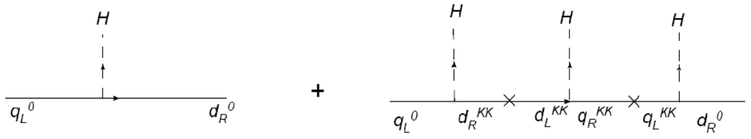

Figure 4: Higgs mediated corrections to masses and Yukawa couplings of SM fermions in the mass insertion approximation. The 4D effective Higgs field is defined here as $H = v + h$ and contains the physical Higgs field $h$.

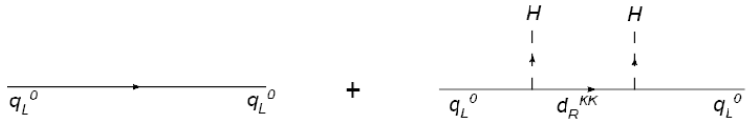

Figure 5: Higgs mediated corrections to kinetic terms of SM fermions in the mass insertion approximation.

while the corrected Yukawa interactions with the physical 4D Higgs $h$ are generally given by

$$\left(\hat{y}^{SM}_{ij_d} + 3A^d_{ij}\frac{v^2}{\Lambda^2}\right) h\bar{Q}_{L_i} D_{R_j} \, , \tag{87}$$

and analogously for the up contributions $A^u_{ij}$ and $C_{ij}$, where $\hat{y}^{SM}_{ij_{u,d}} \simeq \hat{Y}^{LO}_{ij_{u,d}} f^{-1}_{Q_i} f^{-1}_{u_j,d_j} r^{H\Phi}_{00}(c_{Q_i}, c_{u_j,d_j}, \beta)$ are the SM leading order Yukawa couplings. The origin of the misalignment between Yukawa couplings and SM masses [19] resides in the simple fact that an additional multiplicity factor 3 is associated with the corrected Yukawa couplings to the physical Higgs $h$. In the mass insertion approximation, the leading corrections to Yukawa couplings and fermion masses are generated by the second diagram in Fig. 4, while the corrections to the fermion kinetic terms are generated by the second diagram in Fig. 5 via the exchange of KK modes.

After redefining the fermion fields to canonically normalize the corrected fermion action, the total misalignment between SM masses and Yukawa couplings in the mass insertion approximation is given by [19]

$$\hat{\Delta}^{u,d}_{H} = \hat{m}^{SM}_{u,d} - \hat{y}^{SM}_{u,d}\, v = \hat{\Delta}^{u,d}_{H_1} + \hat{\Delta}^{u,d}_{H_2}, \tag{88}$$

where

$$\hat{\Delta}^{u,d}_{H_1} = -2A^{u,d}_{ij}\frac{v^2}{\Lambda^2} \qquad \hat{\Delta}^{u(d)}_{H_2} = -\left(K_{ij}\frac{v^2}{\Lambda^2} + C_{ij}(B_{ij})\frac{v^2}{\Lambda^2}\right) . \tag{89}$$

It is clear that, after the shift in Eq. (88), the SM mass matrix and Yukawa couplings are in general not diagonalized by the same biunitary transformation. Thus, in the diagonal mass basis, non-diagonal Yukawa interactions are in general present and induce FCNC processes by tree level Higgs exchange.

In [15] the contributions of Higgs mediated FCNC to $\Delta F = 2$ processes were estimated in the framework of flavor anarchy. It was found that the dominant contribution to the misalignment is in this case due to $(--)$ KK modes, and does not vanish for an IR localized Higgs, contrary to the conclusions of previous analyses [27]. Also, the overall misalignment was calculated by mass diagonalization in the one-generation approximation, and generalized to three generations using a spurion analysis in the mass insertion approximation [10]. Here, we analyze the same misalignment in the context of RS-A$_4$ to establish whether a significant suppression of Higgs mediated FCNC contributions to $\Delta F = 2$ processes can be induced by the particular structure of up and down diagonalization matrices of A$_4$.

We start with writing the explicit flavor structure of the corrections in Eq. (89), in the IR localized case and using the spurion analysis in the mass insertion approximation. In the special interaction basis one would in this case obtain

$$\left(\hat{\Delta}^{u,d}_{H_1}\right)_{ij} = -\frac{2v^3 R'^2}{3}\left[F_Q \hat{Y}_{u,d}\hat{Y}^\dagger_{u,d}\hat{Y}_{u,d}F_{u,d}\right]_{ij}\,, \tag{90}$$

$$\left(\hat{\Delta}^{u,d}_{H_2}\right)_{ij} = -R'^2\left[\hat{m}_{u,d}\left(\hat{m}^\dagger_{u,d}\hat{K}(c^L_q) + \hat{K}(c_{u_i,d_i})\hat{m}^\dagger_{u,d}\right)\hat{m}_{u,d}\right]_{ij}, \tag{91}$$

where $\hat{K}(c_i) = \mathrm{d}iag(K(c_i))$ and

$$K(c) = \frac{1}{1-2c}\left[-\frac{1}{\varepsilon^{2c-1}-1} + \frac{\varepsilon^{2c-1}-\varepsilon^2}{(\varepsilon^{2c-1}-1)(3-2c)} + \frac{\varepsilon^{1-2c}-\varepsilon^2}{(1+2c)(\varepsilon^{2c-1}-1)}\right], \tag{92}$$

with $(R')^{-1} = k\,e^{-k\pi R} \approx 1.8$ TeV the UV cutoff of the 4D theory and $\varepsilon = R/R' = e^{-k\pi R}$. The function $K(c)$ was obtained in [19] by taking the brane localized Higgs limit ($\beta_H \to \infty$) of the original bulk function for one generation of down-type quarks. The $c$ dependence of $K(c)$ renders the shift from kinetic terms subdominant w.r.t. the one arising from Yukawa interactions, in the case of first and second generation quarks that interest us.

To account for bulk effects in the three-generation case we use the spurion-overlap approximation of Sec. 3.3. One can easily realize that the general flavor structure of the shift in Eq. (90) for the up and down sectors is identical to the one of the down-type contributions to dipole operators. This means that we can rewrite Eq. (90) in the form of Eq. (29) with a new factor $B^H_{P_{u,d}}$ that quantifies to a good approximation the overall effect of overlap corrections present in the second diagram of Fig. 4. The difference with the dipole operator case in Eq. (21) stems from the different type of KK modes: $d^{KK}_L$ and $q^{KK}_R$ in Fig. 4 denote $(--)$ and $(+-)$ KK states in custodial RS-A$_4$. The flavor structure of the dominant contribution to the misalignment $\hat{\Delta}^{u,d}_{H_1}$ thus contains two terms

$$\begin{aligned}(\hat{\Delta}^{d,u}_{H_1})_{(++)} &\propto F_Q\hat{Y}_{d,u}\,r_{01}(c_{Q_i}, c_{d_{\ell_1},u_{\ell_1}}, \beta)\,\hat{Y}^\dagger_{d,u}\,r_{1-1-}(c_{d_{\ell_1},u_{\ell_1}}, c_{Q_{\ell_2}}, \beta)\,\hat{Y}_{d,u}\,r_{10}(c_{Q_{\ell_2}}, c_{d_j,u_j})F_{d,u}\,,\\ (\hat{\Delta}^{d,u}_{H_1})_{(-+)} &\propto F_Q\hat{Y}_{u,d}\,r_{01-+}(c_{Q_i}, c_{u_{\ell_1},d_{\ell_1}}, \beta)\,\hat{Y}^\dagger_{u,d}\,r_{1+-1}(c_{u_{\ell_1},d_{\ell_1}}, c_{Q_{\ell_2}}, \beta)\,\hat{Y}_{d,u}\,r_{10}(c_{Q_{\ell_2}}, c_{d_j,u_j}, \beta)F_{d,u}\,.\end{aligned} \tag{93}$$

Given the almost degeneracy of overlap factors as shown in appendix A.1, we can again work in the approximation analogous to Eq. (29), and define $B^H_{P_{u,d}}$

$$B^H_{P_{u,d}} = \mathrm{m}ax\left( (\hat{r}^{u,d}_{00})^{-3} (\hat{r}^{u,d}_{01} \hat{r}^{u,d}_{1^-1^-} + \hat{r}^{u,d}_{01^{-+}} \hat{r}^{u,d}_{1^{+-}1^-})\, \hat{r}^{u,d}_{10} \right) \tag{94}$$

as an overall multiplicative overlap factor. It is now important to notice that the IR peaked profile of both $\Phi$ and the Higgs and the vanishing of the $(--)$ and $(+-)$ profiles at the IR brane, provide a suppression by almost an order of magnitude of the overlap factors $r_{1^-1^-}$ and $r_{1^{+-}1^-}$ compared to $r_{11}$ and $r_{1^{-+}1}$, rendering $\hat{\Delta}^{u,d}_{H_1}$ smaller, but still dominant over $\hat{\Delta}^{u,d}_{H_2}$. In the same approximation of Eq. (29) and in the mass basis $\hat{\Delta}^{u,d}_{H_1}$ reduces to

$$(\hat{\Delta}^{u,d}_{H_1})_{ij} \;=\; -\frac{2R'^2 f_Q^2 m_{u_i,d_i} m^2_{u_j,d_j} B^H_{P_{u,d}}}{3} \sum_{n=1}^{3} (V_R^{u,d})^*_{ni} (V_R^{u,d})_{nj} f^2_{u_n,d_n}\,. \tag{95}$$

Disregarding $\hat{\Delta}^{u,d}_{H_2}$, the off-diagonal Yukawa couplings in the mass basis are then obtained by dividing the contribution in Eq. (95) by the Higgs VEV, $v$. Recalling the structure of the right-handed diagonalization matrices in Eq. (13) and the hierarchy of $f_{u_i,d_i}$, it is straightforward to identify the dominant corrections. Defining $(\Delta\hat{y}^{u,d}_{SM})_{ij} \equiv a^{u,d}_{ij} \equiv (\hat{\Delta}^{u,d}_{H_1})_{ij}/v$ we obtain

$$a^{u,d}_{ij} \simeq \frac{-2R'^2 f_Q^2 m_{u_i,d_i} m^2_{u_j,d_j} B^H_{P_{u,d}}}{3v} \begin{pmatrix} f^2_{u,d} & f^2_{u,d}\Delta^{u,d}_1 & f^2_{u,d}\Delta^{u,d}_2 \\ -f^2_{u,d}(\Delta^{u,d}_1)^* & f^2_{c,s} & f^2_{c,s}\Delta^{u,d}_3 \\ -f^2_{u,d}(\Delta^{u,d}_2)^* & -f^2_{c,s}(\Delta^{u,d}_3)^* & f^2_{t,b} \end{pmatrix}_{ij} . \tag{96}$$

Hence, new 4D effective operators of the form $a^d_{ij} h \bar{d}^i_L \bar{d}^j_R + (d \to u) + \mathrm{h.}c.$ will induce tree level Higgs mediated FCNC. One can already notice that the suppression of third-generation couplings, as for $\bar{t}t$, is much milder than in the flavor anarchic case [19]. For $R' \simeq 1.8$ TeV, the suppression amounts to $\Delta y_t/y_t \sim 4 \times 10^{-3}$. This is due to the degeneracy of the left-handed fermion profiles $f_Q$ and the consequent factorization of the left-handed matrices $V_L$.

## 6.1 Low energy physics bounds from $\Delta F = 2$ processes

The Higgs flavor violating couplings can induce tree level FCNC contributions to various observables. The most stringent constraints on their size may come from experimental bounds on $\Delta F = 2$ processes, such as $K - \bar{K}$, $B_{d,s} - \bar{B}_{d,s}$ and $D - \bar{D}$ mixing. $\Delta F = 2$ processes are described by the general effective Hamiltonian [23, 28]:

$$\mathcal{H}^{\Delta F=2}_{eff} = \sum_{a=1}^{5} C_a O^{q_i q_j}_a + \sum_{a=1}^{3} C'_a O'^{q_i q_j}_a, \tag{97}$$

where

$$O_1^{q_iq_j} = \bar{q}_{jL}^{\alpha}\gamma_\mu q_{iL}^{\alpha}\bar{q}_{jL}^{\beta}\gamma^\mu q_{iL}^{\beta}, \quad O_2^{q_iq_j} = \bar{q}_{jR}^{\alpha}q_{iL}^{\alpha}\bar{q}_{jR}^{\beta}q_{iL}^{\beta}, \quad O_3^{q_iq_j} = \bar{q}_{jR}^{\alpha}q_{iL}^{\beta}\bar{q}_{jR}^{\beta}q_{iL}^{\alpha}$$
$$O_4^{q_iq_j} = \bar{q}_{jR}^{\alpha}q_{iL}^{\alpha}\bar{q}_{jL}^{\beta}q_{iR}^{\beta}, \quad O_5^{q_iq_j} = \bar{q}_{jR}^{\alpha}q_{iL}^{\beta}\bar{q}_{jL}^{\beta}q_{iR}^{\alpha}\,, \tag{98}$$

with color indices $\alpha$, $\beta$. The opposite chirality operators are denoted with a $'$ and obtained from the operators above by the replacement $L \leftrightarrow R$. For $K-\bar{K}$, $B_d - \bar{B}_d$, $B_s - \bar{B}_s$ and $D - \bar{D}$ mixing we have $q_iq_j = sd, bd, bs$ and $uc$, respectively. In particular, Higgs mediated tree-level processes as in Fig. 6 generate new contributions to $C_2$, $C_2'$ (Fig. 6(A)) and $C_4$ (Fig. 6(B)) [19]. They read as follows

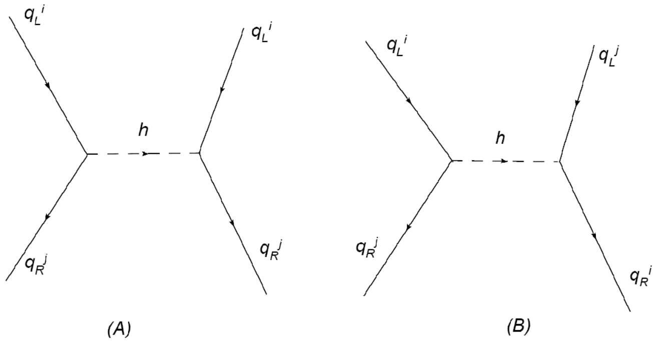

Figure 6: Contributions to $\Delta F = 2$ processes from Higgs exchange at tree level.

$$C_2^h = \frac{a_{ij}^2}{m_h^2} \qquad C_2'^h = \frac{a_{ji}^2}{m_h^2} \qquad C_4^h = \frac{a_{ij}a_{ji}}{m_h^2}, \tag{99}$$

where $m_h$ denotes the mass of the physical Higgs. We adopt the model independent bounds of [28], renormalized at the scale $\mu_h = 200$ GeV as in [19], to make the comparison with the flavor anarchic results in [19] transparent. The bounds

$$\mathrm{I}mC_2^K \leq 2.04 \times 10^{-16} GeV^{-2}, \quad \mathrm{I}mC_4^K \leq 5.9 \times 10^{-17} GeV^{-2}, \quad |C_2^D| \leq 2.77 \times 10^{-13} GeV^{-2},$$
$$|C_4^D| \leq 1.18 \times 10^{-13} GeV^{-2}, \quad |C_2^{B_d}| \leq 1.23 \times 10^{-12} GeV^{-2}, \quad |C_4^{B_d}| \leq 5.1 \times 10^{-13} GeV^{-2},$$
$$|C_2^{B_s}| \leq 1 \times 10^{-10} GeV^{-2}, \quad |C_4^{B_s}| \leq 3.46 \times 10^{-11} GeV^{-2} \tag{100}$$

directly constrain both $m_h$ and $a_{ij}$, and provide lower bounds for the KK mass scale. The most stringent bound in RS-$A_4$ should be provided by $\mathrm{I}mC_4^K$ and comes from $\epsilon_K$. Using Eqs. (99) and (96) in the spurion-overlap approximation with an overall overlap factor, one obtains

$$\mathrm{I}m(C_4^K)_{RS-A_4} \simeq \mathrm{I}m\left(\frac{(2B_P^{H_d}f_Q^2R'^2)^2}{m_h^2(3v)^2}f_d^4 m_d^3 m_s^3 \Delta_1^d \Delta_1^{d*}\right) = 0 \tag{101}$$

for any parameter assignment to first order in $\tilde{x}_i^d$ and $\tilde{y}_i^d$. The next strongest constraint should come from $C_2^K$. Using again Eqs. (99) and (96), assuming $\mathrm{I}m((\Delta_1^d)^2) = (\mathrm{m}ax(|\Delta_1^d|))^2 =$

$4\tilde{y}_D^2(f_\chi^d+f_\chi^s)^2$, choosing $m_h = 300$ GeV and $R' = (1.8\,\mathrm{Te}V)^{-1}$ as reference values, the largest contribution to $C_2^K$ in the same approximation is

$$\mathrm{I}m(C_2^K)_{RS-A_4} \simeq \mathrm{Im}\left(\frac{(2B_P^{H_d} f_Q^2 R'^2)^2}{m_h^2(3v)^2} f_d^4 m_d^2 m_s^4 \Delta_1^d \Delta_1^d\right) \simeq 1.4{\times}10^{-20}\,\mathrm{Ge}V^{-2}\left(\frac{Y^2\tilde{y}_D(1.8\,\mathrm{Te}VR')^4}{(m_h/300\,\mathrm{Ge}V)^2}\right) \tag{102}$$

where we used $f_d = 2.24 \times 10^4$, $f_Q = 3.13$ and $B_P^{H_d} \simeq 0.18$. Thus, both constraints from $C_4$ and $C_2$ are strongly suppressed in our setup. This is again due to the $\mathrm{A}_4$ pattern of the Yukawa matrices. Suppression factors come from the mass ratios in $V_R^d$, due to the mass hierarchy and the consequent hierarchy of right-handed fermion profiles in $\mathrm{A}_4$, the presence of $f_\chi^{d,s,b}$ suppression factors also in $V_L^d$, and the suppressed overlap of $(--)$ and $(+-)$ fermion KK modes with the IR peaked VEV of $\Phi$ and the bulk Higgs. The same sources of suppression are at work in the up sector. For completeness, we obtain the largest possible estimation of the NP contribution to $C_2^D$, the most constraining bound in the up sector. Assuming $\mathrm{I}m((\Delta_1^u)^2) = (\mathrm{m}ax(|\Delta_1^u|))^2 = 4\tilde{y}_U^2(f_\chi^u + f_\chi^c)^2$, and using the same reference values for $m_h$ and $R'$ as before, we obtain

$$|(C_2^D)|_{RS-A_4} = \left|\frac{(2B_P^{H_u} f_Q^2 R'^2)^2}{m_h^2(3v)^2} f_u^4 m_u^2 m_c^4 \Delta_1^u \Delta_1^u\right| \simeq 2.4 \times 10^{-18}\mathrm{Ge}V^{-2}\left(\frac{Y^2\tilde{y}_U(1.8\,\mathrm{Te}VR')^4}{(m_h/300\,\mathrm{Ge}V)^2}\right), \tag{103}$$

where we used $B_P^{H_{u,d}} = 0.18$ from Eq. (90). The above contribution is almost six orders of magnitude suppressed compared to the model independent bound in Eq. (100). Higher order corrections in $\tilde{x}_i^{u,d}$ and $\tilde{y}_i^{u,d}$ will induce terms which are suppressed by at least $O(f_\chi^{u_i,d_i})$ compared to the first order terms and they will generally combine incoherently. Hence, it seems safe to expect that Higgs mediated FCNC contributions to $\Delta F = 2$ processes do not provide the most stringent bounds on the KK mass scale in the RS-$\mathrm{A}_4$ model, even going beyond the spurion-overlap approximation and taking full account of generational mixing. Far more stringent constraint thus remains the one coming from the $Zb_L\bar{b}_L$ coupling, which is fairly satisfied for the choice $c_q^L = 0.4$, $R'^{-1} = 1.8$ TeV, $m_h = 150$ GeV and order one Yukawa couplings. Fig. 7 also shows how the bound on the KK mass $M_{KK} \simeq 2.55\,R'^{-1}$ becomes weaker upon increasing the Higgs mass.

# 7 Conclusions

We have illustrated how the presence of an additional $\mathrm{A}_4$ flavor symmetry in the bulk of a warped two-brane scenario allows to relax the most stringent lower bounds on the KK mass scale typical of flavor anarchic models. The most relevant difference between the RS-$\mathrm{A}_4$ model proposed in [1] and flavor anarchy stems from the degeneracy of the left-handed fermion bulk profiles, and the consequent factorization of the left-handed rotation matrices in many contributions to dipole operators. The flavor hierarchy of the Standard Model is induced by the $\mathrm{A}_4$ texture of the 5D Yukawa couplings and the bulk mass parameters of the right-handed fermions.

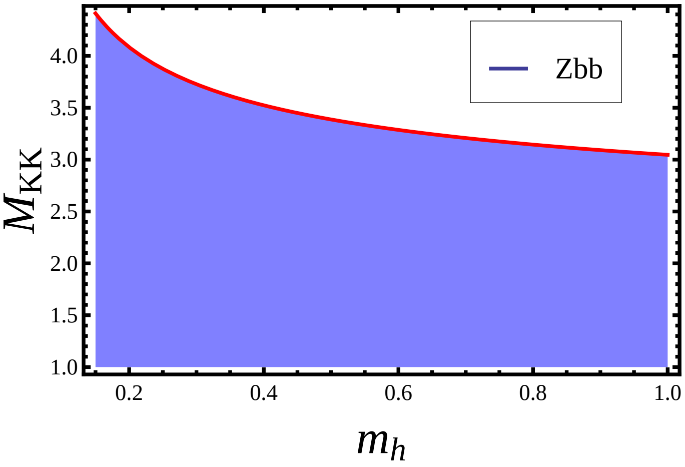

Figure 7: Bound on the KK mass scale $M_{KK}$(TeV) from $Zb_L\bar{b}_L$ as a function of the Higgs mass, $m_h$(TeV).

At leading order in an expansion in powers of the UV cutoff of RS-A$_4$, i.e. in the absence of cross-talk interactions [1], the CKM matrix is the unit matrix and no quark mixing is generated in the effective 4D theory. At next-to-leading order, an almost realistic CKM matrix is obtained in a rather economical way, due to the presence of cross-talk higher-dimensional operators and cross-brane interactions. We have also shown in [1] that the structure of the leading order Yukawa couplings may induce exact cancellations in the contributions to dipole operators. It is hence natural to expect the suppression of many contributions to the same operators, once the next-to-leading order corrections to the Yukawa couplings are taken into account, as compared with flavor anarchic descriptions.

It should also be noticed that whenever a flavor symmetry is present in the 5D theory, it is important – and more relevant than in flavor anarchic models – to fully account for non-degeneracies and KK mixing patterns within the same generation and among generations. For this reason, we have considered various analytical approximations and compared their prediction with an *exact* analysis based on a fully numerical diagonalization of the complete KK mass matrix, a $12 \times 12$ matrix in the custodial case for three generations.

Concerning flavor violating processes, the first relevant difference with flavor anarchic models is the fact that new physics contributions are dominated by the same chirality operators as in the Standard Model and no enhancement of the opposite chirality operators is in place. Another relevant feature is the vanishing of the dominant new-physics contribution to $\epsilon_K$, mediated by a KK gluon exchange at tree level. This has striking consequences, due to the fact that this contribution to $\epsilon_K$ is inversely proportional to the Yukawa scale, while other relevant observables such as $\epsilon'/\epsilon_K$, $b \to s\gamma$ and the neutron EDM are directly proportional to the Yukawa scale. The consequence in flavor anarchic models [16] is that the combined constraints from $\epsilon_K$, $\epsilon'/\epsilon_K$ and $b \to s\gamma$ force large Yukawa couplings, closer to the perturbativity bound, and an overall bound $M_{KK} \gtrsim 7.5$ TeV. In addition, the little CP problem [10], related to the generation of a far too large neutron EDM in flavor anarchy, remains to be solved. In contrast, given the vanishing of the leading new physics contributions to $\epsilon_K$ in RS-A$_4$, the most relevant constraints on the new physics scale should come from the remaining FCNC processes, while relaxing the constraints on the size of the Yukawa couplings.

Fig. 3 is a summary of the most relevant results for FCNC processes in RS-A$_4$, expressed in terms of the lower bounds on the KK mass scale $M_{KK} \simeq 2.55\, R'^{-1}$ and by varying the typical size of Yukawa couplings. Given the absence of the constraint from $\epsilon_K$, an $O(1)$ Yukawa coupling is allowed, providing the overall bound $M_{KK} \gtrsim 1.3$ TeV, induced by $b \to s\gamma$. The latter bound is weaker than any flavor anarchic bound and less stringent than the bound $M_{KK} \gtrsim 4.6$ TeV, from $Zb_L\bar{b}_L$ in RS-A$_4$ [1]. Another salient feature in Fig. 3 is the substantial suppression of new physics contributions to the neutron EDM. This stems from the A$_4$-induced degeneracies in the left-handed fermion sector, which determine the vanishing of these contributions to the EDM also at next-leading-order in the Yukawa couplings, in the spurion-overlap analysis within the mass insertion approximation.

The pattern of HMFCNC in RS-A$_4$ shows a much milder suppression of the top Yukawa coupling if compared with flavor anarchic models, and more in general the A$_4$ flavor structure guarantees weak bounds on the KK mass scale induced by Higgs mediated FCNC processes. We defer to future work the study of potentially interesting features of an extended $P_{LR}$ custodial symmetry [29, 21] within a A$_4$ warped flavor model. Such an additional symmetry is known [21] to relax the constraints from $Zb_L\bar{b}_L$.

We conclude that the little CP problem related to the neutron EDM in flavor anarchic models is avoided in the custodial RS-A$_4$, while the most stringent bounds on the KK mass scale come from EWPM, in particular the $Zb_L\bar{b}_L$ coupling. The dominance of the constraint induced by $b \to s\gamma$ over the constraints from $\epsilon'/\epsilon_K$ and the neutron EDM mainly stems from the amount of non-degeneracy of the third-generation Yukawa coupling, in turn induced by the degeneracy of the left-handed 5D profiles of all quarks in A$_4$.

### Acknowledgments

We thank Aleksander Azatov, Yuval Grossman and Gilad Perez for useful discussions. The work of A.K is supported in part by the Ubbo Emmius scholarship program at the University of Groningen.

# A Explicit Calculation of Overlap Corrections

In this appendix we define and obtain explicitly the various overlap correction factors introduced in Eq. (1) and discussed through the text. We start by some definitions. The bulk geometry is a slice of $AdS_5$ compactified on an orbifold $S_1/Z_2$ and can be described by the proper distance metric

$$ds^2 = dy^2 + e^{-2k|y|}\eta_{\mu\nu}dx^\mu dx^\nu, \tag{104}$$

where $k \simeq M_{Pl}$ is the $AdS_5$ curvature scale and $-\pi R \leq y \leq \pi R$. The UV and IR branes are located at the orbifold fixed points $y = 0$ and $y = \pi R$, respectively. The same problem is also studied by many authors in an interval setup with conformal coordinates. The corresponding metric is in this case

$$ds^2 = \left(\frac{R}{z}\right)^2 \left(-dz^2 + \eta_{\mu\nu} dx^\mu dx^\nu\right), \tag{105}$$

where $z = e^{ky}/k$, defined on the interval $(R, R')$ with $R = z_h = 1/k$ and $R' = z_v = e^{k\pi R}/k$. One feature of the interval setup is that it naturally allows for more general boundary conditions (BC) for the bulk fields, as compared to the orbifold case. On the other hand, only the orbifold fixed points can be naturally interpreted as the location of physical branes due to source terms originating from the "jump" of derivatives at the fixed points; in the interval picture branes can only be assumed to be located at the edges of the interval, namely $z_h$ and $z_v$. Since in the orbifold case the behavior of all bulk fields in the interval $[-\pi R, 0]$ is determined by their transformation law under the orbifold $Z_2$ symmetry, we normalize all wave functions and perform all integrals on the interval $[0, \pi R]$ without loss of generality.

The normalized wave function for a fermion left-handed zero mode as a function of its bulk mass is

$$\chi_0(c_{f_i}, y) = \sqrt{\frac{2k(1/2 - c_{f_i})}{e^{\pi k R(1-2c_{f_i})} - 1}}\, e^{(2-c_{f_i})k|y|}, \tag{106}$$

where $f_i = Q_i, \ell_i, u_i, d_i, e_i$ and $c_{f_i}$ is the corresponding bulk mass given in units of $k$. A right-handed zero mode is obtained with the replacement $c \to -c$. The canonically normalized wave function on the IR brane, $\hat{\chi}_0$, is defined as $\hat{\chi}_0(c_{f_i}, \pi R) = e^{(-3/2)k\pi R}\chi_0(c_{f_i}, \pi R)$.

The induced 4D VEV's of the IR peaked bulk scalars $\Phi$ and $H$, required for the definition of the IR localized Higgs limit, are related to the 5D VEV's as follows

$$H_0(\Phi_0) = \sqrt{\frac{2k(1+\beta_{H(\Phi)})}{1 - e^{-k\pi R(2+2\beta_{H(\Phi)})}}}\, v^{4D}_{H(\Phi)} e^{k\pi R} \simeq \sqrt{2k(1+\beta_{H(\Phi)})}\, v^{4D}_{H(\Phi)} e^{k\pi R}, \tag{107}$$

where $\beta_{H,\Phi} = \sqrt{4 + \mu^2_{H,\Phi}}$ tunes the amount of localization from the UV to the IR and $\mu_{H,\Phi}$ is the corresponding bulk mass in units of $k$. The above relation is obtained by integrating the solution (for $H$ or $\Phi$) of the bulk equation of motion along the extra dimension [22]. In the IR localized Higgs and $\Phi$ case, the charged fermion masses arising from the Yukawa coupling to the Higgs, and before diagonalization, are obtained via [30]:

$$(\hat{m}_f)^{ij}_{IR} = (\hat{y}^f_{ij})_{LO} \frac{v v^{4D}_\Phi e^{k\pi R}}{k^2} \hat{\chi}_0(c_{\ell_i}(c_{Q_i}), \pi R)\hat{\chi}_0(c_{e_{R_j}}(c_{q_{R_j}}), \pi R) = \frac{2(\hat{y}^f_{ij})_{LO}\, v v^{4D}_\Phi e^{k\pi R}}{k f_{\ell_i, Q_i} f_{e_j, u_j(d_j)}}, \tag{108}$$

where $q = u, d$, the matrix $(\hat{y}^f_{ij})_{LO}$ of dimensionless 5D couplings is defined in Eq. (5) and $v \equiv v^{4D}_H = 174$ GeV is the Higgs VEV. In the second equality we write the fermion masses in similar notations to [10], where $f_{f_i} = \sqrt{2k}/\hat{\chi}_{0_{f_i}}$ to make the comparison with their results more transparent. In the setup we use, where charged fermion masses are generated by the

Yukawa interactions with bulk $H$ and $\Phi$ and where LH fermion bulk masses are degenerate, we have to consider the overlap of scalar VEV profiles and zero mode fermion profiles, leading to the following masses before diagonalization:

$$(\hat{m}_f)^{ij}_{Bulk} = (\hat{y}^f_{ij})_{LO}\frac{H_0\Phi_0}{k^2}\int_0^{\pi R} dy e^{-4k|y|}e^{(4+\beta_H+\beta_\Phi)(k|y|-\pi R)}\chi_0(c_{\ell_i}(c_{Q_i}),y)\chi_0(c_{e_{R_j}}(c_{q_{R_j}}),y)\,. \tag{109}$$

As a natural choice for the bulk scalar profile, we assume [22] $\beta_{H,\Phi} \simeq 2+\epsilon$, with $\epsilon$ a small parameter for stabilisation purposes. To obtain the physical quark masses at the scale $ke^{-k\pi R} \simeq 1.8$ TeV we used the following assignment [1]:

$$c^L_q = 0.4, \quad c_u = 0.79, \quad c_d = 0.77, \quad c_s = 0.683, \quad c_c = 0.602, \quad c_b = 0.557, \quad c_t = -0.17\,, \tag{110}$$

with $y_{u,c,d,s,b} = 1$ and $y_t \simeq 2.8$, which is still required to match $m_t(\mu = 1.8TeV) \simeq 140$ GeV. The integration in Eq. (109) is straightforward, given that all functions are simple exponentials and only depend on $\beta = \beta_H + \beta_\Phi$. Dividing Eq. (109) by Eq. (108), we obtain the definition of the (LO) RS-A$_4$ zero-zero overlap correction factors

$$(r^{H\Phi}_{00})_{ij} = \frac{(\hat{m}_f)^{ij}_{Bulk}}{(\hat{m}_f)^{ij}_{IR}} \simeq \frac{(2\sqrt{(1+\beta_H)(1+\beta_\Phi)}v^{4D}_\Phi v e^{2k\pi R})}{(4+\beta_H+\beta_\Phi - c^L_q - c_{u_i,d_i})v^{4D}_\Phi v e^{2k\pi R}} \simeq \frac{6}{8-c^L_q-c_{u_i,d_i}}, \tag{111}$$

where we used $\beta_H = \beta_\Phi \simeq 2$, $H_0 = 0.396M^{3/2}_{Pl}$, $\Phi_0 = 0.577M^{3/2}_{Pl}$, $k \simeq M_{Pl} = 2.44\times 10^{18}TeV$ and $k\pi R \simeq 34.8$. The numerical values of the bulk parameters in Eq. (110) lead to

$$r^{u,d}_{00} \simeq 0.88 \quad r^s_{00} \simeq 0.87 \quad r^c_{00} \simeq 0.86 \quad r^b_{00} \simeq 0.85 \quad r^t_{00} \simeq 0.77\,, \tag{112}$$

with a rather mild flavor dependence. In an analogous way we obtain $r^{H\Phi\chi}_{00}$, the overlaps associated with the NLO Yukawa interactions of Eq.(7), for which the corresponding integration for $\beta_\chi = 2$ was already performed in [1]:

$$\begin{aligned} r^{H\Phi\chi}_{00}(\beta_{H,\Phi,\chi}, c^L_q, c_{u_i,d_i}) &\simeq \frac{4\sqrt{2}\beta_\chi\sqrt{(1+\beta_H)(1+\beta_\Phi)(1+\beta_\chi)}}{(6+\beta_H+\beta_\Phi+\beta_\chi-c^L_q-c_{u_i,d_i})(6+\beta_H+\beta_\Phi-\beta_\chi-c^L_q-c_{u_i,d_i})} \\ &\simeq \frac{24\sqrt{6}}{(12-c^L_q-c_{u_i,d_i})(8-c^L_q-c_{u_i,d_i})}, \end{aligned} \tag{113}$$

where in the second equality we used $\beta_{H,\Phi,\chi} = 2+\epsilon_{H,\Phi,\chi}$ and $\epsilon_{H,\Phi,\chi} << 1$. Notice that the interactions with $\chi$ are vanishing identically on the IR brane, for $\beta_\chi = 2$, due to the VEV profile of $\chi$; thus the IR localized limit of Yukawa interactions involving $\chi$ is naturally suppressed. The correction $r^{H\Phi\chi}_{00}$, as defined in Eq. (113), is just a way for us to parametrize the bulk NLO Yukawa interactions in a way similar to the LO Yukawa interactions. The same goes for the definition of the 4D VEV for the $\chi$ field, $\chi_0 = v^{4D}_\chi e^{k\pi R}\sqrt{(1+\beta_\chi)}$. The overlap correction factors from Eq. (113) range from $(r^{H\Phi\chi}_{00})_t \simeq 0.64$ to $(r^{H\Phi\chi}_{00})_u \simeq 0.8$. Finally, the function $f_\chi^{u_i,d_i}$, defined after Eq. (7) and measuring the relative strength of NLO and LO Yukawa interactions in the bulk case for generic $\beta_{H,\Phi,\chi}$, is given by:

$$f_\chi^{u_i,d_i} \equiv \frac{(v_\chi^{4D} e^{k\pi R}/k)\, r_{00}^{H\Phi\chi}(c_q^L, c_{u_i,d_i}, \beta_{H\Phi\chi})}{r_{00}^{H\Phi}(c_q^L, c_{u_i,d_i}, \beta_{H\Phi})} \simeq \frac{2\beta_\chi C_\chi}{6+\beta_H+\beta_\Phi+\beta_\chi - c_q^L - c_{u_i,d_i}}. \tag{114}$$

We then consider the overlap correction factors associated with the interaction of KK and zero mode fermions. They enter at each Higgs vertex (and mass insertion) in the one-loop diagrams of Figs. 1 and 2. The wave functions for the KK fermion modes are [30]:

$$\chi_n(c,y) = \frac{e^{5k|y|/2}}{N_n\sqrt{\pi R}}\left[J_\alpha\left(m_n\frac{e^{k|y|}}{k}\right) + b_\alpha(m_n) Y_\alpha\left(m_n\frac{e^{k|y|}}{k}\right)\right], \tag{115}$$

where $\alpha = |c+1/2|$ and $\chi_n$ denotes the normalized wave function of the level $n$ KK mode. The coefficients $b_\alpha(m_n)$ and the mass spectrum $m_n$ are determined by the BC imposed on the corresponding fermion. For (++) BC, one obtains [30, 10]

$$-\,b_n = \frac{J_{\alpha-1}(m_n/k)}{Y_{\alpha-1}(m_n/k)} = \frac{J_{\alpha-1}(m_n e^{k\pi R}/k)}{Y_{\alpha-1}(m_n e^{k\pi R}/k)}. \tag{116}$$

The coefficient $\tilde{b}_n$, for the wave function of the $(--)$ KK mode, is obtained by the replacement $\alpha - 1 \to \alpha$, and the replacement $c \to -c$ should also be made. The coefficient $b_n'(m_n)$ for the $(-+)$ KK mode is instead given by:

$$-\,b_n' = \frac{J_\alpha(m_n/k)}{Y_\alpha(m_n/k)} = \frac{J_{\alpha-1}(m_n e^{k\pi R}/k)}{Y_{\alpha-1}(m_n e^{k\pi R}/k)}\,, \tag{117}$$

while the coefficient $\tilde{b}_n'(m_n)$, for the wave function of the $(+-)$ KK mode, is obtained by the replacement $\alpha \leftrightarrow \alpha - 1$. The normalization factor $N_n$, for (++) modes, is as follows

$$\begin{aligned}(N_n^2)_{(++)} \;&=\; \frac{1}{2k\pi R}\left[e^{2k\pi R}\left(J_\alpha(m_n\frac{e^{k\pi R}}{k}) + b_\alpha(m_n)Y_\alpha(m_n\frac{e^{k\pi R}}{k})\right)^2\right. \\ &\quad \left. -\left(J_\alpha(\frac{m_n}{k}) + b_\alpha(m_n)Y_\alpha(\frac{m_n}{k})\right)^2\right]\,, \end{aligned} \tag{118}$$

and the one for $(--)$ KK modes is given by the replacement $\alpha \to \alpha - 1$. The normalization factor $N_n$, for $(-+)$ KK modes, is instead

$$\begin{aligned}(N_n^2)_{(-+)} \;&=\; \frac{1}{2k\pi R}\left[e^{2k\pi R}\left(J_\alpha(m_n\frac{e^{k\pi R}}{k}) + b_\alpha(m_n)Y_\alpha(m_n\frac{e^{k\pi R}}{k})\right)^2\right. \\ &\quad \left. -\left(J_{\alpha-1}(\frac{m_n}{k}) + b_\alpha(m_n)Y_{\alpha-1}(\frac{m_n}{k})\right)^2\right]\,, \end{aligned} \tag{119}$$

and the one for $(+-)$ KK modes is given by the replacement $\alpha \leftrightarrow \alpha - 1$. For all KK modes, in the limit $m_n << k$ and $kR >> 1$, the normalization factor is well approximated by

$$N_n \simeq \frac{e^{k\pi R}}{\sqrt{2k\pi R}} J_\alpha \left( m_n \frac{e^{k\pi R}}{k} \right) \simeq \frac{e^{k\pi R/2}}{\sqrt{\pi^2 R m_n}} \,. \tag{120}$$

In this way the value of all KK modes on the IR brane is approximately $\sqrt{2k}$, as also in [16] and others. The above definitions of the fermionic KK normalization constants are needed when writing the 4D Lagrangian of Eq. (1) in terms of the Yukawa couplings in Eqs. (5) and (7).

The overlap correction factors for the KK modes in Eq. (1) are thus defined as follows

$$r^{H\Phi}_{nm}(c_n, c_m, y) = \frac{\int_0^{\pi R} dy \sqrt{-g}\, \chi_n(c_n, y) \chi_m(c_m, y) (H_0 \Phi_0 / k^2) e^{(4+\beta_H+\beta_\Phi)k(|y|-\pi R)}}{\chi_n(c_n, \pi R) \chi_m(c_m, \pi R) (v v_\Phi^{4D})/(k^2 e^{2k\pi R})} \,, \tag{121}$$

where $n, m = 0, 1, 1^{-+}, 1^{-}, 1^{+-}, 2, \ldots$ denote the KK states. In the following, we will only consider the effects of the first KK level, thus taking $n, m = 0, 1, 1^{-+}, 1^{-}, 1^{+-}$. Notice also that the overlap integral of Eq. (121) with two bulk scalar fields is equivalent to the overlap integral of a single bulk Higgs field with $\beta = 2 + \beta_H + \beta_\Phi$, rescaled by a $\mathcal{O}(1)$ correction factor, $R_{H\Phi}$

$$R_{H\Phi} = \frac{H_0 \Phi_0 / k^2}{(v v_\Phi^{4D} e^{2k\pi R}/k) \sqrt{2(3 + \beta_H + \beta_\Phi)}} \simeq \frac{2\sqrt{(1+\beta_H)}\sqrt{(1+\beta_\Phi)}}{\sqrt{2(1+\beta_H+\beta_\Phi)}} \simeq 1.6 \,. \tag{122}$$

All overlap factors can eventually be rewritten in terms of $R_{H\Phi}$, in order to make a direct comparison with the case of a single bulk scalar field, the Higgs, and no flavon fields.

Since $c_q^L$ is strongly constrained by electroweak precision measurements [1], and $H$ and $\Phi$ are exponentially peaked towards the IR brane, the $c_{u_i,d_i}$ dependence of the various overlap corrections in Eq. (121) is mild. In addition, the continuous $(--)$ and $(+-)$ wave functions vanish at the IR brane, thus further suppressing the corresponding overlap corrections. It is also important to notice that Eqs. (116) – (119) imply that the $(-+)$ modes imitate the $(++)$ modes, while the $(+-)$ modes imitate the $(--)$ modes. The same behavior should be reflected in the corresponding overlap correction factors.

## A.1 Numerical results for the overlap correction factors

We calculate the overlap integrals in Eq. (121) numerically for the first level KK modes and for the bulk masses assignments in [1] and Eq. (110). In the following $n, m = 0, 1$ and we define:

$$r^{u_i,d_i}_{n(n^-)m(m^-)} \equiv r^{H\Phi}_{n(n^-)m(m^-)}(c_q^L, c_{u_i,d_i}, \beta) \qquad r^{u_i,d_i}_{nm^{-+}} \equiv r^{H\Phi}_{nm^{-+}}(c_q^L, c_{d_i,u_i}, \beta). \tag{123}$$

Similarly we also define:

$$r^{u_i,d_i}_{n^-m^{+-}} \equiv r^{H\Phi}_{n^-m^{+-}}(c_{d_i,u_i}, c_q^L, \beta). \tag{124}$$

The (++) and (−+) KK-KK overlap corrections are given by:

$$\begin{array}{lll} r^{u,d}_{11} \simeq r^{u,d}_{11^{-+}} \simeq 0.747 & r^{s}_{11} \simeq r^{s}_{11^{-+}} \simeq 0.744 & r^{c}_{11} \simeq r^{c}_{11^{-+}} \simeq 0.740 \\ r^{b}_{11} \simeq r^{b}_{11^{-+}} \simeq 0.738 & r^{t}_{11} \simeq 0.645 & r^{t}_{11^{-+}} \simeq 0.708. \end{array} \tag{125}$$

The (− −) and (+ −) KK-KK overlap corrections are given by:

$$\begin{array}{lll} r^{u,d}_{1^-1^-} \simeq 0.096 & r^{u,d}_{1^-1^{+-}} \simeq 0.070 & r^{s}_{1^-1^-} \simeq 0.093 \\ r^{s}_{1^-1^{+-}} \simeq 0.075 & r^{c}_{1^-1^-} \simeq 0.090 & r^{c}_{1^-1^{-+}} \simeq 0.080 \\ r^{b}_{1^-1^-} \simeq 0.087 & r^{b}_{1^-1^{-+}} \simeq 0.082 & r^{t}_{1^-1^-} \simeq 0.112 \\ r^{t}_{1^-1^{+-}} \simeq 0.048\,. & & \end{array} \tag{126}$$

The (++) KK-zero and (− +) KK-zero overlap corrections $r^{u_i,d_i}_{01}$ are given by:

$$\begin{array}{lll} r^{u,d}_{01} \simeq r^{u,d}_{01^{-+}} \simeq 0.800 & r^{s}_{01} \simeq r^{s}_{01^{-+}} \simeq 0.794 & r^{c}_{01} \simeq r^{c}_{01^{-+}} \simeq 0.790 \\ r^{b}_{01} \simeq r^{b}_{01^{-+}} \simeq 0.780 & r^{t}_{01} \simeq 0.670 & r^{t}_{01^{-+}} \simeq 0.755\,. \end{array} \tag{127}$$

The zero-KK (++) and zero-KK (− +) overlap corrections $r^{u_i,d_i}_{10}$ are given by:

$$\begin{array}{llll} r^{u,d}_{10} \simeq 0.806 & r^{u,d}_{1^{-+}0} \simeq 0.822 & r^{s}_{10} \simeq 0.795 & r^{s}_{1^{-+}0} \simeq 0.811 \\ r^{c}_{10} \simeq 0.790 & r^{c}_{1^{-+}0} \simeq 0.803 & r^{b}_{10} \simeq 0.784 & \\ r^{b}_{1^{-+}0} \simeq 0.798 & r^{t}_{10} \simeq 0.720 & r^{t}_{1^{-+}0} \simeq 0.730\,. & \end{array} \tag{128}$$

Using Eqs. (112) and (125) − (128) we obtain the coefficients $B^{u,d}_P$ to be used in the spurion-overlap formula in Eq. (28),

$$B^u_P = B^d_P \simeq 1.5. \tag{129}$$

Notice that, while $B^{u,d}_P$ is larger than one, each independent overlap correction factor is always smaller than one in magnitude and approaches one for IR localized $H$ and $\Phi$ fields.

# B Diagonalization of the KK mass matrices

We provide more details of the diagonalization procedure described in Sec. 4, starting from the one-generation case, and then considering three generations. We first specify the KK mass spectrum corresponding to the bulk parameters assignment in Eq. (110). Masses are obtained by solving Eqs. (116) and (117) numerically. The common left-handed bulk mass parameter $c^L_q$ determines the mass of all LH (++) KK modes, $Q^{(1)_{u_i,d_i}}_L$, providing $M^{KK}_{Q_L} \equiv M_{KK} \simeq 2.55\,ke^{-k\pi R}$. The rest of the KK mass spectrum for the down-sector, in units of $R'^{-1} = ke^{-k\pi R}$ and omitting the label KK to ease the notation, is

$$\begin{array}{lll} M_{d_R^{(1)}} = 2.8 & M_{\tilde{d}_R^{(1)-+}} = 2.8 & M_{s_R^{(1)}} = 2.75 \\ M_{\tilde{s}_R^{(1)-+}} = 2.55 & M_{b_R^{(1)}} = 2.5 & M_{\tilde{b}_R^{(1)-+}} = 1.23\,, \end{array} \tag{130}$$

while the mass spectrum in the up sector is given by:

$$\begin{array}{ccc} M_{u_R^{(1)}} = 2.8 & M_{\tilde{u}_R^{(1)-+}} = 2.8 & M_{c_R^{(1)}} = 2.56 \\ M_{\tilde{c}_R^{(1)-+}} = 2.7 & M_{t_R^{(1)}} = 3.4 & M_{\tilde{t}_R^{(1)-+}} = 2.5\,. \end{array} \tag{131}$$

Considering the above numerical values, we are going to treat two of the three KK modes for each generation as almost degenerate, when diagonalizing the one-generation mass matrices to $\mathcal{O}(x)$. Naively, this approximation may cease to be a good one for differences in KK masses of $\mathcal{O}(0.2ke^{-k\pi R})$, which happens to be characteristic of the first two generations since their masses are only three times larger than $x = v/M_{KK}$. For this reason, we kept track of $\mathcal{O}(x^2)$ terms in the perturbative diagonalization process, and verified a posteriori that they are sufficiently suppressed and can be neglected within the $\mathcal{O}(x)$ approximation.

## B.1 Diagonalization of the one-generation mass matrices

Starting from the down sector KK mass matrix in Eq. (31), and using Eq. (130) we realize that we have to perform a $\pi/4$ rotation in the $(2,4)$ plane when obtaining $O_L^{d_{KK}}$ and a $\pi/4$ rotation in the $(2,3)$ plane, when obtaining $O_R^{d_{KK}}$. These rotations act on $\hat{\mathbf{M}}_d^{KK}(\hat{\mathbf{M}}_d^{KK})^\dagger$ for $O_L^{d_{KK}}$ and $(\hat{\mathbf{M}}_d^{KK})^\dagger\hat{\mathbf{M}}_d^{KK}$ for $O_R^{d_{KK}}$. Once these rotations are performed and the corresponding degenerate subspaces have been diagonalized, the resulting matrix can be diagonalized using non degenerate perturbation theory. The same holds for all the one-generation mass matrices, where the main differences reside in the degenerate subspaces. The resulting diagonalization matrix for the down sector of the first generation is

$$O_L^{d_{KK}} = \left(\begin{array}{cccc} 1 & 0.64f_Q^{-1}(r_{01}\breve{y}_d - r_{101}\breve{y}_u)x & \mathcal{O}(x^2) & 0.64f_Q^{-1}(r_{01}\breve{y}_d + r_{101}\breve{y}_u)x \\ -0.91f_Q^{-1}r_{01}\breve{y}_d^*x & \frac{1}{\sqrt{2}} & (-5.24r_{11} - 4.76r_{111})\breve{y}_d^*x & \frac{1}{\sqrt{2}} \\ \mathcal{O}(x^2) & (3.7(r_{11} - r_{111})\breve{y}_u + 3.37(r_{22} - r_{222})\breve{y}_d)x & 1 & (3.7(r_{11} + r_{111})\breve{y}_u + 3.37(r_{22} + r_{222})\breve{y}_d)x \\ -0.91f_Q^{-1}r_{101}\breve{y}_u^*x & \frac{-1}{\sqrt{2}} & (-5.24r_{11} - 4.76r_{111})\breve{y}_u^*x & \frac{1}{\sqrt{2}} \end{array}\right) \tag{132}$$

Since the KK mass spectrum in the up sector of the first generation is substantially identical to the one in the down sector ($c_d = 0.77, c_u = 0.79$), the matrix $O_L^{u_{KK}}$ can be obtained from the above equation by the replacement $\breve{y}_u \leftrightarrow \breve{y}_d$. For the right diagonalization matrix, we obtain:

$$O_R^{d_{KK}} = \left(\begin{array}{cccc} 1 & f_d^{-1}r_{10}\breve{y}_dx & \mathcal{O}(x^2) & \mathcal{O}(x^2) \\ -f_d^{-1}r_{10}\breve{y}_dx & 1 & 3.37(r_{11} + r_{22})\breve{y}_dx - 3.7(r_{111} + r_{222})\breve{y}_ux & 3.37(r_{11} + r_{22})\breve{y}_dx + (3.7(r_{111} + r_{222})\breve{y}_ux \\ \mathcal{O}(x^2) & -(4.76r_{11} + 5.24r_{22})\breve{y}_d^*x & \frac{1}{\sqrt{2}} & \frac{1}{\sqrt{2}} \\ \mathcal{O}(x^2) & -(4.76r_{111} + 5.24r_{222})\breve{y}_u^*x & \frac{-1}{\sqrt{2}} & \frac{1}{\sqrt{2}} \end{array}\right) \tag{133}$$

where, once again, $O_R^{u_{KK}}$ is obtained with the replacement $\breve{y}_u \leftrightarrow \breve{y}_d$. Next, we turn to the $s$-quark sector, which due to the "fake" $SU(2)_R$ partner of the $c_R$ quark, $\tilde{s}_R^{(1)^{-+}}$, shows the same KK mass degeneracy pattern as the one in the $t$-quark sector. Then $O_L^{s_{KK}}$ is given by:

$$O_L^{s_{KK}} =$$

$$\begin{pmatrix} 1 & 0.94 f_Q^{-1} r_{01} \breve{y}_s x & \frac{f_Q^{-1}}{\sqrt{2}} r_{101} \breve{y}_c x & \frac{f_Q^{-1}}{\sqrt{2}} r_{101} \breve{y}_c x \\ -0.94 f_Q^{-1} r_{01} \breve{y}_s x & 1 & (6.06 r_{11} + 4.72 r_{22}) e^{i\theta_c} \breve{y}_s^* x & -(6.06 r_{11} + 4.72 r_{22}) e^{i\theta_c} \breve{y}_s^* x \\ \mathcal{O}(x^2) & (8.6 r_{11} + 8.1 r_{22}) \breve{y}_s x & -\frac{e^{i\theta_c}}{\sqrt{2}} + \frac{(r_{111}^2 - r_{222}^2)\breve{y}_c + r_{11}^2 (|\breve{y}_s|^2/\breve{y}_c^*)}{4\sqrt{2}(r_{111}+r_{222})} x & \frac{e^{i\theta_c}}{\sqrt{2}} + \frac{(r_{111}^2 - r_{222}^2)\breve{y}_c + r_{11}^2 (|\breve{y}_s|^2/\breve{y}_c^*)}{4\sqrt{2}(r_{111}+r_{222})} x \\ -f_Q^{-1} r_{101} \breve{y}_c^* x & \mathcal{O}(x^2) & \frac{1}{\sqrt{2}} + \frac{(r_{111}^2 - r_{222}^2)\breve{y}_c + r_{11}^2 (|\breve{y}_s|^2/|\breve{y}_c|)}{4\sqrt{2}(r_{111}+r_{222})} x & \frac{1}{\sqrt{2}} - \frac{(r_{111}^2 - r_{222}^2)\breve{y}_c + r_{11}^2 (|\breve{y}_s|^2/|\breve{y}_c|)}{4\sqrt{2}(r_{111}+r_{222})} x \end{pmatrix} \tag{134}$$

where $\theta_c$ denotes the phase of $\breve{y}_c$. The right diagonalization matrix, $O_R^{s_{KK}}$, is instead

$$O_R^{s_{KK}} =$$

$$\begin{pmatrix} 1 & -\frac{f_s^{-1}}{\sqrt{2}} r_{10} e^{i\theta_c} \breve{y}_s^* x & \mathcal{O}(x^2) & \frac{f_s^{-1}}{\sqrt{2}} r_{10} e^{i\theta_c} \breve{y}_s^* x \\ -f_s^{-1} r_{10} \breve{y}_s x & -\frac{e^{i\theta_c}}{\sqrt{2}} + \frac{(r_{222}^2 - r_{111}^2)\breve{y}_c + r_{22}^2 (|\breve{y}_s|^2/\breve{y}_c^*)}{4\sqrt{2}(r_{111}+r_{222})} x & (8 r_{11} + 8.5 r_{22}) \breve{y}_s x & \frac{e^{i\theta_c}}{\sqrt{2}} + \frac{(r_{222}^2 - r_{111}^2)\breve{y}_c + r_{22}^2 (|\breve{y}_s|^2/\breve{y}_c^*)}{4\sqrt{2}(r_{111}+r_{222})} x \\ \mathcal{O}(x^2) & (5.7 r_{11} + 6 r_{22}) e^{i\theta_c} \breve{y}_s^* x & 1 & -(5.7 r_{11} + 6 r_{22}) e^{i\theta_c} \breve{y}_s^* x \\ \mathcal{O}(x^2) & \frac{1}{\sqrt{2}} + \frac{(r_{222}^2 - r_{111}^2)\breve{y}_c + r_{22}^2 (|\breve{y}_s|^2/|\breve{y}_c|)}{4\sqrt{2}(r_{111}+r_{222})} x & \mathcal{O}(x^2) & \frac{1}{\sqrt{2}} - \frac{(r_{222}^2 - r_{111}^2)\breve{y}_c + r_{22}^2 (|\breve{y}_s|^2/|\breve{y}_c|)}{4\sqrt{2}(r_{111}+r_{222})} x \end{pmatrix} \tag{135}$$

The diagonalization matrices for the $t$-quark sector, similar in structure to the matrices in the $s$-sector, are as follows

$$O_L^{t_{KK}} =$$

$$\begin{pmatrix} 1 & 0.75 f_Q^{-1} r_{01} \breve{y}_t x & \frac{f_Q^{-1}}{\sqrt{2}} r_{101} \breve{y}_b x & \frac{f_Q^{-1}}{\sqrt{2}} r_{101} \breve{y}_b x \\ -0.75188 f_Q^{-1} r_{01} \breve{y}_t x & 1 & (1.22 r_{11} + 0.92 r_{22}) e^{i\theta_b} \breve{y}_t^* x & -(1.22 r_{11} + 0.92 r_{22}) e^{i\theta_b} \breve{y}_t^* x \\ \mathcal{O}(x^2) & (1.73 (r_{11} + 1.3 r_{22}) \breve{y}_t x & -\frac{e^{i\theta_b}}{\sqrt{2}} + \frac{(r_{111}^2 - r_{222}^2)\breve{y}_b + (f_t^2 r_{10}^2 + r_{11}^2)(|\breve{y}_t|^2/\breve{y}_b^*)}{4\sqrt{2}(r_{111}+r_{222})} x & \frac{e^{i\theta_b}}{\sqrt{2}} + \frac{(r_{111}^2 - r_{222}^2)\breve{y}_b + (f_t^2 r_{10}^2 + r_{11}^2)(|\breve{y}_t|^2/\breve{y}_b^*)}{4\sqrt{2}(r_{111}+r_{222})} x \\ -f_Q^{-1} r_{101} \breve{y}_b^* x & \mathcal{O}(x^2) & \frac{1}{\sqrt{2}} + \frac{(r_{111}^2 - r_{222}^2)\breve{y}_b + (f_t^2 r_{10}^2 + r_{11}^2)(|\breve{y}_t|^2/|\breve{y}_b|)}{4\sqrt{2}(r_{111}+r_{222})} x & \frac{1}{\sqrt{2}} - \frac{(r_{111}^2 - r_{222}^2)\breve{y}_b + (f_t^2 r_{10}^2 + r_{11}^2)(|\breve{y}_t|^2/|\breve{y}_b|)}{4\sqrt{2}(r_{111}+r_{222})} x \end{pmatrix} \tag{136}$$

where $\theta_b$ denotes the phase of $\breve{y}_b$, and

$$O_R^{t_{KK}} =$$

$$\begin{pmatrix} 1 & -\frac{f_t^{-1}}{\sqrt{2}} r_{10} e^{i\theta_b} \breve{y}_t^* x & \mathcal{O}(x^2) & \frac{f_t^{-1}}{\sqrt{2}} r_{10} e^{i\theta_b} \breve{y}_t^* x \\ -f_t^{-1} r_{10} \breve{y}_t x & -\frac{e^{i\theta_b}}{\sqrt{2}} + \frac{(r_{222}^2 - r_{111}^2)\breve{y}_b + r_{22}^2 (|\breve{y}_t|^2/\breve{y}_b^*)}{4\sqrt{2}(r_{111}+r_{222})} x & (1.33 r_{11} + 1.8 r_{22}) \breve{y}_t x & \frac{e^{i\theta_b}}{\sqrt{2}} + \frac{(r_{222}^2 - r_{111}^2)\breve{y}_b + r_{22}^2 (|\breve{y}_t|^2/\breve{y}_b^*)}{4\sqrt{2}(r_{111}+r_{222})} x \\ \mathcal{O}(x^2) & (0.92 r_{11} + 1.22 r_{22}) e^{i\theta_b} \breve{y}_t^* x & 1 & -(0.92 r_{11} + 1.22 r_{22}) e^{i\theta_b} \breve{y}_t^* x \\ \mathcal{O}(x^2) & \frac{1}{\sqrt{2}} + \frac{(r_{222}^2 - r_{111}^2)\breve{y}_b + r_{22}^2 (|\breve{y}_t|^2/|\breve{y}_b|)}{4\sqrt{2}(r_{111}+r_{222})} x & \mathcal{O}(x^2) & \frac{1}{\sqrt{2}} - \frac{(r_{222}^2 - r_{111}^2)\breve{y}_b + r_{22}^2 (|\breve{y}_t|^2/|\breve{y}_b|)}{4\sqrt{2}(r_{111}+r_{222})} x \end{pmatrix} \tag{137}$$

Finally, we consider the $b$-quark sector and the analogous $c$-quark sector. Starting with $O_L^{b_{KK}}$, we obtain:

$$O_L^{b_{KK}} =$$

$$\begin{pmatrix} 1 & -\frac{f_Q^{-1}}{\sqrt{2}} r_{01} |\breve{y}_b| x & \frac{f_Q^{-1}}{\sqrt{2}} r_{01} |\breve{y}_b| x & 2 f_Q^{-1} r_{101} \breve{y}_t x \\ -f_Q^{-1} r_{01} \breve{y}_b^* x & -\frac{e^{-i\theta_b}}{\sqrt{2}} - \frac{(r_{11}^2 - r_{22}^2)\breve{y}_b^* + r_{111}^2 (|\breve{y}_t|^2/\breve{y}_b)}{4\sqrt{2}(r_{111}+r_{222})} x & \frac{e^{-i\theta_b}}{\sqrt{2}} - \frac{(r_{11}^2 - r_{22}^2)\breve{y}_b^* + r_{111}^2 (|\breve{y}_t|^2/\breve{y}_b)}{4\sqrt{2}(r_{111}+r_{222})} x & \mathcal{O}(x^2) \\ \mathcal{O}(x^2) & \frac{1}{\sqrt{2}} - \frac{(r_{11}^2 - r_{22}^2)|\breve{y}_b| + r_{111}^2 (|\breve{y}_t|^2/|\breve{y}_b|)}{4\sqrt{2}(r_{111}+r_{222})} x & \frac{1}{\sqrt{2}} + \frac{(r_{11}^2 - r_{22}^2)|\breve{y}_b| + r_{111}^2 (|\breve{y}_t|^2/|\breve{y}_b|)}{4\sqrt{2}(r_{111}+r_{222})} x & -\frac{2}{3}(r_{111} y_t + 2 r_{222} y_t) x \\ -2 f_Q^{-1} r_{101} \breve{y}_t^* x & 0.47 (r_{111} + 2 r_{222}) y_t^* x & 0.47 (r_{111} + 2 r_{222}) y_t^* x & 1 \end{pmatrix} \tag{138}$$

and for the right-handed diagonalization matrix

$$O_R^{b_{KK}} =$$

$$\begin{pmatrix} 1 & -\frac{f_b^{-1}}{\sqrt{2}} r_{10}|\breve{y}_b|x & \frac{f_b^{-1}}{\sqrt{2}} r_{10}|\breve{y}_b|x & \mathcal{O}(x^2) \\ -f_b^{-1} r_{10}\breve{y}_b x & -\frac{e^{i\theta_b}}{\sqrt{2}} + \frac{(r_{22}^2 - r_{11}^2)\breve{y}_b^* + r_{222}^2(|\breve{y}_t|^2/\breve{y}_b)}{4\sqrt{2}(r_{11}+r_{22})}x & \frac{e^{i\theta_b}}{\sqrt{2}} + \frac{(r_{22}^2 - r_{11}^2)\breve{y}_b^* + r_{222}^2(|\breve{y}_t|^2/\breve{y}_b)}{4\sqrt{2}(r_{11}+r_{22})}x & -\frac{2}{3}(2r_{111} + r_{222})y_t x \\ \mathcal{O}(x^2) & \frac{1}{\sqrt{2}} + \frac{(r_{22}^2 - r_{11}^2)|\breve{y}_b| + r_{222}^2(|\breve{y}_t|^2/|\breve{y}_b|)}{4\sqrt{2}(r_{11}+r_{22})}x & \frac{1}{\sqrt{2}} - \frac{(r_{22}^2 - r_{11}^2)|\breve{y}_b| + r_{222}^2(|\breve{y}_t|^2/|\breve{y}_b|)}{4\sqrt{2}(r_{11}+r_{22})}x & \mathcal{O}(x^2) \\ \mathcal{O}(x^2) & -\frac{\sqrt{2}}{3}(r_{111} + 2r_{222})e^{i\theta_b}\breve{y}_t^* x & \frac{\sqrt{2}}{3}(r_{111} + 2r_{222})e^{i\theta_b}\breve{y}_t^* x & 1 \end{pmatrix} \tag{139}$$

Analogously, $O_L^{c_{KK}}$ is given by:

$$O_L^{c_{KK}} =$$

$$\begin{pmatrix} 1 & -\frac{f_Q^{-1}}{\sqrt{2}} r_{01}|\breve{y}_c|x & \frac{f_Q^{-1}}{\sqrt{2}} r_{01}|\breve{y}_c|x & 0.94 f_Q^{-1} r_{101}\breve{y}_s x \\ -f_Q^{-1} r_{01}\breve{y}_c^* x & -\frac{e^{-i\theta_c}}{\sqrt{2}} - \frac{(r_{11}^2 - r_{22}^2)\breve{y}_c^* + r_{111}^2(|\breve{y}_s|^2/\breve{y}_c)}{4\sqrt{2}(r_{111}+r_{222})}x & \frac{e^{-i\theta_c}}{\sqrt{2}} - \frac{(r_{11}^2 - r_{22}^2)\breve{y}_c^* + r_{111}^2(|\breve{y}_s|^2/\breve{y}_c)}{4\sqrt{2}(r_{111}+r_{222})}x & \mathcal{O}(x^2) \\ \mathcal{O}(x^2) & \frac{1}{\sqrt{2}} - \frac{(r_{11}^2 - r_{22}^2)|\breve{y}_c| + r_{111}^2(|\breve{y}_s|^2/|\breve{y}_c|)}{4\sqrt{2}(r_{111}+r_{222})}x & \frac{1}{\sqrt{2}} + \frac{(r_{11}^2 - r_{22}^2)|\breve{y}_c| + r_{111}^2(|\breve{y}_s|^2/|\breve{y}_c|)}{4\sqrt{2}(r_{111}+r_{222})}x & (8.6r_{111} + 8.1r_{222})y_s x \\ -0.94 f_Q^{-1} r_{101}\breve{y}_s^* x & -(6.1r_{111} + 5.7r_{222})y_s^* x & -(6.1r_{111} + 5.7r_{222})y_s^* x & 1 \end{pmatrix} \tag{140}$$

while $O_R^{c_{KK}}$ is

$$O_R^{c_{KK}} =$$

$$\begin{pmatrix} 1 & -\frac{f_c^{-1}}{\sqrt{2}} r_{10}|\breve{y}_c|x & \frac{f_c^{-1}}{\sqrt{2}} r_{10}|\breve{y}_c|x & \mathcal{O}(x^2) \\ -f_c^{-1} r_{10}\breve{y}_c x & -\frac{e^{i\theta_c}}{\sqrt{2}} + \frac{(r_{22}^2 - r_{11}^2)\breve{y}_c^* + r_{222}^2(|\breve{y}_s|^2/\breve{y}_c)}{4\sqrt{2}(r_{11}+r_{22})}x & \frac{e^{i\theta_c}}{\sqrt{2}} + \frac{(r_{22}^2 - r_{11}^2)\breve{y}_c^* + r_{222}^2(|\breve{y}_s|^2/\breve{y}_c)}{4\sqrt{2}(r_{11}+r_{22})}x & (8r_{111} + 8.5r_{222})y_s x \\ \mathcal{O}(x^2) & \frac{1}{\sqrt{2}} + \frac{(r_{22}^2 - r_{11}^2)|\breve{y}_c| + r_{222}^2(|\breve{y}_s|^2/|\breve{y}_c|)}{4\sqrt{2}(r_{11}+r_{22})}x & \frac{1}{\sqrt{2}} - \frac{(r_{22}^2 - r_{11}^2)|\breve{y}_c| + r_{222}^2(|\breve{y}_s|^2/|\breve{y}_c|)}{4\sqrt{2}(r_{11}+r_{22})}x & \mathcal{O}(x^2) \\ \mathcal{O}(x^2) & (5.65r_{111} + 6r_{222})e^{i\theta_c}\breve{y}_s^* x & -(5.65r_{111} + 6r_{222})e^{i\theta_c}\breve{y}_s^* x & 1 \end{pmatrix} \tag{141}$$

We also provide the KK mass spectrum obtained in the one-generation approximation. The mass spectrum for the first generation, $u$ and $d$, KK modes remains unchanged at $\mathcal{O}(x)$ and given by

$$(\mathbf{M}_{u,d}^{KK})_{diag} = M_{KK}\,\mathrm{d}iag\left(\breve{y}_{u,d} f_Q^{-1} f_{u,d}^{-1} r_{00} x, 1.1, 1, 1.1\right) \tag{142}$$

The mass spectrum for the $s$ and $t$ KK modes is modified in a similar manner, as follows

$$\begin{aligned} (\mathbf{M}_s^{KK})_{diag} &= M_{KK}\,\mathrm{d}iag\left(\breve{y}_s f_Q^{-1} f_s^{-1} r_{00} x, 1.125, 1 - (r_{111} + r_{222})|\breve{y}_c|x, 1 + (r_{111} + r_{222})|\breve{y}_c|x\right) \\ (\mathbf{M}_t^{KK})_{diag} &= M_{KK} \times \mathrm{d}iag\left(\breve{y}_t f_Q^{-1} f_t^{-1} r_{00} x, 1.33, 1 - (r_{111} + r_{222})|\breve{y}_b|x, 1 + (r_{111} + r_{222})|\breve{y}_b|x\right) \end{aligned} \tag{143}$$

The mass spectrum for the $b$ and $c$ KK modes is also modified in a similar manner

$$\begin{aligned} (\mathbf{M}_b^{KK})_{diag} &= M_{KK}\,\mathrm{d}iag\left(\breve{y}_b f_Q^{-1} f_b^{-1} r_{00} x, 1 - (r_{111} + r_{222})|\breve{y}_b|x, 1 + (r_{11} + r_{22})|\breve{y}_b|x, 0.5\right) \\ (\mathbf{M}_c^{KK})_{diag} &= M_{KK} \times \mathrm{d}iag\left(\breve{y}_c f_Q^{-1} f_c^{-1} r_{00} x, 1 - (r_{11} + r_{22})|\breve{y}_c|x, 1 + (r_{11} + r_{22})|\breve{y}_c|x, 1.125\right) \end{aligned} \tag{144}$$

## B.2 Overlap dependence of Dipole Operators in the one-generation approximation

In this section we evaluate the coefficients $B_P^{u,d}$ that enter the spurion-overlap analysis of the new physics contributions to the neutron EDM, $\epsilon'/\epsilon$ and $b \to s\gamma$, when it is combined with the direct diagonalization of the one-generation mass matrices. The approach is described in Sec. 4.1 and makes use of Eqs. (33) and (34), the Yukawa matrices of Eqs.(35)–(37) and the diagonalization matrices of appendix B.1. In the evaluation of $B_P^{u,d}$ for this case, we neglect the very moderate generational dependence of overlap corrections and use their maximal value, leading to the most conservative estimate.

We start with the down-type contribution to the neutron EDM. The overlap dependence of this contribution in the one-generation KK diagonalization scheme is encoded in $(B_P^d)_{nEDM}^{KK(1gen)}$, for which the most dominant contributions are as follows

$$(B_P^d)_{nEDM}^{KK(1gen)} = (r_{01} + r_{101}) \left[2.6 r_{10}(r_{11} + r_{111}) + 1.88 r_{10}(r_{22} + r_{222}) + 0.91 f_Q^2 r_{00}(r_{01} + r_{101})\right] . \tag{145}$$

Here and in the following $r_{111} = r_{11-+}$, $r_{101} = r_{01-+}$, $r_{22} = r_{1-1-}$, $r_{222} = r_{1-1^+-}$ and the notation for the rest of the overlaps is the same as in Eq. (1). As we naively expect from the spurion-overlap analysis in the mass insertion approximation, each term in the above equation is cubic in the overlap correction factors and of the characteristic form $(0 - KK)(KK - KK)(KK - 0)$, or $(0 - 0)(0 - KK)(0 - KK)$ for $f_Q^2$ proportional terms. Notice that the latter, with $f_Q^2 \approx 0.1$, is suppressed compared to other $\mathcal{O}(x) \approx \mathcal{O}(0.1)$ terms. For this reason we can safely neglect the overlap correction terms proportional to $\mathcal{O}(0.5) f_Q^2$ in the expressions below.

The overlap dependence of the up-type contribution to the neutron EDM is encoded in $(B_P^u)_{nEDM}^{KK(1gen)}$, for which the most dominant contributions are as follows

$$(B_P^u)_{nEDM}^{KK(1gen)} = (r_{10} + r_{101}) \left[2.6 r_{10}(r_{11} + r_{111}) + 2.9 r_{10}(r_{22} + r_{222}) + 0.46 f_Q^2 r_{00}(r_{01} + r_{101})\right] . \tag{146}$$

The overlap dependence of the up- and down-type contributions within the first generation is almost identical, due to the similarity of the corresponding one-generation KK diagonalization matrices of Eqs. (132) and (133) and given that $c_d = 0.77$ and $c_u = 0.79$. More substantial differences between the overlap dependence of up- and down-type contributions to $\epsilon'/\epsilon$ and $b \to s\gamma$ are to be expected, since they involve less degenerate bulk parameters from the second and third generation. In addition, to account conservatively for the generational dependence within the one-generation approximation, we will take the maximum over all generations for the following $B_P^{u,d}$ factors.

The overlap dependence of the down-type (neutral Higgs) contribution to $\epsilon'/\epsilon$ is thus encoded in $(B_P^d)_{\epsilon'/\epsilon}^{KK(1gen)}$, for which the dominant terms are as follows

$$(B_P^d)_{\epsilon'/\epsilon}^{KK(1gen)} = max \left[ r_{01} r_{10} \left( \frac{1}{4} r_{111} - \frac{5}{4} r_{222} + \frac{r_{11}^2}{4(r_{111} + r_{222})} + f_Q^2 r_{00} r_{101} \right) \right] . \tag{147}$$

For the up-type (charged Higgs) contribution to $\epsilon'/\epsilon$ we obtain

$$\begin{aligned}(B_P^u)^{KK(1gen)}_{\epsilon'/\epsilon} &= max\left[\frac{r_{01}r_{10}}{r_{11}+r_{22}}\left(3.24r_{11}^2 - 6.06r_{111}(r_{11}+r_{22}) - 0.125r_{111}^2 + 5.93r_{11}r_{22}\right.\right.\\ &\left. +2.68r_{22}^2 - 6.43r_{222}(r_{11}+r_{22})\right) + \frac{r_{10}r_{101}}{r_{11}+r_{22}}\left(\frac{1}{8}(r_{11}^2+r_{111}^2) + 0.5r_{11}r_{22}\right.\\ &\left.\left. -2.7r_{111}(r_{11}+r_{22}) + 0.375r_{22}^2 - 3.37r_{222}(r_{11}+r_{22})\right)\right]\,. \end{aligned} \tag{148}$$

For the down-type (neutral Higgs) contribution to $b \to s\gamma$, the dominant overlap dependence is as follows

$$\begin{aligned}(B_P^d)^{KK(1gen)}_{b\to s\gamma} &= \max\left\{\frac{r_{10}}{r_{11}+r_{22}}\left[r_{01}\left(0.2\,r_{11}^2 + \sqrt{2}\,r_{111}^2 - (\sqrt{2}/2)\,r_{11}r_{22} - 0.9r_{22}^2\right)\right.\right.\\ &\left. + r_{101}\left(-0.125\,r_{11}^2 - r_{111}^2 + 0.5\,r_{11}r_{22} + 0.625\,r_{22}^2\right)\right]\\ &+\frac{r_{10}}{r_{111}+r_{222}}\left[r_{01}\left(4r_{11}r_{111} + 4.8r_{111}r_{22} + 4.04r_{11}r_{222} + 4.76r_{22}r_{222}\right)\right.\\ &\left. + r_{101}\left(-0.1r_{111}^2 + 0.125r_{22}^2 + 0.54r_{111}r_{222} + 0.625r_{222}^2\right)\right]\\ &\left. - r_{101}\left(1.32r_{10}r_{111} + 4.62r_{10}r_{222}\right)\right\}, \end{aligned} \tag{149}$$

while the dominant up-type (charged Higgs) contribution is

$$\begin{aligned}(B_P^u)^{KK(1gen)}_{b\to s\gamma} &= \max\left\{\frac{r_{10}}{r_{11}+r_{22}}\left[r_{01}\left(-0.18\,r_{11}^2 + \sqrt{2}\,r_{111}^2 - 2\,r_{11}r_{22} - 1.8r_{22}^2\right)\right.\right.\\ &\left. + r_{101}\left(0.125\,r_{11}^2 + r_{111}^2 + \sqrt{2}\,r_{11}r_{22} + 1.275\,r_{22}^2\right)\right]\\ &+\frac{r_{10}}{r_{111}+r_{222}}\left[r_{01}\left(-4r_{11}r_{111} - 3.8r_{111}r_{22} - 4.04r_{11}r_{222} - 3.8r_{22}r_{222}\right)\right.\\ &\left. + r_{101}\left(0.125r_{111}^2 - 0.125r_{22}^2 + 0.47r_{111}r_{222} + 0.347r_{222}^2\right)\right]\\ &\left. + r_{101}\left(1.32r_{10}r_{111} - 2.9r_{10}r_{222}\right)\right\}. \end{aligned} \tag{150}$$

Using the numerical results for the overlap corrections in the RS-A$_4$ setup, as given in appendix A.1, we obtain the following conservative estimate for the modified $B_P^{u,d}$ overlap factors

$$\begin{gathered}(B_P^d)^{KK(1gen)}_{nEDM} \simeq 5.4 \quad (B_P^u)^{KK(1gen)}_{nEDM} \simeq 5.3 \quad (B_P^d)^{KK(1gen)}_{\epsilon'/\epsilon} \simeq 0.2,\\ (B_P^u)^{KK(1gen)}_{\epsilon'/\epsilon} \simeq -2.63, \quad (B_P^d)^{KK(1gen)}_{b\to s\gamma} \simeq 0.98, \quad (B_P^u)^{KK(1gen)}_{b\to s\gamma} \simeq -1.54\,, \end{gathered} \tag{151}$$

to be used in the combined spurion-overlap analysis with the diagonalization of the one-generations mass matrices – see Sec. 4.1.

## B.3 Approximate analytical diagonalization of the three-generation mass matrices

This section collects more details of the approximate analytical diagonalization scheme described in Sec. 4.2. In particular, we are going to inspect the structure of the down-type mass matrix, $\hat{\mathbf{M}}^D_{Full}$, once it is rotated by the block KK diagonalization matrices, $\mathbf{O}^{D_{KK}}_{L,R}$. This allows to understand why an additional rotation by the A$_4$ $12 \times 12$ matrices, $\hat{\mathbf{O}}^{D_{A_4}}_{L,R}$ may provide an almost complete diagonalization. Similar arguments hold for the up-type mass matrix, $\hat{\mathbf{M}}^U_{Full}$, which is of an analogous structure. Using the $4 \times 4$ block notation, we write:

$$\begin{aligned}\frac{(\mathbf{O}^{D_{KK}}_L)^\dagger \hat{\mathbf{M}}^D_{Full} \mathbf{O}^{D_{KK}}_R}{M_{KK}} &\equiv \tilde{\mathbf{M}}^D_{(KK)} \\ &= \begin{pmatrix} (\hat{\mathbf{M}}^d_{KK})_{diag}/M_{KK} & (O^{d_{KK}}_L)^\dagger \hat{Y}'^{KK}_s O^{s_{KK}}_R x & (O^{d_{KK}}_L)^\dagger \hat{Y}'^{KK}_b O^{b_{KK}}_R x \\ (O^{s_{KK}}_L)^\dagger \hat{Y}'^{KK}_d O^{d_{KK}}_R x & (\hat{\mathbf{M}}^s_{KK})_{diag}/M_{KK} & (O^{s_{KK}}_L)^\dagger \hat{Y}''^{KK}_b O^{b_{KK}}_R x \\ (O^{b_{KK}}_L)^\dagger \hat{Y}''^{KK}_d O^{d_{KK}}_R x & (O^{b_{KK}}_L)^\dagger\ \hat{Y}''^{KK}_s O^{s_{KK}}_R x & (\hat{\mathbf{M}}^b_{KK})_{diag}/M_{KK} \end{pmatrix}\end{aligned} \tag{152}$$

In the above equation, $\hat{Y}^{(\prime,\prime\prime)KK}_{d,s,b}$ is a shorthand notation for the off-diagonal entries in Eq. (38), namely $\hat{Y}'^{KK}_d = \hat{Y}^{KK}_d((\hat{y}^{LO}_{21} + \hat{y}^{NLO}_{21}, f_d)$ and so on. Using this notation, the matrix $\hat{Y}'^{KK}_d$ has the same structure as $\hat{Y}^{KK}_d$ in Eq. (35), up to the replacement $\breve{y}_{u,d} \to \breve{y}'_{u,d}$. At LO, from Eq. 5, one also has $\breve{y}'_{u,d} \equiv (\hat{Y}^{u,d}_{12})_{LO} = 2(\hat{y}^{u,d}_{12})_{LO} v^{4D}_\Phi e^{k\pi R}/k$, while Eq. 7 provides the NLO contribution. Since we want to perform the diagonalization to $\mathcal{O}(x)$, the slight generational dependence of the overlap corrections is numerically negligible at this order. The same goes for the zero-zero interaction terms in each of the off-diagonal blocks. It is important to notice that the latter are proportional to $x$, hence it is clear that only the $\mathcal{O}(1)$ terms in $O^{(d,s,b)_{KK}}_{L,R}$ will supplement us with off-diagonal $\mathcal{O}(x)$ entries in the "KK-rotated" mass matrix of Eq. (152). The $\mathcal{O}(1)$ terms in the KK diagonalization matrices arise from the rotations that diagonalize the corresponding nearly degenerate subspaces.

To illustrate it, we first focus on the (12) block in Eq. (152) and write it explicitly. From Eqs. (132) and (133), we learn that the $\mathcal{O}(1)$ terms in $O^{d_{KK}}_{L,R}$ correspond to $\pi/4$ rotations in the (24) and (34) subspaces, respectively. Similarly the $\mathcal{O}(1)$ terms in $O^{s_{KK}}_{L,R}$ of Eqs. (134)–(135), correspond to $\pi/4$ rotations (plus a phase $\theta_c \equiv \mathrm{A}rg(y_c)$) in the (34) and (24) subspaces, respectively. Using $(\hat{y}^{u,d}_{12})_{LO} = (\hat{y}^{u,d}_{11})_{LO}$, we have $\breve{y}'_{c,s} \simeq \breve{y}_{c,s}$ [7] and the (12) block of $\tilde{\mathbf{M}}^D_{(KK)}$ turns out to be:

$$\left(\tilde{\mathbf{M}}^D_{(KK)}\right)_{12} = \begin{pmatrix} f_Q^{-1} f_s^{-1} r_{00} \breve{y}_s x & f_Q^{-1} r_{101} \breve{y}_c x & f_Q^{-1} r_{10} \breve{y}_s x & \frac{f_Q^{-1} r_{101}}{\sqrt{2}} \breve{y}_c x \\ 0 & \frac{e^{i\theta_c}}{2}\left(r_{222}\breve{y}^*_c - r_{22}\breve{y}^*_s\right) x & 0 & \frac{e^{i\theta_c}}{2}\left(r_{222}\breve{y}^*_c - r_{22}\breve{y}^*_s\right) x \\ f_s^{-1} r_{10} \breve{y}_s x & \frac{1}{2} r_{111} \breve{y}_c x & r_{11} \breve{y}_s x & \frac{1}{2} r_{111} \breve{y}_c x \\ 0 & -\frac{e^{i\theta_c}}{2}\left(r_{222}\breve{y}^*_c + r_{22}\breve{y}^*_s\right) x & 0 & -\frac{e^{i\theta_c}}{2}\left(r_{222}\breve{y}^*_c + r_{22}\breve{y}^*_s\right) x \end{pmatrix} \tag{153}$$

---

[7] Notice that we also have $\breve{y}_c \simeq \breve{y}_s$, which is an exact equality for the LO Yukawa interactions.

Because of the near degeneracy of $r_{22}$ and $r_{222}$, one concludes that the second row is approximately vanishing. A similar pattern will emerge for the (21) block, where the third column will be the one that approximately vanishes at this order. Considering the (13) block, we recall that $(\hat{y}^{u,d}_{13})_{LO} = (\hat{y}^{u,d}_{11})_{LO}$, which implies $\breve{y}'_{t,b} \simeq \breve{y}_{t,b}$, thus leading to

$$\left(\tilde{\mathbf{M}}^D_{(KK)}\right)_{13} = \\ \begin{pmatrix} f_Q^{-1} f_b^{-1} r_{00} \breve{y}_b x & \frac{f_Q^{-1}}{\sqrt{2}} r_{01} \breve{y}_b x & \frac{f_Q^{-1}}{\sqrt{2}} r_{01} \breve{y}_b x & f_Q^{-1} r_{101} \breve{y}_t x \\ 0 & \frac{e^{i\theta_b}}{2} \left(r_{222} \breve{y}_t^* - r_{22} \breve{y}_b^*\right) x & \frac{e^{i\theta_c}}{2} \left(r_{222} \breve{y}_t^* - r_{22} \breve{y}_b^*\right) x & 0 \\ f_b^{-1} r_{10} \breve{y}_b x & \frac{r_{11}}{\sqrt{2}} \breve{y}_b x & \frac{r_{11}}{\sqrt{2}} \breve{y}_b x & r_{111} \breve{y}_t x \\ 0 & -\frac{e^{i\theta_b}}{2} \left(r_{222} \breve{y}_t^* + r_{22} \breve{y}_b^*\right) x & -\frac{e^{i\theta_b}}{2} \left(r_{222} \breve{y}_t^* + r_{22} \breve{y}_b^*\right) x & 0 \end{pmatrix} \tag{154}$$

It is already at this level that we notice the modifications induced by $y_t \simeq 2.8$, as compared to $y_{u,c,d,s,b} = 1$. The difference of Yukawa couplings now spoils the vanishing of the second row for the (13) block, differently from the (12) block. An analogous situation arises in the third column of the (31) block.This will be the main obstacle in obtaining a fully analytical diagonalization of all blocks involving the third generation.
Finally, we focus on the (23) block of $\tilde{\mathbf{M}}^D_{(KK)}$. From Eqs. (138) and (139) it is clear that the $\mathcal{O}(1)$ terms in $O^{b_{KK}}_{L,R}$ correspond to a $\pi/4$ rotations in the (23) subspace of the $(\tilde{\mathbf{M}}^D_{(KK)})_{23}$ block plus a phase $\theta_b = \mathrm{A}rg(y_b)$. Using $(\hat{y}^{u,d}_{23})_{LO} = \omega^2 (\hat{y}^{u,d}_{11})_{LO}$, we get $\breve{y}''_{t,b} \simeq \omega^2 \breve{y}_{t,b}$ and the (23) block turns out to be:

$$\left(\tilde{\mathbf{M}}^D_{(KK)}\right)_{23} = \\ \begin{pmatrix} \omega^2 f_Q^{-1} f_b^{-1} r_{00} \breve{y}_b x & \omega^2 \frac{f_Q^{-1}}{\sqrt{2}} r_{01} \breve{y}_b x & \omega^2 \frac{f_Q^{-1}}{\sqrt{2}} r_{01} \breve{y}_b x & \omega^2 f_Q^{-1} r_{101} \breve{y}_t x \\ 0 & \frac{-\omega e^{i\theta_b}}{\sqrt{2}} r_{22} \breve{y}_b^* x & \frac{\omega e^{i\theta_b}}{\sqrt{2}} r_{22} \breve{y}_b^* x & 0 \\ \frac{-\omega^2 e^{i\theta_c}}{\sqrt{2}} f_Q^{-1} r_{10} \breve{y}_b & -(\frac{\omega^2 e^{i\theta_c}}{2} \breve{y}_b r_{11} + \frac{\omega e^{i\theta_b}}{2} \breve{y}_t^* r_{222}) x & (\frac{-\omega^2 e^{i\theta_c}}{2} \breve{y}_b r_{11} + \frac{\omega e^{i\theta_b}}{2} \breve{y}_t^* r_{222}) x & \frac{-\omega^2 e^{i\theta_c}}{\sqrt{2}} r_{111} \breve{y}_t x \\ \frac{\omega^2 e^{i\theta_c}}{\sqrt{2}} f_Q^{-1} r_{10} \breve{y}_b & (\frac{\omega^2 e^{i\theta_c}}{2} \breve{y}_b r_{11} - \frac{\omega e^{i\theta_b}}{2} \breve{y}_t^* r_{222}) x & (\frac{-\omega^2 e^{i\theta_c}}{2} \breve{y}_b r_{11} + \frac{\omega e^{i\theta_b}}{2} \breve{y}_t^* r_{222}) x & \frac{\omega^2 e^{i\theta_c}}{\sqrt{2}} r_{111} \breve{y}_t x \end{pmatrix} \tag{155}$$

As expected, the cancellation pattern we encountered in the (12) block gets modified even further than in the (13) block, due to the different rotations involved in the (23) block of $\tilde{\mathbf{M}}^D_{(KK)}$. Observing Eqs. (153)– (155), we realize that the distribution of the 1, $\omega$ and $\omega^2$ factors in the off-diagonal blocks of $\tilde{\mathbf{M}}^D_{(KK)}$ approximately corresponds to the one of the leading order Yukawa couplings $(\hat{y}^{u,d}_{ij})_{LO}$, up to complex conjugations of terms proportional to $\breve{y}^*_{u,c,t,d,s,b}$. For this reason, we expect the A$_4$ $12 \times 12$ rotation matrices defined as $\mathbf{O}^{(U,D)_{A_4}}_{L,R} \equiv V^{u,d}_{L,R} \otimes \mathbb{1}_{4\times 4}$ to induce some cancellations among the various blocks of $\tilde{\mathbf{M}}^D_{(KK)}$. However, due to the difference of $y_t$ from the rest of the LO Yukawa couplings and due to the different rotations in each of the off-diagonal blocks of $\tilde{\mathbf{M}}^D_{(KK)}$, it is clear that the cancellations induced by $\mathbf{O}_{L,R}^{(U,D)_{A_4}}$ can never be exact, even if we only consider the LO Yukawa interactions. Thus, the above diagonalization scheme will still fail to fully diagonalize the degenerate subspace. On the other hand, off-diagonal elements in the non degenerate subspaces like the zero-KK and a few KK-KK entries can be treated using non degenerate perturbation theory.

At this level, the exact structure of the approximate $12 \times 12$ diagonalization matrices composed of the $\mathbf{O}_{L,R}^{D_{KK}}$, $\mathbf{O}_{L,R}^{(U,D)_{A_4}}$ and the perturbative rotation matrices, used in attempting the analytical diagonalization, is very complicated and impossible to write in a compact way. Instead, to better estimate the inaccuracy of this diagonalization scheme, we assign $y_{u,c,d,s,b} = 1$, $y_t \simeq 2.8$ and set the bulk masses according to Eq. (110), which yield the physical running quark masses at the scale $R'^{-1} \simeq 1.8$ TeV and fix all the overlap correction factors. The NLO Yukawas are assigned according to Eq. (12), to provide a realistic CKM matrix in the ZMA. The $x$ parameter is left unassigned. We then write the magnitude of the off-diagonal elements in the degenerate subspace of $\tilde{\mathbf{M}}^{D}_{(KK)}\tilde{\mathbf{M}}^{D\dagger}_{(KK)}$ to gain an insight into the "contaminations", which can not be treated using non degenerate perturbation theory and can only be partly reduced by the $\mathbf{O}_{L}^{(D)_{A_4}}$ rotation matrices. A similar procedure is followed for $\tilde{\mathbf{M}}^{D\dagger}_{(KK)}\tilde{\mathbf{M}}^{D}_{(KK)}$ and the right-handed rotations.

From Eqs. (142)–(144), we learn that the degenerate subspace approximately decomposes in two blocks, one corresponding to the $(2, 4, 6)$ subspace, where all KK masses are approximately $1.1 M_{KK}$ and the $(3, 7, 8, 10, 11)$ subspace[8], where all KK masses are approximately $M_{KK} \simeq 2.55\, R'^{-1}$. In $\tilde{\mathbf{M}}^{D}_{(KK)}\tilde{\mathbf{M}}^{D\dagger}_{(KK)}$ these masses appear squared, since every diagonal block is proportional to a diagonalized one-generation KK mass matrix squared plus additional $\mathcal{O}(x^2)$ terms. Hence in total, we have the squared spectrum $(1.21, 1, 1.21, 1.21, 1, 1, 1, 1)$ on the diagonal of the $(2, 3, 4, 6, 7, 8, 10, 11)$ subspace of $\tilde{\mathbf{M}}^{D}_{(KK)}\tilde{\mathbf{M}}^{D\dagger}_{(KK)}$, and the contaminations in the same subspace amount to

$$(\tilde{\mathbf{M}}^{D}\tilde{\mathbf{M}}^{D\dagger})_{(KK_{Deg.})} \approx \\ \begin{pmatrix} 1.21 & \mathcal{O}(x^2) & \mathcal{O}(x^2) & 0.03x & 0.02x & 0.02x & -0.1x & -0.15x \\ \mathcal{O}(x^2) & 1 & \mathcal{O}(x^2) & 0.2x & 0.25x & 0.2x & 0.25x & 0.25x \\ \mathcal{O}(x^2) & \mathcal{O}(x^2) & 1.21 & -0.03x & -0.25x & 0.25x & 0.05x & 0.2x \\ 0.03x & 0.2x & -0.03x & 1.21 & \mathcal{O}(x^2) & \mathcal{O}(x^2) & (-0.05+0.15i)x & -0.05+0.1ix \\ 0.02x & 0.25x & -0.25x & \mathcal{O}(x^2) & 1 & \mathcal{O}(x^2) & 0.25ix & 0.2ix \\ 0.02x & 0.2x & 0.25x & \mathcal{O}(x^2) & \mathcal{O}(x^2) & 1 & -0.1x & -0.14x \\ -0.1x & 0.3x & 0.05x & (-0.05+0.15i)x & 0.25ix & -0.1x & 1 & \mathcal{O}(x^2) \\ -0.15x & 0.3x & 0.2x & (-0.05+0.1i)x & 0.2ix & -0.14x & \mathcal{O}(x^2) & 1 \end{pmatrix} \tag{156}$$

We realize that the largest contaminations of $\mathcal{O}(0.25x)$ are numerically suppressed by three orders of magnitude compared to the diagonal entries for $x \simeq 0.04$, which corresponds to $R'^{-1} = 1.8$ TeV. For this reason, the results of the approximate analytical diagonalization scheme can still provide an order of magnitude estimate for the physical couplings between zero modes and KK modes. From the above matrix, one can also infer the way $\mathbf{O}_{L}^{D_{KK}}$

---

[8] Since the contaminations in the off-diagonal elements of the degenerate subspace are of $\mathcal{O}(x)$, the $\mathcal{O}(x)$ corrections to the KK masses will have a minor effect on this estimation.

deviates from the "true" diagonalization matrix; in particular it is evident that the first row of $\mathbf{O}_L^{D_{KK}}$ is the least contaminated. This qualitatively explains why the semianalytical estimation for the neutron EDM is in better agreement with the numerical result than in the case of $\epsilon'/\epsilon$ and $b \to s\gamma$. We have failed to find a better analytical method which would allow us to further diagonalize the contaminated subspace of Eq. (156). Nevertheless, the adopted scheme allows to qualitatively understand the way some of the cancellation mechanisms still act in the full $12 \times 12$ case. An analogous situation occurs for $(\tilde{\mathbf{M}}^{D\dagger}\tilde{\mathbf{M}}^{D})_{(KK_{Deg.})}$ and the right-handed diagonalization matrix $\mathbf{O}_R^{D_{KK}}$.

# References

[1] A. Kadosh and E. Pallante, JHEP **1008**, 115 (2010) [arXiv:1004.0321 [hep-ph]].

[2] E. Ma and G. Rajasekaran, Phys. Rev. **D64**, 113012 (2001) K. S. Babu, E. Ma and J. W. F. Valle, Phys. Lett. **B552** 207 2003; E. Ma, Phys. Rev. **D70**, 031901(2004) Talk at SI2004, Fuji-Yoshida, Japan, hep-ph/0409075.

[3] L. Randall and R. Sundrum, Phys. Rev. Lett. **83**, 3370 (1999) [arXiv:hep-ph/9905221]; L. Randall and R. Sundrum, Phys. Rev. Lett. **83**, 4690 (1999) [arXiv:hep-th/9906064].

[4] C. Csaki, C. Delaunay, C. Grojean and Y. Grossman, JHEP **0810**, 055 (2008) [arXiv:0806.0356 [hep-ph]].

[5] X. G. He, Y. Y. Keum and R. R. Volkas, JHEP **0604**, 039 (2006) [arXiv:hep-ph/0601001].

[6] K. Agashe, A. Delgado, M. J. May and R. Sundrum, JHEP **0308**, 050 (2003) [arXiv:hep-ph/0308036].

[7] M. Carena, E. Ponton, J. Santiago and C.E.M. Wagner, arXiv:hep-ph/0701055.

[8] K. Agashe, G. Perez and A. Soni, Phys. Rev. Lett. **93**, 201804 (2004) [arXiv:hep-ph/0406101];

[9] G. Cacciapaglia, C. Csaki, J. Galloway, G. Marandella, J. Terning and A. Weiler, JHEP **0804**, 006 (2008) [arXiv:0709.1714 [hep-ph]].

[10] K. Agashe, G. Perez and A. Soni, Phys. Rev. D **71**, 016002 (2005) [arXiv:hep-ph/0408134];

[11] K. Agashe, M. Papucci, G. Perez and D. Pirjol, arXiv:hep-ph/0509117; Z. Ligeti, M. Papucci and G. Perez, Phys. Rev. Lett. **97**, 101801 (2006) [arXiv:hep-ph/0604112]. A. L. Fitzpatrick, G. Perez and L. Randall, arXiv:0710.1869 [hep-ph].

[12] M. C. Chen and H. B. Yu, Phys. Lett. B **672**, 253 (2009) [arXiv:0804.2503 [hep-ph]].

[13] G. Perez and L. Randall, JHEP **0901**, 077 (2009) [arXiv:0805.4652 [hep-ph]].

[14] C. Csaki, G. Perez, Z. Surujon and A. Weiler, arXiv:0907.0474 [hep-ph].

[15] K. Agashe, A. Azatov and L. Zhu, Phys. Rev. D **79**, 056006 (2009) [arXiv:0810.1016 [hep-ph]].

[16] O. Gedalia, G. Isidori and G. Perez, Phys. Lett. **B 682**, 200 (2009).

[17] F. Feruglio, C. Hagedorn, Y. Lin and L. Merlo, Nucl. Phys. B **775**, 120 (2007) [arXiv:hep-ph/0702194]; M. C. Chen, K. T. Mahanthappa and F. Yu, arXiv:0909.5472 [hep-ph]; P. H. Frampton and T. W. Kephart, Int. J. Mod. Phys. A **10**, 4689 (1995) [arXiv:hep-ph/9409330]; A. Aranda, C. D. Carone and R. F. Lebed, Phys. Lett. B **474**, 170 (2000) [arXiv:hep-ph/9910392]; A. Aranda, C. D. Carone and R. F. Lebed, Phys. Rev. D **62**, 016009 (2000) [arXiv:hep-ph/0002044].

[18] K. Agashe and R. Contino, Phys. Rev. D **80**, 075016 (2009) [arXiv:0906.1542 [hep-ph]].

[19] A. Azatov, M. Toharia and L. Zhu, Phys. Rev. D **80**, 035016 (2009) [arXiv:0906.1990 [hep-ph]].

[20] C. Amsler *et al.* [Particle Data Group], Phys. Lett. **B667** 1 (2008).

[21] K. Agashe, R. Contino, L. Da Rold and A. Pomarol, Phys. Lett. B **641**, 62 (2006) [arXiv:hep-ph/0605341].

[22] W. D. Goldberger and M. B. Wise, Phys. Rev. Lett. **83**, 4922 (1999) [arXiv:hep-ph/9907447]; G. Cacciapaglia, C. Csaki, G. Marandella and J. Terning, JHEP **0702**, 036 (2007) [arXiv:hep-ph/0611358].

[23] G. Buchalla, A. J. Buras and M. E. Lautenbacher, Rev. Mod. Phys. **68**, 1125 (1996) [arXiv:hep-ph/9512380].

[24] C. A. Baker *et al.*, Phys. Rev. Lett. **97**, 131801 (2006) [arXiv:hep-ex/0602020].

[25] V. Cirigliano, Eur. Phys. J. C **33**, S333 (2004); W. Lee, PoS **LAT2006**, 015 (2006) [arXiv:hep-lat/0610058]; S. Bertolini, J. O. Eeg and M. Fabbrichesi, Phys. Rev. D **63**, 056009 (2001) [arXiv:hep-ph/0002234]; A. Pich, [arXiv:hep-ph/0410215]. A. J. Buras and J. M. Gerard, Phys. Lett. B **517**, 129 (2001) [arXiv:hep-ph/0106104].

[26] A. J. Buras, G. Colangelo, G. Isidori, A. Romanino and L. Silvestrini, Nucl. Phys. B **566**, 3 (2000) [arXiv:hep-ph/9908371].

[27] A. J. Buras, B. Duling and S. Gori, arXiv:0905.2318 [hep-ph]; M. Blanke, A. J. Buras, B. Duling, S. Gori and A. Weiler, JHEP **0903**, 001 (2009) [arXiv:0809.1073 [hep-ph]].

[28] M. Bona *et al.* [UTfit Collaboration], JHEP **0803**, 049 (2008) [arXiv:0707.0636 [hep-ph]].

[29] S. Casagrande et al., arXiv:1005.4315 [hep-ph]

[30] Y. Grossman and M. Neubert, Phys. Lett. B **474**, 361 (2000) [arXiv:hep-ph/9912408]; T. Gherghetta and A. Pomarol, Nucl. Phys. B **586**, 141 (2000) [arXiv:hep-ph/0003129]; S. J. Huber and Q. Shafi, Phys. Lett. B **498**, 256 (2001) [arXiv:hep-ph/0010195]; S. J. Huber and Q. Shafi, Phys. Lett. B **512**, 365 (2001) [arXiv:hep-ph/0104293].